The Dissertation Committee for Gideon Johannes van Zyl
certifies that this is the approved version of the following dissertation:

The Analysis of Nonlinear Systems Driven by Almost Periodic Inputs

Committee:

Irwin W. Sandberg, Supervisor

Edward J. Powers Jr.

Aristotle Arapostathis

Jerry L. Bona

Joydeep Ghosh

The Analysis of Nonlinear Systems Driven by Almost Periodic Inputs

by

Gideon Johannes van Zyl, B.Eng., M.Eng., Hons.-B.Sc.

Dissertation

Presented to the Faculty of the Graduate School of

The University of Texas at Austin

in Partial Fulfillment

of the Requirements

for the Degree of

Doctor of Philosophy

The University of Texas at Austin

May 2003

To Sonia.

Acknowledgments

None of this work would have been possible without the pioneering work of my supervisor, Prof. I.W. Sandberg. I gratefully acknowledge his help in many aspects of this work.

Thanks are also due to Reutech Radar Systems who sponsored the author to spend a year at the University of Texas at Austin and for allowing the author to take time off to study mathematics at the University of Stellenbosch.

To the National Research Foundation in South Africa, the University of Texas at Austin through research assistantships as well as Advanced Energy Industries, Inc. I am thankful for financial support.

To my family I am very thankful for their support and encouragement.

Gideon Johannes van Zyl

The University of Texas at Austin

May 2003

The Analysis of Nonlinear Systems Driven by Almost Periodic Inputs

Publication No. _____

Gideon Johannes van Zyl, Ph.D.
The University of Texas at Austin, 2003

Supervisor: Irwin W. Sandberg

We start in Chapter 1 by motivating the research, defining almost periodic and asymptotically almost periodic functions, reviewing known properties of these functions and introducing notation to be used in the other chapters.

In Chapter 2 we show how input-output stability theory bears on the problem of obtaining a frequency-domain stability criterion that can be used to design periodically driven varactor (nonlinear capacitor) circuits with guaranteed stability. We present an example of how a varactor frequency doubler with guaranteed stability may be designed using this criterion.

In Chapter 3 we give an analytical basis for evaluating the spectral coefficients for a large family of systems. This involves a convergent iterative process and certain bounds on the errors incurred in truncating the process.

In Chapter 4 we consider the equations of a large class of nonlinear circuits driven by asymptotically almost periodic inputs, and give an analytical basis for the use of harmonic balance to find steady-state solutions. More specifically, we show

that in a certain setting there is a unique solution to the problem of obtaining a harmonic balance approximation, and that the approximations approach the actual solution as additional spectral components are included.

The results in Chapters 2–4 all involve a key circle-criterion hypothesis. In Chapter 5 we give an example that shows that this hypothesis cannot be relaxed significantly.

In Chapter 6 we give a generalization of the techniques in the first chapters that allows us to extend the theory to include non-diagonal nonlinearities. We give an example that shows the generalization is useful even in the case that the nonlinearity is diagonal.

In Chapter 7 we derive an integral equation that describes a nonlinear resistor in parallel with a nonlinear capacitor driven by a Thévenin equivalent source. We show how to obtain a contraction mapping operator on the set of square integrable functions and show the optimality of certain constants used in the construction of the contraction mapping operator.

We end in Chapter 8 by looking at an alternative method for determining the stability of steady state regimes in nonlinear circuits. We point out some problems in the theory and suggest a solution for one problem, but conclude that this method has some serious shortcomings.

Table of Contents

List of Tables

List of Figures

Chapter 1

Introduction

This research was triggered by a desire to obtain stability criteria for periodically driven nonlinear microwave circuits. In the microwave literature a number of methods have been proposed for evaluating the stability of periodic steady state solutions obtained by numerical methods [10], [7], [27]. Although these methods appear to have some success in solving a difficult problem, no stability criteria are provided that can serve as a guide at design time. Furthermore the methods do not all appear to have a firm analytical basis and all address only the stability of a particular large signal solution or the stability of some set of large signal solutions in the case of continuation methods. By contrast, the operator-theoretic methods described in [15] and earlier papers by the same author do provide criteria that can be used as a guide at design time, have a solid analytical basis, and apply to all solutions of the system equations. (Under the conditions of the theorems there is generally a unique solution within the class of solutions considered.) The stronger results do not come free and generally the circuit or system has to satisfy stringent conditions before the theorems can be applied. Part of the work described here is to make the theory applicable to a wider class of problems than was previously possible. Although the initial focus was on microwave circuits, the results apply equally (and perhaps more

so) to control systems and other circuits and systems encountered in engineering.

While researching this field it became clear that the class of functions can be extended to include the class of asymptotically almost periodic functions without significantly reducing the class of circuits for which stability criteria can be obtained. (E.g. if a circuit satisfies all the conditions required to conclude that the circuit is stable in a certain sense when the input is a periodic signal, it is generally also stable in a related sense when the input is only asymptotically almost periodic.) Since the class of asymptotically almost periodic functions plays an important role in communication systems, the scope of the research was enlarged to include this interesting class of functions. In order to introduce this class of functions we start with a number of definitions.

A function f given by

$$f(t) = \sum_m A_m \sin(\omega_m t + \theta_m), \quad t \in (-\infty, \infty) \tag{1.1}$$

in which the sum is finite and the A_m, ω_m, and θ_m are real constants, is called a *trigonometric polynomial* (because of its exponential-form representation). In (1.1) the frequencies $\{\omega_m\}$ need not be integrally related. The set of real-valued *almost periodic functions* consists of these trigonometric polynomials together with all limits, with respect to the usual uniform norm, of sequences of trigonometric polynomials. *Asymptotically almost periodic functions* are defined only for $t \geq 0$. They are sums of the restriction to $[0, \infty)$ of an almost periodic function and a continuous function that approaches zero as $t \to \infty$. Asymptotically almost periodic functions often arise in the study of communication systems. They often describe the system input or a modified input that takes into account initial conditions.

1.1 General Notation

In the following, $\mathbb{R}$ and $\mathbb{C}$ denote the real and complex numbers, respectively, $\mathbb{Z}$ stands for the set of all integers, and $\mathbb{N}$ denotes $\{1, 2, 3, \cdots\}$. We use j for $\sqrt{-1}$.

We use 0 to denote the null element of any of the vector spaces defined below and t always denotes a real scalar. The symbol s denotes a scalar complex variable with $\sigma = \text{Re } (s)$ and $\omega = \text{Im}(s)$.

We use $\mathbb{R}^N$ ($\mathbb{C}^N$) to denote the set of real (complex) N-vectors. In equations involving matrices we view $x \in \mathbb{R}^N$ ($x \in \mathbb{C}^N$) as a column vector. The k-th component of $x \in \mathbb{R}^N$ ($x \in \mathbb{C}^N$) is denoted by x_k. For $x \in \mathbb{R}^N$ ($x \in \mathbb{C}^N$) define

$$|x|_2 = \left(\sum_{k=1}^{N} |x_k|^2 \right)^{\frac{1}{2}}$$

as the 2-norm, and

$$|x|_\infty = \max_k |x_k|$$

as the ∞-norm on $\mathbb{R}^N$ ($\mathbb{C}^N$).

Let M denote an arbitrary matrix. Denote the transpose, the complex conjugate transpose, and the inverse of M by M^T, M^* and M^{-1}, respectively. The positive square root of the largest eigenvalue of M^*M is denoted by $\Lambda\{M\}$ and 1_N denotes the identity matrix of order N.

With $a, b \in \mathbb{R} \bigcup \{-\infty, \infty\}$ and $a < b$, the set of complex (Lebesgue) measurable N-vector-valued functions of the real variable t defined on (a, b) (or $[a, b)$ etc. as appropriate) is denoted by $\mathbb{H}_N(a, b)$ and the k-th component of $f \in \mathbb{H}_N(a, b)$ is denoted by f_k. The set $L_{2,N}(a, b)$ is defined by

$$L_{2,N}(a, b) = \left\{ f : f \in \mathbb{H}_N(a, b), \ \int_a^b f^*(t) f(t)\, dt < \infty \right\}.$$

The norm of $f \in L_{2,N}(0, \infty)$ is denoted by $\|f\|_2$ and is defined by

$$\|f\|_2 = \left(\int_0^\infty f^*(t) f(t)\, dt \right)^{\frac{1}{2}}.$$

More generally the norm of $f \in L_{2,N}(a,b)$ is denoted by $\|f\|_{2(a,b)}$ and is defined by

$$\|f\|_{2(a,b)} = \left(\int_a^b f^*(t) f(t)\, dt \right)^{\frac{1}{2}}.$$

With this norm $L_{2,N}(a,b)$ is a Banach space [31, p. 132]. The norm of a linear operator T taking $L_{2,N}(0,\infty)$ into $L_{2,N}(0,\infty)$ (induced by the norm $\|\cdot\|_2$ on $L_{2,N}(0,\infty)$) is denoted by $\|T\|_2$.

The set $L_{\infty,N}(0,\infty)$ is defined by

$$L_{\infty,N}(0,\infty) = \left\{ f : f \in \mathbb{H}_N(0,\infty), \sup_{t \geq 0} [f^*(t) f(t)] < \infty \right\}.$$

For $b > 0$ the set $L_{\infty,N}(0,b)$ is defined by

$$L_{\infty,N}(0,b) = \left\{ f : f \in \mathbb{H}_N(0,b), \sup_{t \in [0,b]} [f^*(t) f(t)] < \infty \right\}.$$

The set $L_{\infty,N}(-\infty,\infty)$ is defined by

$$L_{\infty,N}(-\infty,\infty) = \left\{ f : f \in \mathbb{H}_N(-\infty,\infty), \sup_{t \in \mathbb{R}} [f^*(t) f(t)] < \infty \right\}.$$

The norm of $f \in L_{\infty,N}(0,\infty)$ is denoted by $\|f\|_\infty$ and is defined by

$$\|f\|_\infty = \sup_{t \geq 0} |f(t)|_\infty .$$

Let $y \in (0,\infty)$ and define f_y by

$$f_y(t) = \begin{cases} f(t), & t \in [0,y] \\ 0, & t > y \end{cases}$$

for any $f \in \mathbb{H}_N(0,\infty)$, and let

$$\begin{aligned} L_{2,N_{loc}}(0,\infty) &= \{ f : f \in \mathbb{H}_N(0,\infty), f_y \in L_{2,N}(0,\infty) \text{ for } y \in [0,\infty) \} \\ L_{\infty,N_{loc}}(0,\infty) &= \{ f : f \in \mathbb{H}_N(0,\infty), f_y \in L_{\infty,N}(0,\infty) \text{ for } y \in [0,\infty) \}. \end{aligned}$$

With A an arbitrary measurable $N \times N$ matrix-valued function of the real variable t with elements $\{a_{nm}\}$ defined on $[0,\infty)$, let $\mathbb{K}_{p,N}$ ($p \in \{1,2\}$) denote

$$\left\{ A : \int_0^\infty |a_{nm}(t)|^p\, dt < \infty \text{ for } n,m \in \{1,2,\ldots,N\} \right\}.$$

We shall say that a (not necessarily linear) operator T with domain $\mathcal{D}(\mathcal{T}) \subset \mathbb{H}_N(0,\infty)$ is *causal* if and only if for an arbitrary $\delta > 0$

$$(Tf)(t) = (Tg)(t) \text{ a.e. on } (0,\delta)$$

whenever $f,\ g \in \mathcal{D}(\mathcal{T})$ and $f(t) = g(t)$ a.e.[1] on $(0,\delta)$.

Let S and V be open balls in $L_{\infty,N}(0,\infty)$ and $L_{\infty,N}(-\infty,\infty)$, respectively, centered at the origin. Let $T_y : L_{\infty,N}(0,\infty) \to L_{\infty,N}(0,\infty)$ be defined by

$$(T_y u)(t) = \begin{cases} 0, & t < y \\ u(t-y), & t \geq y, \end{cases}$$

for $y > 0$.

We say that $G : S \to L_{\infty,N}(0,\infty)$ is *time invariant* if G commutes with T_y on S for $y > 0$ and $F : V \to L_{\infty,N}(-\infty,\infty)$ is *time invariant* if $F[v(\cdot + a)] = (Fv)(\cdot + a)$ for $v \in V$ and $a \in \mathbb{R}$.

We say $G : S \to L_{\infty,N}(0,\infty)$ has *approximately finite memory* if for each $\gamma > 0$ there is a $\Delta > 0$ such that

$$|(Gs)(t) - (GW_{t,\alpha}s)(t)|_\infty < \gamma,\ t \geq 0$$

for $\alpha \geq \Delta$ and $s \in S$, where $W_{t,\alpha}$ is given by

$$(W_{t,\alpha}s)(\tau) = \begin{cases} s(\tau), & t - \alpha \leq \tau \leq t \\ 0, & \text{otherwise.} \end{cases}$$

By $\mathbb{R}^+$ we mean the interval $[0,\infty)$.

For scalar-valued functions we use the usual notation, namely with f a measurable real or complex valued function of a real variable, we define the following function spaces. On $\mathbb{R}$ we define

$$\begin{aligned} L_\infty(-\infty,\infty) &= \{f : \sup_t |f(t)| < \infty\} \\ L_p(-\infty,\infty) &= \{f : \int_{-\infty}^{\infty} |f(t)|^p dt < \infty\},\ p \in \{1,2,\ldots\} \end{aligned}$$

[1] We abbreviate *almost everywhere* a.e. A property holds a.e. in a set S if it holds in S except in some subset of S with measure zero [31, page 52].

and on $\mathbb{R}^+$

$$\begin{aligned} L_\infty(0,\infty) &= \{f : \sup_{t \geq 0} |f(t)| < \infty\} \\ L_p(0,\infty) &= \{f : \int_0^\infty |f(t)|^p dt < \infty\},\ p \in \{1,2,\ldots\} \\ L_{p\ \mathrm{loc}} &= \{f : \int_0^y |f(t)|^p dt < \infty \text{ for } 0 < y < \infty\},\ p \in \{1,2,\ldots\}. \end{aligned}$$

1.2 Definitions and Known Results Concerning Almost Periodic Functions

The set of real-valued almost periodic functions, which we denote by AP, is defined in the introduction. An equivalent definition is the following.[2] AP is the set of continuous real-valued functions x defined on $\mathbb{R}$ with the property that for each x and each $\epsilon > 0$ there is a real number $\ell > 0$ such that every interval in $(-\infty, \infty)$ of length ℓ contains at least one number τ for which

$$|x(t+\tau) - x(t)| < \epsilon, \quad t \in \mathbb{R}.$$

Notice that all continuous real-valued periodic functions on $\mathbb{R}$ are almost periodic.

We will use the fact that AP is a vector space over $\mathbb{R}$ and that any AP function is bounded.

For any locally integrable x we define

$$M(x) = \lim_{T \to \infty} \frac{1}{2T} \int_{-T}^{T} x(t)dt,$$

provided the limit exists (as a complex number). It is known that $M(x)$ and $M(x^2)$ exist for $x \in AP$.

[2]The material in this section concerning AP is drawn from [4] and [2]. See especially [4, pp. 11–23] and [2, pp. 2, 3, 5, 12, 27, 28, 104]. The notation in [2] is different from our notation and the notation in [4]. In [2] the term *uniformly almost periodic* is used instead of *almost periodic*.

For $x \in AP$ we define

$$\|x\|_B = \left[M(x^2)\right]^{\frac{1}{2}}.$$

We refer to this norm as the B-norm. (Note that $\|\cdot\|_B$ is not the usual norm on AP, nor is AP complete in this norm. The fact that this is indeed a norm follows from the Parseval-like equality for AP functions [see (1.2) below] and the fact that if two AP functions have the same Fourier series they are identical.)

For any $x \in$ AP, the function $a : \mathbb{R} \to \mathbb{C}$ given by $a(\omega) = M(x(\cdot)\exp(-j\omega\,\cdot))$ exists and the set $\{\omega : a(\omega) \neq 0\}$ is countable. Let this set be $\{\omega_1, \omega_2, \cdots\}$. We refer to $A_n^x \stackrel{\text{def}}{=} a(\omega_n)$ as the n^{th} spectral coefficient of x. For $x \in AP$, the "generalized Fourier series"

$$\sum_n A_n^x e^{j\omega_n t}$$

converges to x with respect to $\|\cdot\|_B$. We define the module $\bar{\Lambda}_x$ of x as $\{q \in \mathbb{R} : q = \sum_{l=1}^m k_l\omega_l, k_l \in \mathbb{Z}, m \in \mathbb{N}\}$. By the module of an asymptotically almost periodic function we mean the module of its almost periodic part.

We will make use of the fact that the Parseval-like identity holds for AP functions, i.e., that

$$\sum_{n=1}^{\infty} |A_n^x|^2 = \|x\|_B^2. \tag{1.2}$$

In addition to the space of AP functions, we will also make use of the class of functions B-AP. This class is the closure under the B-norm of the family of trigonometric polynomials. The space AP is a subset of the B-AP functions. Elements x of the family of B-AP functions also have Fourier series representations, the identity (1.2) holds, and we have an analog of the Riesz-Fisher theorem, namely that to any generalized Fourier series

$$\sum_n A_n e^{j\omega_n t}$$

for which

$$\sum_n |A_n|^2$$

converges, there corresponds a B-AP function having this series as its Fourier series.

We can extend the definition of AP functions [16] to include $\mathbb{R}^N$-valued functions by defining a $\mathbb{R}^N$-valued AP function as the set of continuous $\mathbb{R}^N$-valued functions x defined on $\mathbb{R}$ with the property that for each x and each $\epsilon > 0$ there is a real number $\ell > 0$ such that every interval in $(-\infty, \infty)$ of length ℓ contains at least one number τ for which

$$|x(t+\tau) - x(t)|_\infty < \epsilon, \quad t \in \mathbb{R}.$$

A property of AP functions that is useful (and does not hold for periodic functions) is that if f_1 and f_2 are respectively $\mathbb{R}^{N_1}$ and $\mathbb{R}^{N_2}$-valued AP functions, then the $\mathbb{R}^{N_1+N_2}$ valued function (f_1, f_2) is an AP function.[3] Of course the converse, namely that every element x_k of a $\mathbb{R}^N$ valued AP function x is an AP function, follows directly from the definition.

1.3 Special Notation

Throughout the rest of the chapters, α and β denote positive constants such that $\alpha \leq \beta$.

We say that $k \in \Phi(\alpha, \beta)$ if $k \in L_1(0, \infty)$, and with

$$K(j\omega) = \int_0^\infty k(t) e^{-j\omega t}\, dt,$$

the locus of $K(j\omega)$ for $\omega \in \mathbb{R}$ lies outside the circle C_1 of radius $0.5(\alpha^{-1} - \beta^{-1})$ centered on the real axis of the complex plane at $[-0.5(\alpha^{-1} + \beta^{-1}), 0]$ and does not encircle C_1. We refer to C_1 as the *critical disk*. This is a special case of the *circle criterion* [15, page 876].

Let ϕ be a real-valued function defined on $\mathbb{R}$. We say that $\phi \in \Theta(\alpha, \beta)$ if

(i) $\phi(0) = 0$ and

[3] See Lemma 11.

(ii) $\alpha \leq \dfrac{\phi(b)-\phi(a)}{b-a} \leq \beta$ for all $a \neq b$.

In the following we will often be concerned with systems described by integral equations of the form

$$u(t) = y(t) + \int_0^t k(t-\tau)\psi[y(\tau)]d\tau, \quad t \geq 0 \tag{1.3}$$

where t denotes time, u is the input (or a modified input that takes into account initial conditions), and y is the output. Here $u = u_1 + u_2$ where u_1 is the restriction to $[0,\infty)$ of an AP function g, and u_2 takes into account initial conditions.

The following set of assumptions are often made and are referred to as A.1:

(i) $\psi \in \Theta(\alpha,\beta)$

(ii) $k \in \Phi(\alpha,\beta)$.

(iii) $u_2 \in L_\infty(0,\infty)$ with $\lim_{t\to\infty} u_2(t) = 0$[4] , and

(iv) ξ given by $\xi(t) = t^p k(t),\ t \geq 0$ belongs to $L_1(0,\infty)\bigcap L_2(0,\infty)$ for $p \in \{0,1,2\}$.

Let c_0 denote $\frac{1}{2}(\beta+\alpha)$, and let r be given by

$$r = \frac{1}{2}(\beta-\alpha)\sup_\omega \left|\frac{K(j\omega)}{1+c_0K(j\omega)}\right|.$$

If A.1 is satisfied, it follows that $r < 1$.

We will also be concerned with integral equations of the form of (1.3) in which u and y are $\mathbb{R}^N$-valued functions, $k \in \mathbb{K}_{1,N}$ and $\psi : \mathbb{R}^N \to \mathbb{R}^N$. We say ψ is *diagonal* if the k-th component of ψx depends only on x_k.

[4]For the case of interest, u is asymptotically almost periodic according to the usual definition only if u_2 is continuous. Continuity is not assumed because it is not used in what follows.

Chapter 2

A Stability Criterion for Varactor Circuits

In this chapter we show how input-output stability theory bears on the problem of obtaining a frequency-domain stability criterion that can be used to design periodically driven varactor (nonlinear capacitor) circuits with guaranteed stability. The design criterion requires that the locus of $j\omega Z(j\omega)$ for $-\infty < \omega < \infty$ avoids a critical disk in the complex plane, where $Z(j\omega)$ is the Thévenin equivalent driving-point impedance presented to the varactor at frequency ω. The location and size of the disk is a function only of the minimum and maximum incremental capacitance of the varactor. We present an example of how a varactor frequency doubler with guaranteed stability may be designed using this criterion.

We indicate how the results may be extended to include varactor circuits driven by asymptotically almost periodic inputs.

The material in this chapter was originally published in [22] and [21].

2.1 P-stability

We say that a circuit is *p-stable* if the following conditions are met.

1. If the input approaches a periodic function of time with some period T as $t \to \infty$, then the output approaches a periodic function of time with the same period T, with this periodic function independent of the initial conditions and dependent on the input only through its periodic part.[1]

2. Small changes in the input result in small changes in the output.

This definition admittedly lacks some precision in that, for example, the meaning of "small changes" is not spelled out. Corresponding precise statements are given in 2.4.

2.2 Stability Theorem

We will be concerned with circuits of the type depicted in Figure. 2.1, in which we consider e as the input and v as the output.

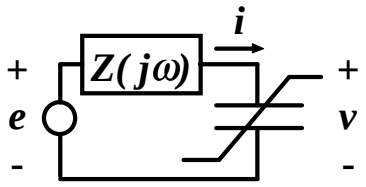

Figure 2.1: Type of circuit considered.

Let $Z(s) = \int_0^\infty z(t)e^{-st}\,dt$ be the Thévenin equivalent driving-point impedance presented to the varactor. We assume that z is integrable [2]and that Z is a positive

[1]E.g., if the input is given by $\sin(2\pi t/T)$ for $t \geq t_0$ then, as $t \to \infty$, the output approaches a periodic function q with period T (which thus contains spectral components only at multiples of $2\pi/T$) and q does not depend on the input before time t_0.

[2]By "integrable", we mean Lebesgue integrable with a finite integral. In this dissertation all functions are legitimate functions, as opposed to generalized functions in which impulses, etc. are

real function in the sense of passive network theory (i.e., that $Z(s)$ is real when s is real, and $\mathrm{Re}\,[Z(s)] \geq 0$ for $\mathrm{Re}\,(s) \geq 0$). We suppose that the varactor charge-voltage law, Q, belongs to $\Theta(\alpha, \beta)$.

We say that Z satisfies the *circle criterion for varactor circuits* if the locus of $j\omega Z(j\omega)$ for all real ω avoids the disk in the complex plane centered on the real axis of the complex s-plane at $\left(-\frac{1}{2}(\alpha^{-1} + \beta^{-1}), 0\right)$ with radius $\frac{1}{2}(\alpha^{-1} - \beta^{-1})$. (In what follows we refer to this disk as the "critical disk".)

We assume that the following two conditions are met:

1. z is differentiable, and its derivative z' is Lipschitz continuous on $[0, a]$ for each $a > 0$.

2. $t^p z'(t)$ is both integrable and square integrable on the interval $[0, \infty)$ for $p \in \{0, 1, 2\}$. (This condition is satisfied whenever z is continuous and there is a constant M for which $|z'(t)| \leq Mt^{-4}$ for all $t \geq 1$.)

Note that conditions 1 and 2 are always met if the circuit consists only of lumped elements. (Assuming also that the reactive lumped elements have some losses so that we exclude the possibility of imaginary axis poles in the Laplace domain representation of the Thévenin equivalent impedance.)

Theorem 1 Suppose that Z satisfies the circle criterion for varactor circuits. Then the circuit is p-stable provided some very reasonable additional conditions are met concerning the input and the way in which initial conditions are taken into account. (See 2.4 for the details.)

Under the conditions of Theorem 1, it is also true that the describing-function (i.e.,harmonic balance) technique for determining the periodic part of the output

allowed. Note that since $\alpha > 0$, a portion of the varactor's capacitance can be lumped in with $Z(j\omega)$ to ensure that z is a legitimate function.

is valid (see the comment concerning describing functions on page 172 as well as Chapter 4).[3]

2.3 Design of a Varactor Frequency Doubler with Guaranteed Stability

The purpose of this section is to illustrate the use of Theorem 1 in the design of a p-stable periodically driven varactor circuit, and to illustrate a consequence of the constraints that the stability criterion imposes on the design.

Consider the design of a varactor frequency doubler with a 100 MHz input frequency. Assume that the diode has an incremental capacitance limited to the range 2 pF to 15 nF. We lump 1 pF of the varactor capacitance in with the matching circuit to make sure that z is a legitimate function. The modified incremental capacitance is thus contained between 1 pF and 15 nF and this determines the size and position of the critical disk in the complex plane. A simple matching circuit can be used consisting of a combination of a singly terminated low pass filter together with its complementary high pass filter. Specifically, consider the use of a singly terminated Butterworth low-pass filter connected as shown in Figure 2.2 to its complementary high pass filter. Both filters are fifth order 50 ohm filters with -3 dB points at 150 MHz. Figure 2.3 shows a plot of $j\omega Z(j\omega)$ for nonnegative ω together with the upper part of the critical disk for such a matching circuit (which includes 1 pF of the varactor's incremental capacitance and, as indicated in Figure 2.2, a series resistance of 0.5 ohm and 2 nH of parasitic inductance) showing that the circle criterion is satisfied.

[3] In addition, using material in [16] and [17] as well as in 2.4, it can be shown that under the conditions of Theorem 1 asymptotically almost periodic inputs (see [16]) produce asymptotically almost periodic outputs, that the almost periodic part of the output is independent of the transient part of the input, and that the frequencies of the output are restricted to the set $\{\omega : \omega = \sum_{j=1}^{q} k_j\omega_j \,;\, \omega_j \in \Lambda,\, k_j \geq 0 \text{ and } q > 0 \text{ integers}\}$ where Λ is the set of frequencies of the input. See Theorems 2 and 3.

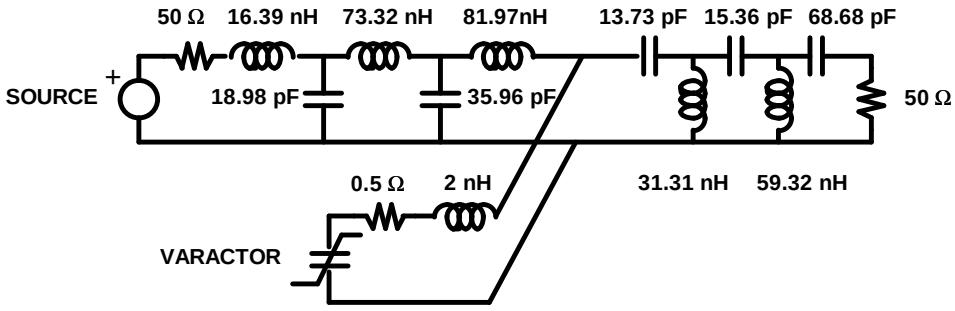

Figure 2.2: Varactor frequency doubler circuit.

In this example the circle criterion is fairly restrictive in the sense that simulations indicate that the conversion loss for the multiplier (excluding loss in the matching circuit) is about 3.7 dB for 16 dBm input, while if there are no constraints on the design of the matching circuits the predicted conversion loss [3] for such a multiplier is close to 0 dB. Simulations of other multiplier configurations indicate that such an additional loss of 3 to 4 dB might be a fairly typical price to pay for compliance with the circle criterion.

In situations where conversion loss is not of extreme importance the circle criterion is a useful design criterion that guarantees stability in a strong sense. But the circle criterion is only a sufficient condition for stability. Thus, where conversion loss is a critical parameter, conventional approaches to the design – in which stability could occur but is not guaranteed – might be more appropriate.

2.4 Proof of the Theorem

The proof presented here involves a few steps to show that the conditions for applying the theorems in [15] are met.

The Thévenin equivalent circuit and the varactor introduce the constraints

$$e(t) + c(t) = v(t) + \int_0^t z(t-\tau)i(\tau)d\tau, \quad t \geq 0$$

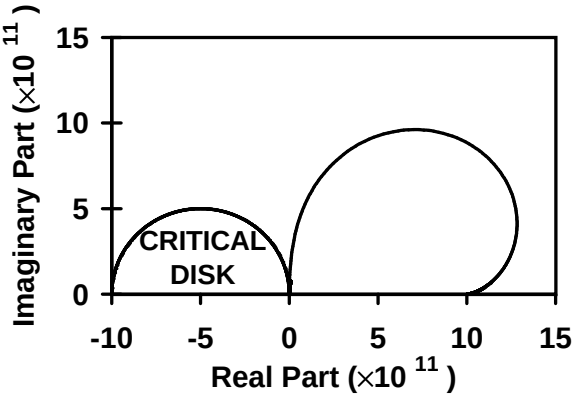

Figure 2.3: Upper part of the critical disk in the complex plane and plot of $j\omega Z(j\omega)$ for ω between 0 and $2\pi \times 50 \times 10^9$.

and $i(t) = \dfrac{d}{dt}Q\left[v(t)\right]$, respectively, where c is assumed to take into account the initial conditions. Thus,

$$e(t) + c(t) = v(t) + \int_0^t z(t-\tau)\frac{d}{d\tau}Q[v(\tau)]d\tau, \quad t \geq 0. \tag{2.1}$$

We seek a solution to (2.1) such that η defined by $\eta(t) = Q[v(t)],\ t \geq 0$ is absolutely continuous on every interval $[0,t] \subset \mathbb{R}$. This ensures that $\dfrac{d}{dt}Q\left[v(t)\right]$ exists a.e. and that charge is conserved in the varactor in the sense that $Q[v(t_b)] = \displaystyle\int_{t_a}^{t_b} i(t)\,dt + Q[v(t_a)]$. See [31, page 116].

We furthermore require that both e and c be absolutely continuous. In practical applications this is not a severe constraint as being differentiable with a continuous derivative is sufficient for a function to be absolutely continuous. (See [31, page 116].) We also assume that e and c are bounded on $[0,\infty)$ and that $\lim_{t\to\infty} c(t) = 0$.

With these assumptions it follows that (2.1) has a unique absolutely continuous on every interval $[0,t]$ solution v defined on the interval $[0,\infty)$, and that integration by parts leading to

$$e(t) + c(t) \quad = \quad v(t) + z(0)Q[v(t)] - z(t)Q[v(0)] +$$

$$\int_0^t u(t-\tau)Q[v(\tau)]d\tau, \quad t \geq 0 \tag{2.2}$$

is justified, where $u(t) = \dfrac{d}{dt}z(t)$.[4]

We will use the fact that it follows from our assumptions that $\lim\limits_{t\to\infty} z(t) = 0$ and that $z(0) \geq 0$. To see that these statements are correct, observe that $z(t) = z(0) + \int_0^t u(\tau)\,d\tau$ for $t \geq 0$, showing that z approaches a limit as $t \to \infty$ (because u is integrable). This limit must be zero, because otherwise it would not be true that z is integrable. Observe also that the Laplace transform U of u, which satisfies $U(s) = sZ(s) - z(0)$ for $\mathrm{Re}\,(s) \geq 0$, also satisfies $U(\sigma) \to 0$ as $\sigma \to \infty$ (in which, as usual, σ is real).[5] This shows that $\lim_{\sigma\to\infty} \sigma Z(\sigma)$ exists and equals $z(0)$. Since Z is a positive real function, we have $z(0) \geq 0$.

Define y by

$$y(t) = v(t) + z(0)Q[v(t)], \ t \geq 0.$$

Since $\alpha > 0$ and $z(0) \geq 0$, $[I_{\mathbb{R}} + z(0)Q]^{-1}$ exists where $I_{\mathbb{R}}$ is the identity on $\mathbb{R}$. Setting $\psi = Q[I_{\mathbb{R}} + z(0)Q]^{-1}$, (2.2) becomes

$$h(t) = y(t) + \int_0^t u(t-\tau)\psi[y(\tau)]d\tau, \quad t \geq 0 \tag{2.3}$$

where $h(t)$ denotes $e(t) + c(t) + z(t)Q[v(0)]$.

Note that, due to the constraints on Q, we have $\psi(0) = 0$ and

$$\frac{\alpha}{1+z(0)\alpha} \leq \frac{\psi(x_2) - \psi(x_1)}{x_2 - x_1} \leq \frac{\beta}{1+z(0)\beta}$$

for any $x_1 \neq x_2$.[6] If Z satisfies the circle criterion for varactor circuits, then the locus of $j\omega Z(j\omega)$ avoids the disk with diameter $(\alpha^{-1} - \beta^{-1})$ centered on the real axis of the complex plane at $\left(-\frac{1}{2}(\alpha^{-1} + \beta^{-1}), 0\right)$. Since $U(s) = sZ(s) - z(0)$, this implies that $U(j\omega)$ always falls outside the disk with diameter $(\alpha^{-1} - \beta^{-1})$ centered on the real axis at $\left(-\frac{1}{2}(\alpha^{-1} + \beta^{-1}) - z(0), 0\right)$ in the complex plane.

[4] See Lemma 10 for details.

[5] For a proof of this well known fact see Lemma 12.

[6] For a proof of these claims see Lemma 9.

By our assumptions the imaginary part of $j\omega Z(j\omega)$ is nonnegative for ω nonnegative, and thus for such ω the only crossing of the real axis can occur at the point $0 + j0$ when $\omega = 0$ and at $z(0) + j0$ when "$\omega \to \infty$". No crossings can thus occur to the left of the critical disk so that the critical disk cannot be encircled by the locus of $j\omega Z(j\omega)$ for $-\infty < \omega < \infty$, and similarly for the locus of $U(j\omega)$ for $-\infty < \omega < \infty$ and the critical disk shifted to the left by the amount $z(0)$. We thus see that if Z satisfies the condition of the circle criterion for varactor circuits, then U satisfies the circle criterion as described in [15] with α there equal to $\alpha[1 + z(0)\alpha]^{-1}$ here and similarly β there equal to $\beta[1 + z(0)\beta]^{-1}$ here.

The claims about the p-stability of the varactor circuit now follow from (2.3) and Theorem 4 and Corollary 3(a) of [15] which are described in Section C.2.

Chapter 3

Calculating the Spectral Coefficients of the Response of Nonlinear Systems to Asymptotically Almost Periodic Inputs

In communication systems Asymptotically Almost Periodic Inputs often describe the system input or a modified input that takes into account initial conditions.

The determination of the spectral coefficients (i.e., the Fourier series coefficients) of the corresponding output of such systems is thus important in the context of evaluating e.g., intermodulation distortion.

Here, for a large family of systems, we give an analytical basis for evaluating the spectral coefficients. This involves a convergent iterative process and certain bounds on the errors incurred in truncating the process. An example is given in

Section 3.3.

The material in this chapter was originally published in [12], [19] and [18].

3.1 Setting and Assumptions

Many systems of practical interest are described by integral equations of the form

$$u(t) = y(t) + \int_0^t k(t-\tau)\psi[y(\tau)]d\tau, \quad t \geq 0 \tag{3.1}$$

where t denotes time, u is the input (or a modified input that takes into account initial conditions), and y is the output. We are interested in the case where $u = u_1 + u_2$ where u_1 is the restriction to $[0, \infty)$ of an AP function g and u_2 takes into account the initial conditions.

In connection with questions concerning the long-time response of systems governed by (3.1), one is often not interested in transients and it is natural to consider the integral equation

$$g(t) = f(t) + \int_{-\infty}^t k(t-\tau)\psi[f(\tau)]d\tau, \quad t \in \mathbb{R}. \tag{3.2}$$

Assume that A.1. (see page 9) is satisfied.

We define the Fourier transform K of k, by

$$K(\omega) = \int_{-\infty}^{\infty} k(t)\exp(-j\omega t)dt, \quad \omega \in \mathbb{R}.$$

It follows from [28, p. 42] that for every u in the set $\mathcal{B}_0$ of real-valued measurable functions defined on the half-line $t \geq 0$, and bounded on bounded intervals, there is in $\mathcal{B}_0$ a unique y that satisfies (3.1). (See Corollary 1.)

3.2 Theorems

Our first result, Theorem 2 below, establishes an important connection between (3.1) and (3.2).

Theorem 2 Let the conditions indicated be met, and let $g \in$ AP. Then

(a) there is a unique $f \in$ AP such that

$$g(t) = f(t) + \int_{-\infty}^{t} k(t-\tau)\psi[f(\tau)]d\tau, \quad t \in \mathbb{R} \tag{3.3}$$

and

(b) with u_1 the restriction to $[0,\infty)$ of g, and y the solution of

$$u_1(t) + u_2(t) = y(t) + \int_{0}^{t} k(t-\tau)\psi[y(\tau)]d\tau, \quad t \geq 0 \tag{3.4}$$

we have

$$\lim_{t\to\infty} |y(t) - f(t)| = 0.$$

Proof: Let G be the map from $u \in L_\infty(0,\infty)$ to y given by (3.1) [which is (3.4) with u_1+u_2 replaced with u] . It follows from material in [17] that under our assumptions G has approximately finite memory as defined in [16]. By [15, Corollary 3(a)], G is a mapping from $L_\infty(0,\infty)$ into itself that is uniformly continuous. From the iterative construction of the solution of (3.4) (see [28] and Corollary 1) it also follows that G is time invariant and causal [16, p. 554]. We can thus use [16, Theorem 9] from which it follows that if $u = u_1 + u_2$ where u_1 is the restriction to $[0,\infty)$ of an AP function [recall that u_2 satisfies Condition (iii) of A.1], then $Gu = y_1 + y_2$ where y_1 is the restriction to $[0,\infty)$ of an AP function f_1, f_1 does not depend on u_2, and $\lim_{t\to\infty} y_2(t) = 0$. We also note that since both Gu and f_1 are bounded [the former since $Gu \in L_\infty(0,\infty)$ and the latter since AP functions are bounded], so is y_2.

Keeping in mind the observations above, let $g \in$ AP be given. Let $u = g_1+u_2$ in which g_1 is the restriction to $[0,\infty)$ of g. Then we have $Gu = y_1+y_2$ where y_1 is the restriction to $[0,\infty)$ of an AP function z, y_1 does not depend on u_2, $y_2 \in L_\infty(0,\infty)$ and $\lim_{t\to\infty} y_2(t) = 0$.

Define w by

$$w(t) = z(t) + \int_{-\infty}^{t} k(t-\tau)\psi[z(\tau)]d\tau, \quad t \in \mathbb{R}$$

By Lemma 1 (in Section 3.5) $w \in$ AP.

We have both

$$w(t) = z(t) + \int_{0}^{t} k(t-\tau)\psi[z(\tau)]d\tau + \int_{-\infty}^{0} k(t-\tau)\psi[z(\tau)]d\tau, \quad t \geq 0$$

as well as

$$g(t) + u_2(t) = z(t) + y_2(t) + \int_{0}^{t} k(t-\tau)\psi[z(\tau) + y_2(\tau)]d\tau, \quad t \geq 0.$$

Thus for $t \geq 0$,

$$|w(t) - g(t)| \leq |u_2(t)| + |y_2(t)| + \int_{0}^{t} |k(t-\tau)| \ |\psi[z(\tau)] - \psi[z(\tau) + y_2(\tau)]|d\tau$$

$$+ \int_{-\infty}^{0} |k(t-\tau)| \ |\psi[z(\tau)]|d\tau$$

$$\leq |u_2(t)| + |y_2(t)| + \beta \int_{0}^{t} |k(t-\tau)| \ |y_2(\tau)|d\tau + \beta \sup_{t} |z(t)| \int_{t}^{\infty} |k(\tau)|d\tau.$$

Since both integrals on the extreme right side approach zero as $t \to \infty$ [1], we see that

$$\lim_{t\to\infty} |w(t) - g(t)| = 0,$$

and since $w - g \in$ AP we have $w = g$ (see Lemma 3 in Section 3.5). Thus (3.3) is met with $f = z$. This shows the existence of an AP solution of (3.3) and it establishes (b), assuming that the solution is unique.

To see that the solution is unique, suppose that (3.3) has a solution $x \in$ AP different from z. Then

$$g(t) = x(t) + \int_{0}^{t} k(t-\tau)\psi[x(\tau)]d\tau + \int_{-\infty}^{0} k(t-\tau)\psi[x(\tau)]d\tau, \quad t \in \mathbb{R}_+.$$

[1] The first integral approaches zero because $k \in L_1(0,\infty)$ and $y_2 \in L_\infty(0,\infty)$ with $\lim_{t\to\infty} y_2(t) = 0$. See Lemma 2 in Section 3.5.

Since (by the boundedness of x and the integrability of k) the second integral $\to 0$ as $t \to \infty$, we have a contradiction to the fact that y_1 does not depend on u_2. This completes the proof.

Our next theorem leads directly to an algorithm for numerically evaluating the spectral coefficients (i.e., Fourier coefficients) of f, where f is the AP solution of (3.3) corresponding to a given $g \in$ AP. Before proceeding to the theorem we give an indication of how the theorem can be used: In accordance with the theorem, we generate a sequence $\{f_n\}_{n=0}^{\infty}$ of AP functions that approaches f in the B-norm. By the Parseval-like equality

$$\|f - f_n\|_B^2 = \sum_{k=1}^{\infty} |A_k^{f_n - f}|^2.$$

From the construction of the f_n it follows that $\bar{\Lambda}_{f_n} \subset \bar{\Lambda}_g$. We also have $\bar{\Lambda}_f \subset \bar{\Lambda}_g$ [16, Theorem 9]. With $\bar{\Lambda}_g = \{\omega_1, \omega_2, \cdots\}$ we use $A_k^{f_n}$ and A_k^f, respectively, to denote the Fourier coefficients of f_n and f corresponding to ω_k. Thus

$$\|f - f_n\|_B^2 = \sum_{k=1}^{\infty} |A_k^{f_n - f}|^2 = \sum_{k=1}^{\infty} |A_k^{f_n} - A_k^f|^2.$$

The theorem provides error bounds. If, for example, we have the bound $\|f - f_n\|_B < 10^{-3}$ and $|A_k^{f_n}| = 0.1$, then we know that $0.099 \le |A_k^f| \le 0.101$.

In our theorem, $\mathcal{B}$ stands for the space of $\mathbb{R}$-valued bounded continuous functions on $\mathbb{R}$, I denotes the identity operator on $\mathcal{B}$, and $\Psi : \mathcal{B} \to \mathcal{B}$ and $L : \mathcal{B} \to \mathcal{B}$ are defined by

$$(\Psi x)(t) = \psi[x(t)], \quad t \in \mathbb{R}$$

and

$$(Lx)(t) = \int_{-\infty}^{t} k(t - \tau) x(\tau) d\tau, \quad t \in \mathbb{R}.$$

Recall that c_0 denotes $\frac{1}{2}(\beta + \alpha)$,

$$r = \frac{1}{2}(\beta - \alpha) \sup_{\omega} \left| \frac{K(\omega)}{1 + c_0 K(\omega)} \right|$$

and that $r < 1$ if A.1 is satisfied.

Theorem 3 Under the conditions described, $(I + c_0 L)$ is an invertible map of $\mathcal{B}$ onto itself, and for any $g \in$ AP and any $f_0 \in$ AP satisfying $\bar{\Lambda}_{f_0} \subset \bar{\Lambda}_g$ the sequence $\{f_n\}_{n=0}^{\infty}$ given by

$$f_{n+1} = (I + c_0 L)^{-1} g - (I + c_0 L)^{-1} L(\Psi - c_0 I) f_n, \quad n \geq 0 \tag{3.5}$$

belongs to AP and satisfies

$$\|f - f_n\|_B \leq \frac{r^n}{1 - r} \|f_1 - f_0\|_B$$

as well as $\bar{\Lambda}_{f_n} \subset \bar{\Lambda}_g$ for $n \geq 0$, where f is the associate of g via (3.3).

Proof: Since $k \in L_1(0, \infty)$ and $K(\omega)$ satisfies the circle criterion, the point $-c_0^{-1}$ is contained in the critical disk. It follows from [13, Theorem 1] that $(I + c_0 L)$ has a bounded inverse as a function from $\mathcal{B}$ into itself and that there exists an $h \in L_1(-\infty, \infty)$, with Fourier transform $-c_0 K(1 + c_0 K)^{-1}$, such that

$$(I + c_0 L)^{-1} x(t) = x(t) + \int_{-\infty}^{\infty} h(t - \tau) x(\tau) d\tau \tag{3.6}$$

for $x \in \mathcal{B}$. From this representation and Lemma 1 (in Section 3.5), together with the fact that AP is a linear space over $\mathbb{R}$, we see that $(I + c_0 L)^{-1}$ maps AP into itself with $\bar{\Lambda}_{(I + c_0 L)^{-1} f} \subset \bar{\Lambda}_f$.

Using

$$g = f + L\Psi f,$$

as well as the fact that $(I + c_0 L)^{-1}$ exists, and following [14], we have

$$f = (I + c_0 L)^{-1} g - (I + c_0 L)^{-1} L(\Psi - c_0 I) f.$$

The map $(\Psi - c_0 I)$ is clearly continuous and time invariant and thus maps $\mathcal{G} \stackrel{def}{=} \{f \in AP : \bar{\Lambda}_f \subset \bar{\Lambda}_g\}$ into itself [16, Theorem 8]. It is also easy to check that $\|\Psi f - c_0 f\|_B \leq 0.5(\beta - \alpha)\|f\|_B$.

By our comments concerning (3.6) it follows[2] that for $x \in \mathcal{B}$,

$$(I + c_0 L)^{-1}(Lx)(t) = (Lx)(t) + \int_{-\infty}^{\infty} h(t-\tau)(Lx)(\tau)d\tau$$

$$= \int_{-\infty}^{\infty} k(t-\tau)x(\tau)d\tau + \int_{-\infty}^{\infty} h(t-\tau)\int_{-\infty}^{\infty} k(\tau - s)x(s)ds\ d\tau$$

$$= \int_{-\infty}^{\infty} (k + h * k)(t-\tau)x(\tau)d\tau$$

(where $*$ denotes convolution). We note that since $(k + h * k) \in L_1(-\infty, \infty)$, by Lemma 1, $(I + c_0 L)^{-1}L$ maps $\mathcal{G}$ into itself. Also, the Fourier transform of $k + h * k$ is

$$K + K\frac{-c_0 K}{1 + c_0 K} = \frac{K}{1 + c_0 K}\ .$$

Finally consider the map H defined by

$$Hx = (I + c_0 L)^{-1} g - (I + c_0 L)^{-1} L(\Psi - c_0 I)x.$$

From our observations it is clear that H maps $\mathcal{G}$ into itself. Let $h_2 = k + h * k$, $\Psi_2 = \Psi - c_0 I$, and $\delta = 0.5(\beta - \alpha)$. For $x_a, x_b \in \mathcal{G}$ and with $x_c = \Psi_2 x_a - \Psi_2 x_b$ and

$$x_d(t) = \int_{-\infty}^{\infty} h_2(t-\tau)x_c(\tau)d\tau$$

we have

$$\|Hx_a - Hx_b\|_B^2 = \|x_d\|_B^2 = \sum_{l=1}^{\infty} |A_l^{x_d}|^2$$

where

$$A_l^{x_d} = \lim_{T\to\infty} \frac{1}{2T}\int_{-T}^{T} x_d(t)\exp(-j\omega_l t)dt$$

where, as before, $\bar{\Lambda}_g = \{\omega_1, \omega_2, \cdots\}$. Thus

$$A_l^{x_d} = \lim_{T\to\infty} \frac{1}{2T}\int_{-T}^{T}\left(\int_{-\infty}^{\infty} h_2(t-\tau)x_c(\tau)d\tau\right)\exp(-j\omega_l t)dt. \tag{3.7}$$

[2]In what follows it is assumed that k is extended by 0 on $(-\infty, 0)$ so that it is defined on all of $\mathbb{R}$.

Since

$$\int_{-T}^{T}\left(\int_{-\infty}^{\infty}|h_2(t-\tau)|\cdot|x_c(\tau)|\cdot|\exp(-j\omega_l t)|d\tau\right)dt<\infty,$$

by Fubini's theorem the order of integration in (3.7) can be interchanged.

With the order interchange and a change of variable, we find that

$$A_l^{x_d}=\lim_{T\to\infty}\int_{-\infty}^{\infty}h_2(y)\exp(-j\omega_l y)\left(\frac{1}{2T}\int_{-T}^{T}x_c(t-y)\exp[-j\omega_l(t-y)]dt\right)dy.$$

By the Lebesgue dominated-convergence theorem and the fact that

$$\frac{1}{2T}\int_{-T}^{T}x_c(t-y)\exp[-j\omega_l(t-y)]dt$$

converges uniformly in y to

$$A_l^{x_c}=\lim_{T\to\infty}\frac{1}{2T}\int_{-T}^{T}x_c(t-y)\exp[-j\omega_l(t-y)]dt$$

(see [2, p. 15]) we have $A_l^{x_d}=H_2(\omega_l)A_l^{x_c}$, where H_2 is the Fourier transform of h_2.[3]

Thus

$$|A_l^{x_d}|\le\sup_{-\infty<\omega<\infty}|H_2(\omega)|\cdot|A_l^{x_c}|$$

and so

$$\begin{aligned}\sum_{l=1}^{\infty}|A_l^{x_d}|^2&\le\left(\sup_{-\infty<\omega<\infty}|H_2(\omega)|\right)^2\sum_{l=1}^{\infty}|A_l^{x_c}|^2\\&\le\left(\sup_{-\infty<\omega<\infty}\left|\frac{K(\omega)}{1+c_0K(\omega)}\right|\right)^2\delta^2\ \|x_a-x_b\|_B^2.\end{aligned}$$

Thus

$$\|Hx_a-Hx_b\|_B\le r\|x_a-x_b\|_B$$

and (as mentioned earlier) by our assumptions $r<1$.

Proceeding as in the usual proof of the contraction mapping fixed point theorem, we note that the sequence $\{f_n\}_{n=0}^{\infty}$ described in the statement of the theorem satisfies

$$\|f_n-f_{n+k}\|_B\le\frac{r^n}{1-r}\|f_1-f_0\|_B \tag{3.8}$$

[3]This conclusion starting with (3.7) involves known arguments (see, for example, [5, p. 66]). The details are included above for the reader's convenience.

for any $k \in \mathbb{N}$. In particular,

$$\|f_n - Hf_n\|_B = \|f_n - f_{n+1}\|_B \leq \frac{r^n}{1-r}\|f_1 - f_0\|_B \to 0 \text{ as } n \to \infty. \tag{3.9}$$

By Theorem 2 there exists an $f \in \text{AP}$ that satisfies $Hf = f$. By way of contradiction, suppose that $\{f_n\}_{n=0}^{\infty}$ does not converge to f in the B norm. Then there exists an $\epsilon > 0$ and a subsequence $\{f_{n_k}\}_{k=0}^{\infty}$ for which $\|f_{n_k} - f\|_B > \epsilon$ for all k. For all k,

$$\begin{aligned} \|f_{n_k} - f\|_B &= \|f_{n_k} - Hf_{n_k} + Hf_{n_k} - Hf\|_B \\ &\leq \|f_{n_k} - Hf_{n_k}\|_B + r\|f_{n_k} - f\|_B \end{aligned}$$

and so $(1-r)\|f_{n_k} - f\|_B \leq \|f_{n_k} - Hf_{n_k}\|_B$. Thus $\epsilon(1-r) \leq \|f_{n_k} - Hf_{n_k}\|_B \to 0$ as $k \to 0$ which is a contradiction.

Therefore $\{f_n\}_{n=0}^{\infty}$ converges to f in the B norm, and since for any $m \in \mathbb{N}$

$$\|f_n - f\|_B \leq \|f_n - f_m\|_B + \|f_m - f\|_B$$

we have from (3.8) by letting $m \to \infty$ that

$$\|f_n - f\|_B \leq \frac{r^n}{1-r}\|f_1 - f_0\|_B.$$

This completes the proof.

3.3 Example of an Application

Consider the model of a simple amplifier shown in Figure 3.1, and assume zero initial conditions. With V_{L_0} the Laplace transform of the sum of the voltages of the three sources on the left, let V_L stand for of the Thévenin equivalent voltage $1/(1 + R_2C_4s)V_{L_0}$ associated with C_4 in parallel with the series combination of R_2 and the sources, and let Z_1 stand for the corresponding Thévenin impedance $R_2/(1+sC_4R_2)$. Similarly, and referring to C_5 in parallel with the series connection

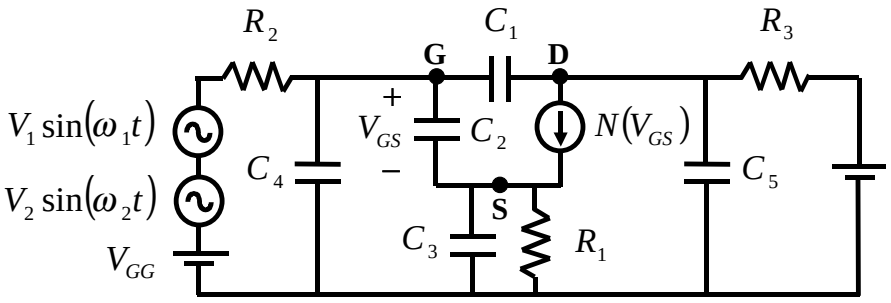

Figure 3.1: Simple amplifier circuit.

of R_3 and the source on the right, let Z_2 and V_R denote the corresponding Thévenin impedance $R_3/(1 + sC_5R_3)$ and Thévenin voltage $1/(1 + R_3C_5s)V_{R_0}$.

With these definitions and with $\mathcal{L}$ denoting the Laplace transform, we can write the circuit equations as

$$\begin{aligned} V_L &= [1 + s(C_1 + C_2)Z_1]V_G - sC_1Z_1V_D - sC_2Z_1V_S \\ V_R &= -s(C_1 + C_2)Z_2V_G + (1 + sC_1Z_2)V_D + [s(C_2 + C_3) + G]Z_2V_S \\ 0 &= -\mathcal{L}[N(v_G - v_S)] + [G + s(C_2 + C_3)]V_S - sC_2V_G \end{aligned}$$

where $G = 1/R_1$, V_G, V_D, and V_S are the transforms of the gate, drain, and source voltages (respectively), and v_G and v_S are the gate and source voltages in the time domain. Letting $y = v_G - v_S$, these relationships lead to

$$y + LNy = L_2v_L + L_3v_R \tag{3.10}$$

in which L, L_2 and L_3 are convolutions and v_L and v_R are the time functions corresponding to V_L and V_R.

In order to apply our results, the right side of (3.10) must be the sum of the restriction to $[0, \infty)$ of an AP function and a bounded function that goes to zero as the argument (time) tends to infinity. This requirement is met if both v_L and v_R are such functions and all poles of the Laplace domain representations of L_2 and L_3 have negative real parts. The requirement that ξ given by $\xi(t) = t^p k(t),\ t \geq 0$

belongs to $L_1(0,\infty)\bigcap L_2(0,\infty)$ for $p \in \{0,1,2\}$ is likewise met if all poles of the Laplace domain representation of L have negative real parts (here k is the impulse response of L).

We assume in this example that $N(v) = C(v-1)^2$ for $v > 1$ and zero otherwise in which C is a positive constant. The incremental slope of N is contained between 0 and ∞, but it is reasonable to assume that the circuit is operated in such a way that the gate-source voltage never exceeds e.g. 10 volts. We thus assume that the slope of N over its domain of interest is contained between 0 and $18C$.

In the case where N (over its domain of interest) is a polynomial, as is the case here, our algorithm for finding y reduces to algebraic manipulation of the sum of complex exponentials. The value of r that determines the rate of convergence of the algorithm can be obtained from a plot of $\delta L_L(j\omega)/[1 + c_0 L_L(j\omega)]$ vs. ω where L_L the Laplace domain representation of L, and $\delta = 0.5(18C - 0) = 9C$.

In this example the method that we use to obtain the approximation to y is to use v_L as the initial estimate and then run the algorithm

$$y_{n+1} = (I + c_0 L)^{-1}(L_2 v_L + L_3 v_R) - (I + c_0 L)^{-1} L(\Psi - c_0 I) y_n, \quad n \geq 0$$

a number of times, each time constraining the order[4] of the intermodulation products. This process of constraining the order of the products keeps the algorithm efficient. We then perform one last iteration in which we keep intermodulation products of all orders. We know that the B-norm of the error is less than

$$\frac{r}{1-r}\|y_{q+1} - y_q\|_B$$

where y_{q+1} is the final (unconstrained) iterate and y_q is the last constrained iterate.

Once we have our estimate y_{q+1} of y, we can obtain an estimate of v_D by applying linear operators to y_{q+1}, v_R and v_L. The dependence of v_d on y (which

[4]In this case where the input consists of two sinusoids of frequencies f_1 and f_2 we define the order of the intermodulation product at frequency $mf_1 + nf_2$ as $|m| + |n|$. To constrain the order we simply discard all terms of order greater than the set limit after applying the operator $(\Psi - c_0 I)$ to y_n.

Table 3.1: Parameter values.

Parameter	Value	Units
$f_1 = \omega_1/(2\pi)$	100	MHz
$f_2 = \omega_2/(2\pi)$	101	MHz
V_1	0.5	V
V_2	0.5	V
$R_1 = 1/G$	10	Ω
R_2	4000	Ω
R_3	4000	Ω

Parameter	Value or formula	Units
C_1	35	fF
C_2	320	fF
C_3	410	fF
C_4	2	fF
C_5	150	fF
$N(\cdot)$	$1.1 \times 10^{-4}(\cdot - 1)^2$	A

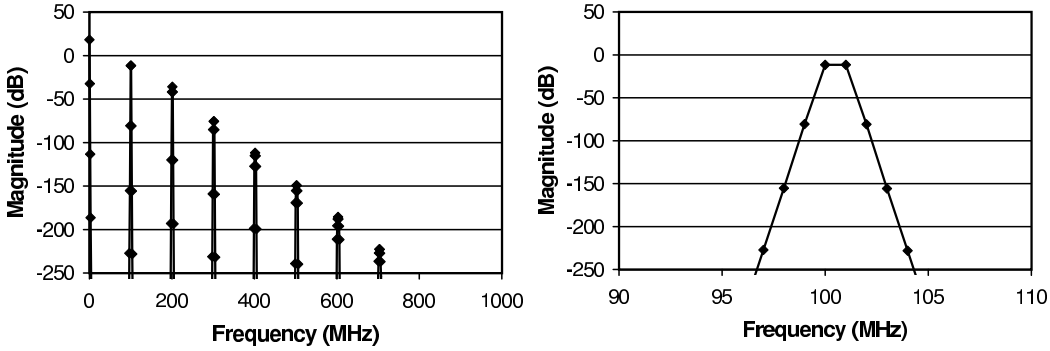

Figure 3.2: Spectral coefficients of the drain voltage.

is approximated by y_{q+1}) leads directly to a bound on the error in estimating the spectral coefficients of v_D.

To give an indication of the numbers involved, consider the model shown in Figure 3.1 with parameter values as in table 3.1. One can verify that all conditions for applying Theorem 3 are met with these values.

Using 20 8-th order iterations before the unconstrained iteration we find that, with y the exact solution to (3.10), $\|y - y_{n+1}\|_B \leq 6.4 \times 10^{-16}$ volt. This means that we can calculate intermodulation products for v_D down to -263 dB volt. (This figure takes into account possible numerical errors.) Errors in this sort of range are at any rate of little practical interest. The entire calculation on a 300 MHz processor takes about 8 seconds. Some of the calculated intermodulation products are shown in Figure 3.2.

3.4 Conclusion

We have given an iterative method for calculating the spectral coefficients of the response of a large family of nonlinear systems to asymptotically almost periodic inputs. We illustrated by way of an example that this method may be used to calculate e.g., intermodulation distortion in amplifier circuits.

An advantage of the method is that it provides error bounds. This may be useful in evaluating the accuracy of methods that ordinarily do not give error bounds, such as harmonic balance or time domain simulations. One weakness is that the theory does not account for all mechanisms by which intermodulation distortion may be generated, such as through nonlinear capacitors (C_5 in Figure 3.1 is normally reasonably nonlinear). However, the algorithm based on the theorems given may be extended to address cases in which the nonlinearity depends on more than one variable. (See Chapter 6.)

3.5 Appendix: Lemmas 1–3

Lemma 1 If $k \in L_1(0,\infty)$[5] and $\eta : \mathbb{R} \to \mathbb{R}$ is Lipschitz continuous, the map $F : L_\infty(-\infty,\infty) \to L_\infty(-\infty,\infty)$ given by

$$(Fx)(t) = \int_{-\infty}^{t} k(t-\tau)\eta[x(\tau)]d\tau, \quad t \in \mathbb{R} \tag{3.11}$$

is time-invariant and Lipschitz continuous, and $f \in \mathrm{AP} \Rightarrow Ff \in \mathrm{AP}$ with $\bar{\Lambda}_{Ff} \subset \bar{\Lambda}_f$.

Proof: It is a simple exercise to check that F is time-invariant and Lipschitz continuous as indicated. Using the time-invariance and continuity, the rest is an application of [16, Theorem 8].

[5]The conclusion remains true if $k \in L_1(-\infty,\infty)$ and F is defined by

$$(Fx)(t) = \int_{-\infty}^{\infty} k(t-\tau)\eta[x(\tau)]\,d\tau, \ t \in \mathbb{R}.$$

Lemma 2 Let $k \in L_1(0,\infty)$ and $x \in L_\infty(0,\infty)$ with $\lim_{t\to\infty} x(t) = 0$. Then

$$\lim_{t\to\infty} \int_0^t k(t-\tau)x(\tau)d\tau = 0.$$

Proof: We assume without loss of generality that

$$\int_0^\infty |k(t)|dt \le 1 \qquad \text{and} \qquad \sup_{t\ge 0} |x(t)| \le 1.$$

Let $\epsilon > 0$ be given. Choose positive constants K and T such that

$$\int_K^\infty |k(t)|dt \le \epsilon/2 \qquad \text{and} \qquad \sup_{t\ge T} |x(t)| \le \epsilon/2.$$

Observe that

$$\left|\int_0^t k(t-\tau)x(\tau)d\tau\right| \le \int_0^T |k(t-\tau)|\cdot|x(\tau)|d\tau + \int_T^t |k(t-\tau)|\cdot|x(\tau)|d\tau$$

$$\le \int_{t-T}^\infty |k(\tau)|d\tau + \int_T^t |k(t-\tau)|\cdot|x(\tau)|d\tau \le \epsilon/2 + \epsilon/2$$

for $t \ge T + K$, which completes the proof.

Lemma 3 If $x, y \in$ AP and $\lim_{t\to\infty}[x(t) - y(t)] = 0$, then $x = y$.

Proof: This follows from the fact $x - y$ is an element of AP (because AP is a linear space). The hypothesis that $\lim_{t\to\infty}[x(t) - y(t)] = 0$ and the assumption that $x(t_0) - y(t_0) \neq 0$ for some t_0 easily leads to a contradiction.

Chapter 4

Harmonic Balance

A common technique for approximating the output spectral coefficients of a nonlinear system driven by an almost periodic input is harmonic balance. The technique is often applied without strict mathematical justification and, as is well known, is often but not always useful. In fact, its results are sometimes grossly misleading. The harmonic balance technique, when it can be carried out, generates a trigonometric polynomial approximation to the actual solution.

In what follows, we consider the equations of a large class of nonlinear circuits driven by asymptotically almost periodic inputs, and give an analytical basis for the use of harmonic balance to find steady-state solutions. More specifically, we show that in a certain setting described in Section 4.1 there is a unique solution to the problem of obtaining a harmonic balance approximation, and that the approximations approach the actual solution as additional spectral components are included.

The material in this chapter was originally published in [20] and [24].

4.1 The Main Result

As in Chapter 3 we are concerned with systems described by integral equations of the form

$$u(t) = y(t) + \int_0^t k(t-\tau)\psi[y(\tau)]d\tau, \quad t \geq 0 \tag{4.1}$$

where t denotes time, u is the input (or a modified input that takes into account initial conditions), and y is the output. We are interested here in the case where $u = u_1 + u_2$ where u_1 is the restriction to $[0, \infty)$ of an AP function g, and u_2 takes into account initial conditions.

We assume that A.1 (see page 9) is satisfied.

Recall that c_0 denotes $\frac{1}{2}(\beta + \alpha)$,

$$r = \frac{1}{2}(\beta - \alpha) \sup_{\omega} \left| \frac{K(j\omega)}{1 + c_0 K(j\omega)} \right|$$

and that it follows from our assumptions that $r < 1$.

Let $\mathcal{B}$ stand for the space of $\mathbb{R}$-valued bounded continuous functions on $\mathbb{R}$, let I denote the identity operator on $\mathcal{B}$, and let $\Psi : \mathcal{B} \to \mathcal{B}$ and $L : \mathcal{B} \to \mathcal{B}$ be defined by

$$(\Psi x)(t) = \psi[x(t)], \quad t \in \mathbb{R}$$

and

$$(Lx)(t) = \int_{-\infty}^t k(t-\tau)x(\tau)d\tau, \quad t \in \mathbb{R}. \tag{4.2}$$

Theorem 2 allows us to pass from functions defined on the half line $[0, \infty)$ to functions defined on $\mathbb{R}$. More specifically, the theorem provides an analytical basis for considering the steady-state response of a large family of systems. (Of course, by the *steady-state response* of a system governed by (4.1), we mean f in (3.3).)

Our main result is Theorem 4, below. Before giving the theorem, we prove two lemmas which are used in the proof of the theorem, and which we feel are of independent interest.

Let Σ be any finite set of real numbers that satisfy $\sigma \in \Sigma \Rightarrow -\sigma \in \Sigma$. Define the projection operator P_Σ that maps AP into the set of trigonometric polynomials by

$$\begin{aligned} \lim_{T\to\infty} \frac{1}{2T} \int_{-T}^{T} (P_\Sigma x) e^{-j\omega_n t}\, dt &= A_n^x,\ \omega_n \in \Sigma \\ &= 0,\ \omega_n \notin \Sigma. \end{aligned}$$

Denote the range of P_Σ by P. Of course P is the family of all real-valued functions that have a representation of the form

$$\sum_{\omega_n \in \Sigma} p_n e^{j\omega_n t}.$$

Lemma 4 Suppose that A.1 holds. Then for any $g \in$ AP there is a unique $f \in$ AP that satisfies

$$P_\Sigma g = f + P_\Sigma L \Psi f. \tag{4.3}$$

Proof: P is a finite dimensional space and is thus complete with respect to $\|\cdot\|_B$. On this space $(I + c_0 L)$ is the operator that multiplies each p_n by $1 + c_0 K(j\omega_n)$. Since $k \in \Phi(\alpha, \beta)$, $K(j\omega) \neq c_0^{-1}$ for all ω, and thus $I + c_0 L$ is an invertible map of P onto itself. Furthermore, since L acts on AP by multiplying the spectral coefficient associated with ω_n by $K(j\omega_n)$[1], L and P_Σ commute.

Thus (4.3) is equivalent to

$$f = (I + c_0 L)^{-1} P_\Sigma g - (I + c_0 L)^{-1} L P_\Sigma (\Psi - c_0 I) f \tag{4.4}$$

for $f \in$ AP. If we define A on P by

$$Af = (I + c_0 L)^{-1} P_\Sigma g - (I + c_0 L)^{-1} L P_\Sigma (\Psi - c_0 I) f$$

then it follows that A maps P into P with

$$\|Af_1 - Af_2\|_B \leq r \|f_1 - f_2\|_B$$

[1] See the proof of Theorem 3.

for any $f_1, f_2 \in P$. Since $r < 1$, the lemma now follows from the contraction mapping fixed point theorem.

Lemma 5 Let L be as defined in (4.2), let A.1 be met, and let c_0 be as described earlier. Then $(I + c_0 P_\Sigma L)$ is an invertible map of B-AP onto itself,

$$\left\| (I + c_0 P_\Sigma L)^{-1} \right\|_B \leq \sup_{\omega \in \mathbb{R}} \left| \frac{1}{1 + c_0 K(j\omega)} \right|$$

and

$$\left\| (I + c_0 P_\Sigma L)^{-1} P_\Sigma L \right\|_B \leq \sup_{\omega \in \mathbb{R}} \left| \frac{K(j\omega)}{1 + c_0 K(j\omega)} \right|.$$

Proof: Let $g \in$ B-AP with Fourier coefficients $\{A_n^g\}$, and let the corresponding set of frequencies be $\{\omega_1, \omega_2, \ldots\}$.

Since $k \in \Phi(\alpha, \beta)$ and $-c_0^{-1}$ is contained in the critical disk C_1,

$$\inf_{\omega \in \mathbb{R}} |1 + c_0 K(j\omega)| > 0.$$

Let

$$a_n = \begin{cases} K(j\omega_n) & \text{if } \omega_n \in \Sigma \\ 0 & \text{otherwise} \end{cases}$$

By the analog of the Riesz-Fisher theorem for B-AP, there is a $f \in$ B-AP with Fourier coefficients given by

$$A_n^f = \frac{A_n^g}{1 + c_0 a_n}.$$

Using the Parseval-like identity on B-AP, we have

$$\| (I + c_0 P_\Sigma L) f - g \|_B = \left(\sum_{n=1}^{\infty} \left| (1 + c_0 a_n) A_n^f - A_n^g \right|^2 \right)^{\frac{1}{2}} = 0,$$

showing that $(I + c_0 P_\Sigma L)$ is onto. Similarly, since $f \in$ B-AP and $\| (I + c_0 P_\Sigma L) f \|_B = 0$ imply that $f = 0$ in B-AP, $(I + c_0 P_\Sigma L)$ is an invertible map of B-AP onto B-AP.

Also,

$$\begin{aligned}\left\|(I+c_0P_\Sigma L)^{-1}\,g\right\|_B &= \left(\sum_{n=1}^{\infty}\left|\frac{A_n^g}{1+c_0a_n}\right|^2\right)^{\frac{1}{2}}\\ &\le \sup_{\omega\in\mathbb{R}}\left|\frac{1}{1+c_0K(j\omega)}\right|\left(\sum_{n=1}^{\infty}|A_n^g|^2\right)^{\frac{1}{2}}\\ &= \sup_{\omega\in\mathbb{R}}\left|\frac{1}{1+c_0K(j\omega)}\right|\|g\|_B\end{aligned}$$

and

$$\begin{aligned}\left\|(I+c_0P_\Sigma L)^{-1}\,P_\Sigma Lg\right\|_B &= \left(\sum_{n=1}^{\infty}\left|\frac{a_nA_n^g}{1+c_0a_n}\right|^2\right)^{\frac{1}{2}}\\ &\le \sup_{\omega\in\mathbb{R}}\left|\frac{K(j\omega)}{1+c_0K(j\omega)}\right|\left(\sum_{k=1}^{\infty}|A_n^g|^2\right)^{\frac{1}{2}}\\ &= \sup_{\omega\in\mathbb{R}}\left|\frac{K(j\omega)}{1+c_0K(j\omega)}\right|\|g\|_B\end{aligned}$$

which completes the proof.

In Theorem 3, which follows and which is our main result, Σ_* denote the family of all sets Σ of the type described.

Theorem 4 Let $g \in$AP, let $\varepsilon > 0$, and let A.1 hold. Then there is a $\Sigma_0 \in \Sigma_*$ such that, for any $\Sigma \in \Sigma_*$ with $\Sigma_0 \subseteq \Sigma$, one has

$$\left\|f-\tilde{f}\right\|_B < \varepsilon$$

where $\tilde{f}$ is the unique trigonometric polynomial that satisfies

$$P_\Sigma g = \tilde{f} + P_\Sigma L\Psi\tilde{f} \tag{4.5}$$

and f is the unique solution in AP of

$$g = f + L\Psi f. \tag{4.6}$$

Proof: The existence and uniqueness of $\tilde{f}$ and f follow from Lemma 4 and Theorem 2 respectively.

Let $\Sigma \in \Sigma_*$. From (4.6) and the linearity of P_Σ,

$$P_\Sigma g = P_\Sigma f + P_\Sigma L \Psi f. \tag{4.7}$$

Using (4.7) and (4.5), we have

$$P_\Sigma f + P_\Sigma L \Psi f = \tilde{f} + P_\Sigma L \Psi \tilde{f}$$

which gives

$$f - (P_\Sigma f + P_\Sigma L \Psi f) = f - \left(\tilde{f} + P_\Sigma L \Psi \tilde{f} \right)$$

and

$$\begin{aligned} (I - P_\Sigma) f &= f - \tilde{f} + P_\Sigma L \left(\Psi f - \Psi \tilde{f} \right) \\ &= (I + c_0 P_\Sigma L)(f - \tilde{f}) + P_\Sigma L \left(\Psi f - \Psi \tilde{f} - c_0 (f - \tilde{f}) \right). \end{aligned}$$

Therefore, by Lemma 5,

$$(f - \tilde{f}) = (I + c_0 P_\Sigma L)^{-1} (I - P_\Sigma) f - (I + c_0 P_\Sigma L)^{-1} P_\Sigma L \left(\Psi f - \Psi \tilde{f} - c_0 (f - \tilde{f}) \right)$$

with the understanding that what is meant by this equation is that the values of the left and right sides agree almost everywhere. Defining

$$h(t) = \begin{cases} \dfrac{\Psi f(t) - \Psi \tilde{f}(t)}{f(t) - \tilde{f}(t)}, & t \in \{x \in \mathbb{R} : f(x) \neq \tilde{f}(x)\} \\ c_0, & t \in \{x \in \mathbb{R} : f(x) = \tilde{f}(x)\} \end{cases}$$

we have

$$\begin{aligned} \left\| \Psi f - \Psi \tilde{f} - c_0 (f - \tilde{f}) \right\|_B &= \left\| (h(\cdot) - c_0)(f(\cdot) - \tilde{f}(\cdot)) \right\|_B \\ &\leq \sup_{t \in \mathbb{R}} |h(t) - c_0| \left\| f - \tilde{f} \right\|_B \\ &\leq \frac{1}{2} (\beta - \alpha) \left\| f - \tilde{f} \right\|_B. \end{aligned}$$

Thus, using Lemma 5,

$$\begin{aligned}
&\left\|(I + c_0 P_\Sigma L)^{-1} P_\Sigma L \left(\Psi f - \Psi \tilde{f} - c_0 (f - \tilde{f})\right)\right\|_B \\
&\quad \leq \frac{1}{2}(\beta - \alpha) \sup_{\omega \in \mathbb{R}} \left| \frac{K(j\omega)}{1 + c_0 K(j\omega)} \right| \left\| f - \tilde{f} \right\|_B \\
&\quad = r \left\| f - \tilde{f} \right\|_B .
\end{aligned}$$

Since $r < 1$, and again using Lemma 5, we have

$$\begin{aligned}
\left\| f - \tilde{f} \right\|_B &\leq \frac{1}{1 - r} \left\| (I + c_0 P_\Sigma L)^{-1} (I - P_\Sigma) f \right\|_B \\
&\leq \frac{1}{1 - r} \sup_{\omega \in \mathbb{R}} \left| \frac{1}{1 + c_0 K(j\omega)} \right| \| (I - P_\Sigma) f \|_B .
\end{aligned}$$

By the Parseval-like identity, given any positive δ there is a $\Sigma_0 \in \Sigma_*$ such that $\| (I - P_\Sigma) f \|_B < \delta$ for any $\Sigma \in \Sigma_*$ with $\Sigma_0 \subseteq \Sigma$. This proves the theorem.

Chapter 5

Experimental results that show that the Circle-Criterion Hypothesis cannot be relaxed significantly

The results in Chapters 2–4 all involve a key circle-criterion hypothesis. (See page 8.) In this chapter we give an example that shows that this hypothesis cannot be relaxed significantly.

The example involves a circuit that exhibits period doubling, and for which the circle criterion is violated – with the locus of $K(j\omega)$ (in which K is the Laplace domain representation of k, the kernel in the integral equation describing the system) not encircling the critical disk and cutting only the upper quarter of the disk. Because the circuit exhibits period doubling, the conclusions of the theorems in Chapters 2–4 do not hold. Our example is based on computation. We know of no earlier examples in which such a small part of the critical disk is cut and the

conclusions of the theorems do not hold.

5.1 Introduction

Much of the theory that forms the basis of the results in this dissertation has been available for almost four decades [15]. The approach in [15] (and in earlier papers by the same writer) is operator theoretic, rather than a differential-equation Lyapunov approach, and the focus is on input-output stability properties of systems. The concepts of extended spaces, truncation operators and causality play a central role, and the main results include the small-gain theorem, the passivity theorem, the circle criterion and several results concerning a time-varying version of (3.1) and L_2 stability, Bounded Input Bounded Output (BIBO) stability, etc. These circle-criterion results include conditions under which bounded or finite-energy changes in inputs produce bounded or finite-energy changes in outputs, respectively, conditions under which inputs whose difference approaches zero as $t \to \infty$ produce outputs whose difference approaches zero as $t \to \infty$, and conditions under which asymptotically periodic inputs yield asymptotically periodic outputs with the same period.

It is an interesting fact that – in the setting described in [15] and under no further assumptions, and over the last thirty-five years – the circle condition has not been replaced with a weaker condition. Nor have there been results showing that the circle condition is actually necessary in some meaningful sense. Popov's work, and the later input-output stability theory multiplier methods, provide some improvement concerning the important but special problem of determining whether a system is asymptotically stable. But the Popov-type results do not provide an improvement of the propositions bearing on the response of systems to inputs that differ as indicated above. That limitation has turned out to be a serious one in practical applications involving systems with inputs – for which one is interested, as in this dissertation, in criteria for the system output to approach a periodic function

or some other special kind of function.

The circle condition is a sufficient condition for certain types of stability. For the purposes of this dissertation, we know of no weaker condition that could have been used in place of that condition. It is known [15, page 882] that the real axis diameter of the critical disk is part of the smallest region that must be avoided by the locus of $K(j\omega)$. But the real axis diameter is only a small part of the critical disk. In this section we give an example of a circuit that exhibits period doubling, and for which the circle criterion is violated – with the locus of $K(j\omega)$ not encircling the critical disk and cutting only the upper quarter of the disk. Because the circuit exhibits period doubling, the conclusions of the theorems stated in Chapters 2–4 do not hold. As will become clear, our example is based on computation. We know of no earlier examples in which such a small part of the critical disk is cut and the conclusions of the theorems do not hold.

5.2 The Example

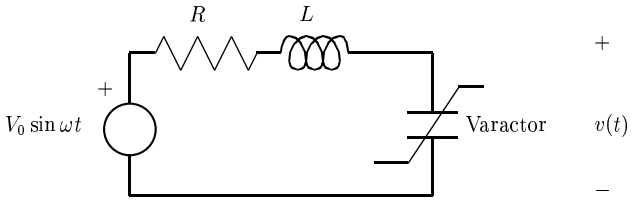

Figure 5.1: Varactor circuit.

Our example concerns the circuit shown in Figure 5.1, with parameters as in Table 5.1. (This was the first context in which we considered this circuit. As it turned out we could use it as an example to illustrate a number of our theorems.) In this circuit the incremental varactor capacitance (i.e., the slope of the plot of charge stored versus voltage) is piecewise linear with one value C_p if the voltage is positive and another, C_m if the voltage is negative. In Chapter 2 it is shown that this circuit

Table 5.1: Parameter values for the varactor circuit of Figure 5.1.

Parameter	Value	Units
ω	1	rad/s
V_0	1	V
L	9.7	H
R	1	Ω
C_p (Varactor incremental capacitance when the varactor voltage is positive.)	0.55	F
C_m (Varactor incremental capacitance when the varactor voltage is negative.)	0.28	F

is described by a Volterra integral equation of the kind considered in Chapters 3–4. In Chapter 2, $j\omega Z(j\omega)$, where Z is the Laplace-domain representation of the Thévenin equivalent source impedance, takes the place of $K(j\omega)$ in Chapters 3–4, in the sense that the circle criterion for varactor circuits is stated in terms of $j\omega Z(j\omega)$.[1] A part C of the varactor capacitance is lumped in with the Thévenin equivalent source impedance to arrange for the inverse Laplace transform of Z to be a legitimate function.

This varactor circuit satisfies the same integral equation as the control system shown in Figure 5.2, where ψ is piecewise linear with slope $C(C_p - C)(C_p)^{-1}$ for positive arguments, and $C(C_m - C)(C_m)^{-1}$ for negative arguments.[2]

To compute the varactor voltage as a function of time, we first assume zero initial conditions and calculate the varactor voltage assuming a linear capacitor of

[1] The Laplace-domain representation of the kernel in the integral equation is $sZ(s) - z(0)$ where z is the time domain representation of the Thévenin equivalent source impedance.

[2] The correspondence between y in the control system and v in the varactor circuit is given by

$$y(t) = \begin{cases} (C_p/C)v(t), & t \in \{x \in [0,\infty) : v(x) \geq 0\} \\ (C_m/C)v(t), & t \in \{x \in [0,\infty) : v(x) < 0\} \end{cases}$$

and $h(t)$ in the control system is equal to the Thévenin equivalent source of the varactor circuit plus some terms that tend to zero as time tends to infinity that result from an integration by parts as well as not-necessarily-zero initial conditions in the varactor circuit.

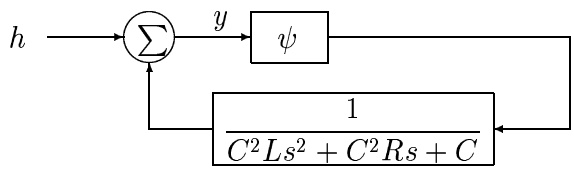

Figure 5.2: Equivalent control system.

value C_p. We solve numerically for the first zero crossing of the varactor voltage. We then calculate the inductor current at the zero crossing and use the zero crossing time and inductor current as initial conditions to calculate the varactor voltage for an incremental capacitance of value C_m. We find the next zero crossing and repeat the process using the corresponding initial inductor current, and so on.

With the chosen circuit parameters, the circuit exhibits period doubling. A plot of the varactor voltage vs. time is shown in Figures 5.3–5.4. The varactor current is shown in Figure 5.5. In order to confirm that the circuit has this property, and that the varactor voltage does not become periodic with the same period as the input after a very long time, we performed a perturbation study: We calculated the varactor voltage for a large number of cycles until the state (i.e., the time of the zero crossing together with the inductor current at the zero crossing) is the same, computationally speaking, from cycle to cycle. We then perturbed the state and calculated the state a number of cycles later (typically 100 cycles later) and have observed that the state returns to the unperturbed state. The result of these calculations is shown in Figure 5.6. We have also carried out numerical integration using SPICE, as well as an independent harmonic balance simulation using 128 harmonics, to further confirm the behavior of the circuit. Comparison with a SPICE simulation using a 0.01 s step size is shown in Figures 5.7–5.8. The difference between the analytical method described here and the SPICE time domain simulation is less than 300 μV. Figures 5.9–5.12 show comparisons with the method described here and a harmonic balance simulation using 128 harmonics. Taken together these

calculations provide compelling evidence that the circuit exhibits period doubling.

A plot of $j\omega Z(j\omega)$ in the vicinity of the critical disk for $\omega \geq 0$ is shown in Figure 5.14[3]. Figure 5.15 shows a plot of $j\omega Z(j\omega)$ for all $\omega \in \mathbb{R}$. To facilitate drawing of this plot the magnitude of all complex numbers are scaled by the function $\ln(1+\cdot)$. We find that the locus of $j\omega Z(j\omega)$ cuts the critical disk for the first time with an imaginary part equal to more than one half the radius of the disk. It never gets closer to the origin of the disk than 60% of the radius of the disk.

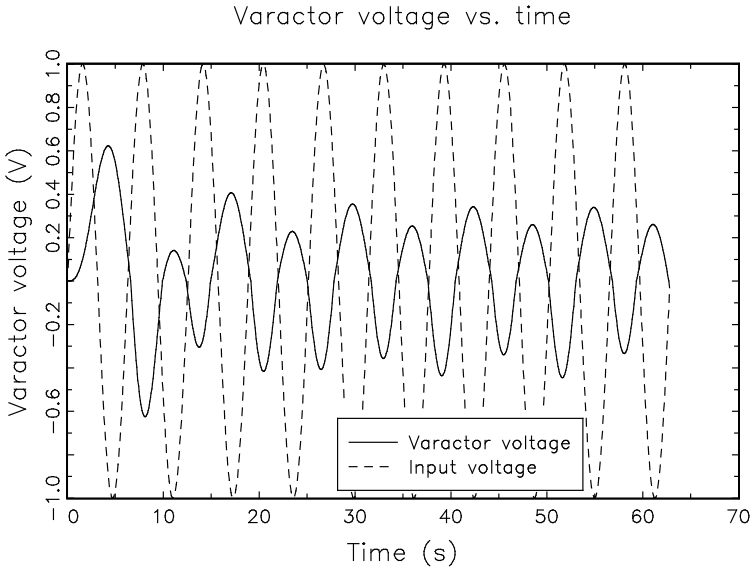

Figure 5.3: Varactor voltage vs. time for small values of time for the varactor circuit of Figure 5.1.

[3]For Figures 5.14 and 5.15 the value of C is 0.01. The optimum (in terms of avoiding the critical disk) choice of C is zero. For a small value of C the effect of C on the locus of $j\omega Z(j\omega)$ is to return to the point $(1/C, 0)$ as $\omega \to \infty$. This is shown in Figure 5.15 for $C = 0.01$ F. The effect of the choice of C on the locus of $j\omega Z(j\omega)$ in the region of the critical disk is shown in Figure 5.13.

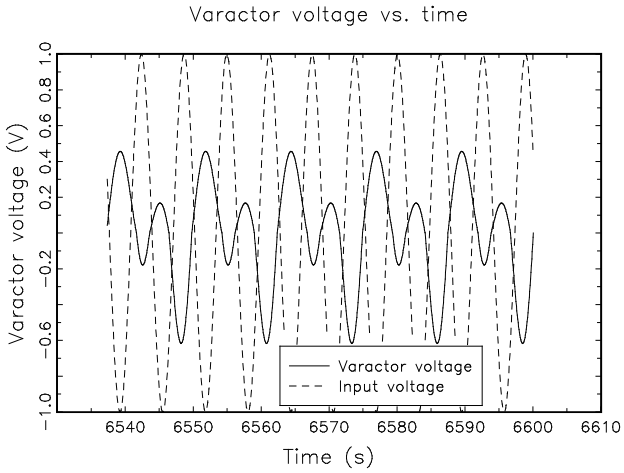

Figure 5.4: Varactor voltage vs. time for large values of time for the varactor circuit of Figure 5.1.

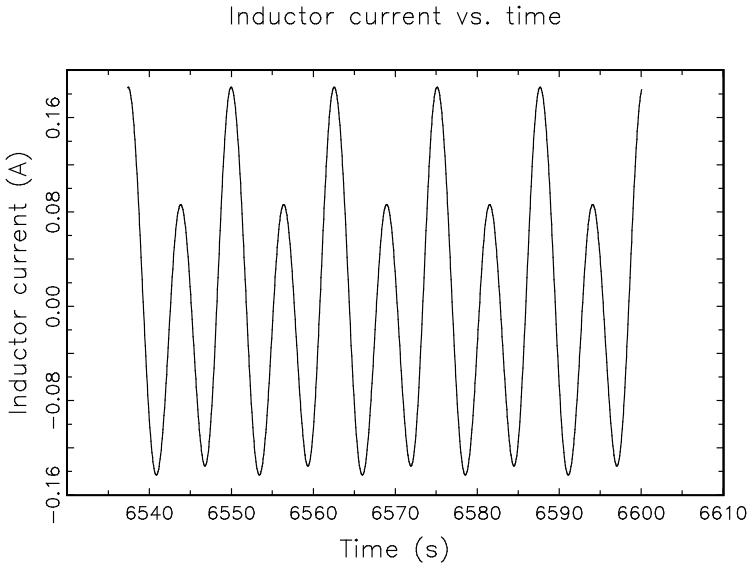

Figure 5.5: Varactor current vs. time for large values of time for the varactor circuit of Figure 5.1.

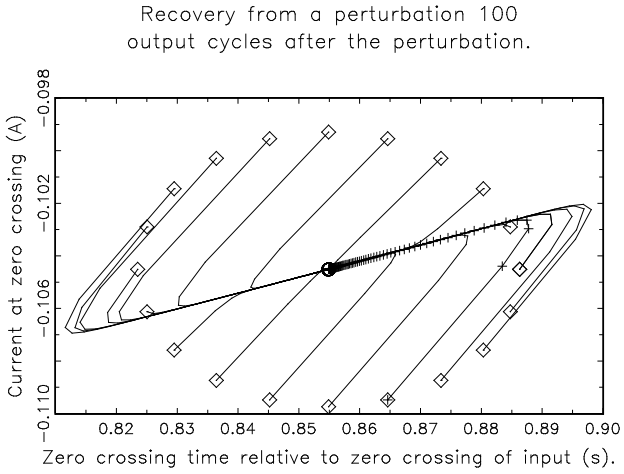

Figure 5.6: Recovery of the zero crossing state from a perturbation after 100 cycles of the output for the varactor circuit of Figure 5.1. Diamonds ($\diamond$) indicate the initial perturbed state and circles ($\circ$) indicate the state 100 output cycles later. Plusses ($+$) indicate the state at zero crossings one output cycle apart along one of the state trajectories.

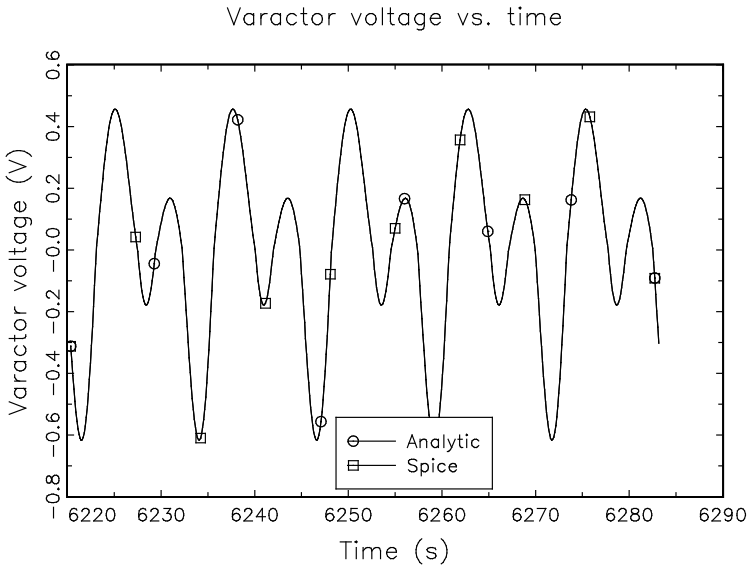

Figure 5.7: A comparison of the varactor voltage calculated for the circuit of Figure 5.1 using the method described in Chapter 5 and a SPICE time domain simulation with a 0.01 s time step.

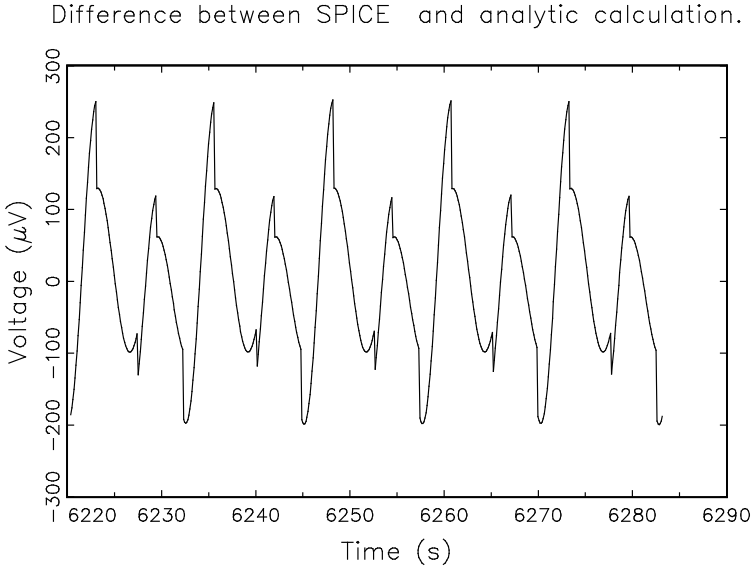

Figure 5.8: The difference between the varactor voltage calculated for the circuit of Figure 5.1 using a SPICE time domain simulation with a 0.01 s time step and the method described in Chapter 5.

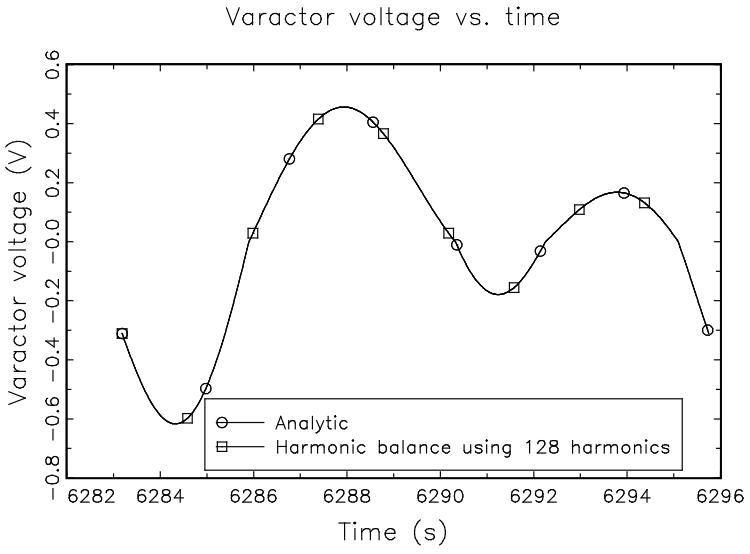

Figure 5.9: A comparison of the varactor voltage calculated for the circuit of Figure 5.1 using the method described in Chapter 5 and a harmonic balance simulation using 128 harmonics. One period of the output is plotted.

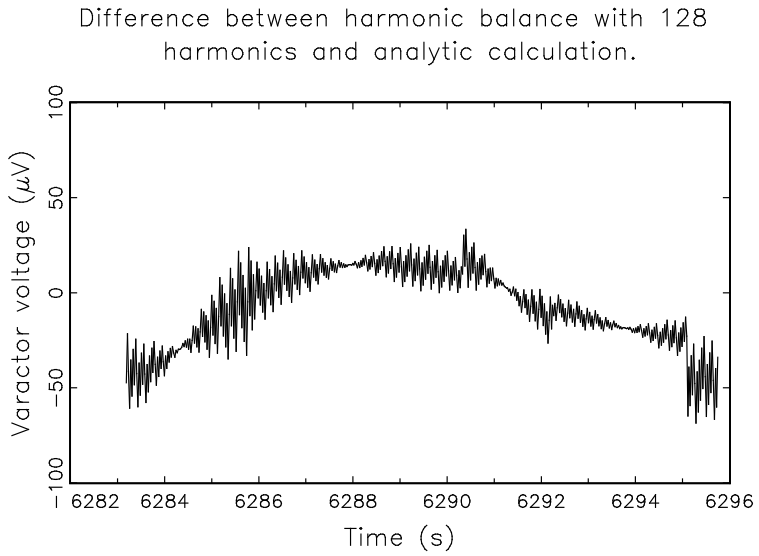

Figure 5.10: The difference between the varactor voltage calculated for the circuit of Figure 5.1 using harmonic balance with 128 harmonics and the method described in Chapter 5. One period of the output is plotted.

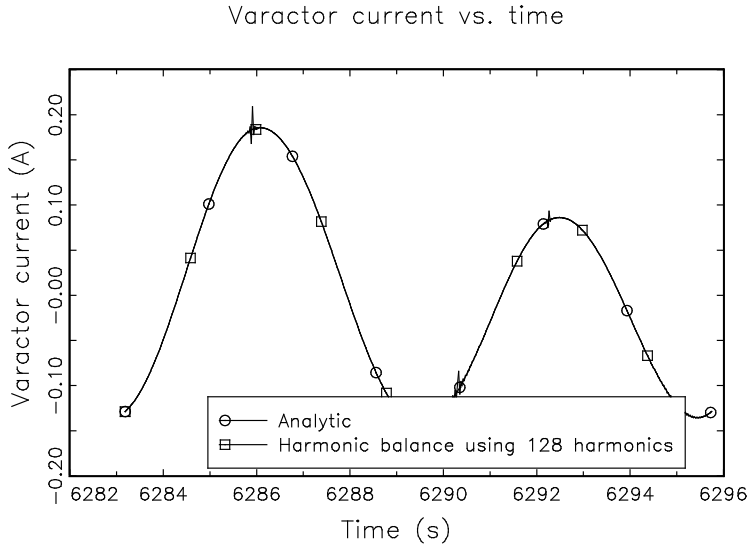

Figure 5.11: A comparison of the varactor current calculated for the circuit of Figure 5.1 using the method described in Chapter 5 and a harmonic balance simulation using 128 harmonics. One period of the output is plotted.

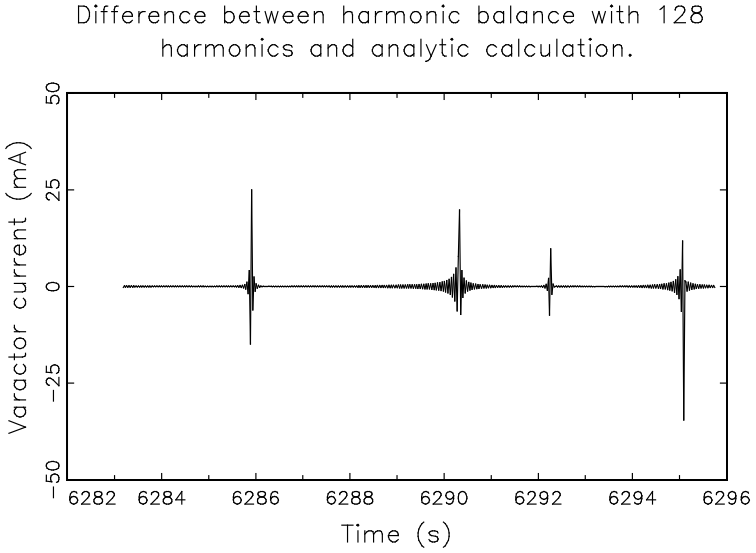

Figure 5.12: The difference between the varactor current calculated for the circuit of Figure 5.1 using harmonic balance with 128 harmonics and the method described in Chapter 5. One period of the output is plotted.

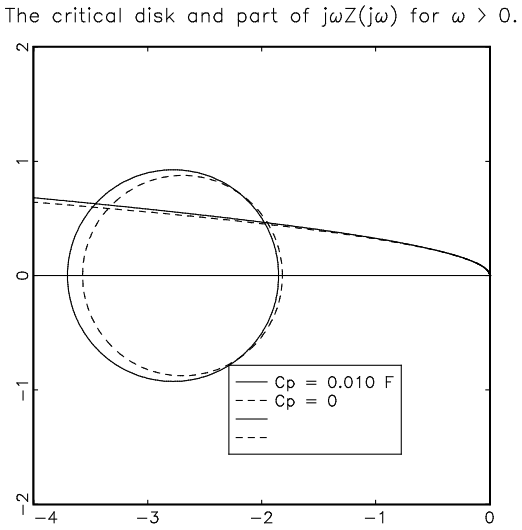

Figure 5.13: The effect of the choice of the part of the varactor capacitance, C, to lump in with the Thévenin impedance on the locus of $j\omega Z(j\omega)$ for the varactor circuit of Figure 5.1.

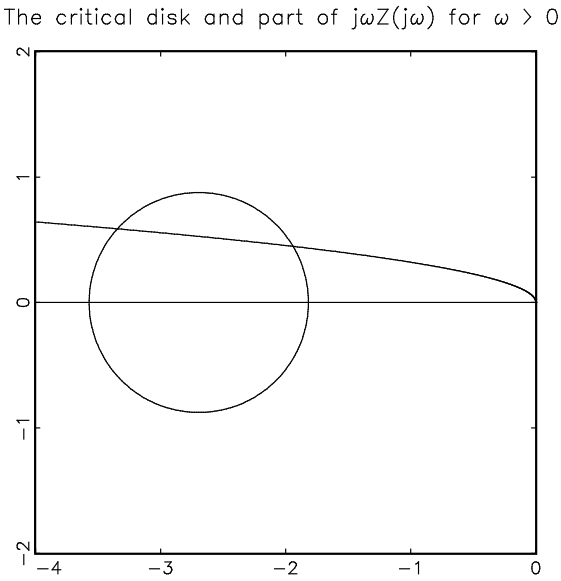

Figure 5.14: Plot of $j\omega Z(j\omega)$ for $\omega > 0$ together with the critical disk for the varactor circuit of Figure 5.1. (Horizontal axis is the real axis and vertical the imaginary.)

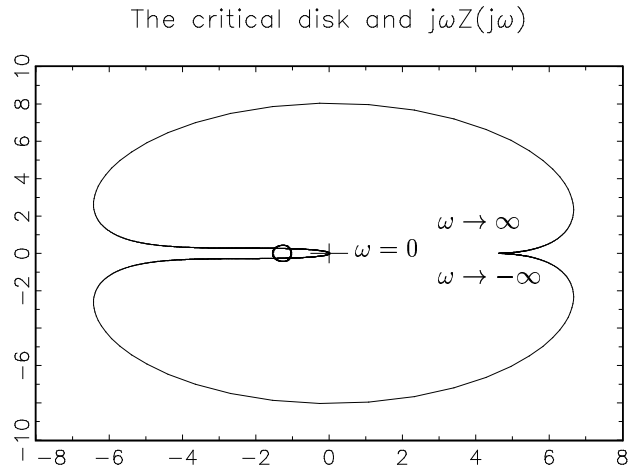

Figure 5.15: Plot of $j\omega Z(j\omega)$ for $-\infty < \omega < \infty$ together with the critical disk for the varactor circuit of Figure 5.1. Magnitudes are scaled by $\ln(1 + \cdot)$ and 0.01 F of the varactor capacitance is lumped in with $Z(j\omega)$. (Horizontal axis is the real axis and vertical the imaginary.)

Chapter 6

Volterra Integral Equations with Non-diagonal Nonlinearities

Nonlinear physical systems can often be described by functional equations of the form

$$g = f + L\Psi f$$

in which g is a known function, f is the solution, L a linear and Ψ a nonlinear operator. Suppose g belongs to $L_{2,N}(0,\infty)$, the set of real square integrable N-vector-valued functions defined on the the interval $[0,\infty)$. To prove that this equation contains a unique solution in $L_{2,N}(0,\infty)$, one can search for a real or complex number x such that $(I + xL)$ is an invertible map of $L_{2,N}(0,\infty)$ onto itself where I is the identity on $L_{2,N}(0,\infty)$.

If such an x exists, the functional equation can be rewritten as

$$f = (I + xL)^{-1}g - (I + xL)^{-1}L(\Psi - xI)f.$$

If there exists a number $c < 1$ such that

$$\left\|(I + xL)^{-1}L\left[(\Psi - xI)f_1 - (\Psi - xI)f_2\right]\right\| \leq c\,\|f_1 - f_2\|$$

for any two elements $f_1,\ f_2 \in L_{2,N}(0,\infty)$, then the contraction mapping fixed point theorem can be used to prove that a unique solution exists in $L_{2,N}(0,\infty)$.

If the operators L and Ψ are causal, then the technique of finding an x as described can be combined with other techniques to prove related results under different settings. In all of these settings the existence of an x such that $(I+xL)$ is an invertible map onto the space of interest (which may not be the space in which the problem is defined as techniques such as truncation are often used in the proofs) and the condition that there exists a number $c<1$ such that either

$$\left\|(I+xL)^{-1}L(\Psi-xI)f_1\right\| \le c\,\|f_1\|$$

or the stronger condition

$$\left\|(I+xL)^{-1}L\left[(\Psi-xI)f_1-(\Psi-xI)f_2\right]\right\| \le c\,\|f_1-f_2\|$$

is satisfied for all f_1 and f_2 in the space of interest, plays a key role. (More can be proved if the latter condition is satisfied.)

If Ψ is diagonal, i.e. the j-th component of Ψf depends only on the j-th component of f, this technique frequently works well. If Ψ is not diagonal, it is often not possible to come up with an x that satisfies the above conditions. Here we report on a generalization of the above technique in that we seek a matrix a and an invertible matrix b such that

$$(I+\mathbb{B}^{-1}L\mathbb{A})$$

is an invertible map onto the space of interest and there exists a number $c<1$ such that either

$$\left\|\left(I+\mathbb{B}^{-1}L\mathbb{A}\right)^{-1}\mathbb{B}^{-1}L\left(\Psi\mathbb{B}-\mathbb{A}\right)f_1\right\| \le c\,\|f_1\|$$

or

$$\left\|\left(I+\mathbb{B}^{-1}L\mathbb{A}\right)^{-1}\mathbb{B}^{-1}L\left[\left(\Psi\mathbb{B}-\mathbb{A}\right)f_1-\left(\Psi\mathbb{B}-\mathbb{A}\right)f_2\right]\right\| \le c\,\|f_1-f_2\|$$

is satisfied for all f_1 and f_2 in the space of interest, where $\mathbb{A}$ and $\mathbb{B}$ are defined by $(\mathbb{A}f)(t) = af(t)$ and $(\mathbb{B}f)(t) = bf(t)$.

To restate and prove the theorems in terms of a and b is rather trivial, but as our examples show, one can obtain a significant improvement in the analysis of practical problems. We give an example that shows the generalization is useful even in the case that Ψ is diagonal.

6.1 Introduction

Many systems of practical interest are described by integral equations of the form

$$u(t) = y(t) + \int_0^t k(t-\tau)\psi[y(\tau),\tau]d\tau, \quad t \geq 0 \tag{6.1}$$

where t denotes time, u is the input (or a modified input that takes into account initial conditions), and y is the output. (See e.g. [15, page 873] in the context of control systems and [21] in connection with circuits.)

In (6.1), u and y are real $N-$vector valued functions of a real variable, k is a real N by N matrix valued function of a real variable, and ψ is a nonlinear N-vector valued function. In many cases u belongs to some interesting class of functions (e.g. the restriction to $[0,\infty)$ of a periodic function plus some bounded continuous function that tends to zero as its argument tends to infinity).

Defining the operators L and Ψ by

$$(Lx)(t) = \int_0^t k(t-\tau)x(\tau)\,d\tau, \ t \geq 0 \tag{6.2}$$

$$(\Psi x)(t) = \psi[x(t),t], \ t \geq 0, \tag{6.3}$$

we can write (6.1) as

$$u = y + L\Psi y. \tag{6.4}$$

It is well known (see e.g. [14, Lemma 5]) that under appropriate conditions one can find a real or complex number x such that $(I + xL)$ is an invertible operator onto

the space of interest. Under these conditions, (6.4) can be written as

$$y = (I + xL)^{-1}u - (I + xL)^{-1}L(\Psi - xI)y. \tag{6.5}$$

If for every f in the space of interest

$$\left\|(I + xL)^{-1}L(\Psi - xI)f\right\| \leq c\,\|f\|$$

for some $c < 1$, then we can conclude that

$$\|y\| \leq \frac{1}{1-c}\left\|(I + xL)^{-1}\right\|\,\|u\|$$

giving a bounded input - bounded output type of result.

If, in addition, there is a $c < 1$ such that for any f_1 and f_2 in the space of interest

$$\left\|(I + xL)^{-1}L\left[(\Psi - xI)f_1 - (\Psi - xI)f_2\right]\right\| \leq c\,\|f_1 - f_2\| \tag{6.6}$$

and the space of interest is complete with respect to the chosen norm, F defined by

$$Fy = (I + xL)^{-1}u + (I + xL)^{-1}L(\Psi - xI)y \tag{6.7}$$

can be used as a contraction mapping. In this case the contraction mapping fixed point theorem [8, page 300] guarantees the existence of a unique solution y of (6.4) in the space of interest. Once a contraction mapping has been obtained in one space, it is sometimes possible to extend the results to other spaces [11].

The case where ψ is diagonal, i.e. the n-th component of $\psi[y(\cdot), \cdot]$ depends only on the n-th component of y, has already been described in many contexts.[1] It is the purpose of this Chapter to give an extension to the case where ψ is not

[1]See e.g. [14], [11], [15]. In [14, page 1595] it is pointed out that $\psi[f(t), t]$ may be replaced by a more general mapping $(Qf)(t)$ as long as there are real constants α and β ($\beta > \alpha$) such that $\|Qh - 0.5(\alpha + \beta)h\| \leq 0.5(\beta - \alpha)\,\|h\|$. In [15, section V] results are also proved for more general mappings, but in each case a scalar quantity times the identity is subtracted from the nonlinear function. In practice, especially when dealing with non-diagonal nonlinearities, it has been found that it is sometimes not possible to satisfy this condition, but that the more general approach described here does work for the same integral equation.

diagonal (i.e. the case where the j-th component of $\psi[y(\cdot),\cdot]$ depends on the k-th component of y with $j \neq k$) so that the large body of results known for the diagonal case may be applied to the non-diagonal case.

The extension to the non-diagonal case is important in applications where the nonlinearity cannot be diagonalized. In addition we show that in some cases involving diagonal nonlinearities the more general technique described here can be used to obtain a contraction mapping when it is not clear whether or not there is an x that satisfies (6.6).

6.2 Results in $L_{2,N}(0,\infty)$

Theorem 5 below is based on results found in [14] and [11].

Theorem 5 Let $k \in \mathbb{K}_{1,N}$, $\Psi : L_{2,N}(0,\infty) \to L_{2,N}(0,\infty)$ be causal and satisfy $\Psi 0 = 0$ and let

$$K(s) = \int_0^\infty k(t)e^{-st}\,dt, \sigma \geq 0.$$

Suppose there are a matrix a and an invertible matrix b and an $M > 0$ such that

(i) $\det\left[1_N + b^{-1}K(s)a\right] \neq 0,\ \sigma \geq 0,$

(ii) $\sup_{\omega\in\mathbb{R}} \Lambda\left\{\left[1_N + b^{-1}K(j\omega)a\right]^{-1} b^{-1}K(j\omega)\right\} M < 1$, and

(iii) for any $f_1,\ f_2 \in L_{2,N}(0,\infty)$,

$$\|(\Psi\mathbb{B} - \mathbb{A})f_1 - (\Psi\mathbb{B} - \mathbb{A})f_2\|_2 \leq M\,\|f_1 - f_2\|_2$$

where $\mathbb{A}$ and $\mathbb{B}$ are defined on $\mathbb{H}_N(0,\infty)$ by $(\mathbb{A}f)(t) = a \times f(t)$ and $(\mathbb{B}f)(t) = b \times f(t)$.

Then,

(i) for each $g \in L_{2,N}(0,\infty)$, there is a unique $f \in L_{2,N}(0,\infty)$ such that

$$g(t) = f(t) + \int_0^t k(t-\tau)(\Psi f)(\tau)d\tau, \quad t \geq 0, \tag{6.8}$$

and furthermore, if $g(t) = 0 \ \forall t \in [0, t_0]$, then $f(t) = 0 \ \forall t \in [0, t_0]$,

(ii) with the mapping F from $L_{2,N}(0,\infty)$ into $L_{2,N}(0,\infty)$ defined by $f = Fg$ where f is the associate of g via (6.8), F is causal,

(iii) there is $\rho > 0$ that depends only on k and Ψ such that

(1) $\|f\|_2 \leq \rho \|g\|_2$

(2) with $g_1, g_2 \in L_{2,N}(0,\infty)$, and f_1 and f_2 the unique solutions in $L_{2,N}(0,\infty)$ of

$$\begin{aligned} g_1(t) &= f_1(t) + \int_0^t k(t-\tau)(\Psi f_1)(\tau)\, d\tau, \ t \geq 0 \\ g_2(t) &= f_2(t) + \int_0^t k(t-\tau)(\Psi f_2)(\tau)\, d\tau, \ t \geq 0, \end{aligned}$$

$\|f_1 - f_2\|_2 \leq \rho \|g_1 - g_2\|_2$.

Proof: Let I be the identity operator on $L_{2,N}(0,\infty)$ and define the operator L on $L_{2,N}(0,\infty)$ by

$$(Lx)(t) = \int_0^t k(t-\tau)x(\tau)\, d\tau, \ t \geq 0.$$

L maps $L_{2,N}(0,\infty)$ into itself [31, page 145], and our assumption that

$$\det\left[1_N + b^{-1}K(s)a\right] \neq 0 \text{ for } \sigma \geq 0$$

ensures [14, Lemma 5] that $\left(I + \mathbb{B}^{-1}L\mathbb{A}\right)$ possesses an inverse on $L_{2,N}(0,\infty)$ and that

$$\begin{aligned} \left\| \left(I + \mathbb{B}^{-1}L\mathbb{A}\right)^{-1} \mathbb{B}^{-1}L \right\|_2 &\leq \sup_{\omega \in \mathbb{R}} \Lambda \left\{ \left[1_N + b^{-1}K(j\omega)a\right]^{-1} b^{-1}K(j\omega) \right\}, \\ \left\| \left(I + \mathbb{B}^{-1}L\mathbb{A}\right)^{-1} \mathbb{B}^{-1} \right\|_2 &\leq \sup_{\omega \in \mathbb{R}} \Lambda \left\{ \left[1_N + b^{-1}K(j\omega)a\right]^{-1} b^{-1} \right\}. \end{aligned}$$

Using this notation we can write (6.8) as

$$g = f + L\Psi f. \tag{6.9}$$

Since $\left(I + \mathbb{B}^{-1}L\mathbb{A}\right)$ is invertible, and letting $h = \mathbb{B}^{-1}f$, we can manipulate (6.9) to get

$$\begin{aligned} g &= f + L\Psi f \\ \Leftrightarrow g &= \mathbb{B}h + L\Psi\mathbb{B}h \\ \Leftrightarrow g &= \mathbb{B}h + L\left(\Psi\mathbb{B}h - \mathbb{A}h\right) + L\mathbb{A}h \\ \Leftrightarrow \mathbb{B}^{-1}g &= \left(I + \mathbb{B}^{-1}L\mathbb{A}\right)h + \mathbb{B}^{-1}L\left(\Psi\mathbb{B} - \mathbb{A}\right)h \\ \Leftrightarrow h &= \left(I + \mathbb{B}^{-1}L\mathbb{A}\right)^{-1}\mathbb{B}^{-1}g \\ &\quad - \left(I + \mathbb{B}^{-1}L\mathbb{A}\right)^{-1}\mathbb{B}^{-1}L\left(\Psi\mathbb{B} - \mathbb{A}\right)h. \end{aligned} \tag{6.10}$$

From the above manipulations we observe that T defined on $L_{2,N}(0,\infty)$ by

$$Th = (I + \mathbb{B}^{-1}L\mathbb{A})^{-1}\mathbb{B}^{-1}g - (I + \mathbb{B}^{-1}L\mathbb{A})^{-1}\mathbb{B}^{-1}L(\Psi\mathbb{B} - \mathbb{A})h$$

is a suitable choice for a contraction operator. We note that T maps $L_{2,N}(0,\infty)$ into itself, and that for any $h_1,\ h_2 \in L_{2,N}(0,\infty)$,

$$\begin{aligned} \|Th_1 - Th_2\|_2 &= \left\| \left(I + \mathbb{B}^{-1}L\mathbb{A}\right)^{-1}\mathbb{B}^{-1}L\left[\left(\Psi\mathbb{B} - \mathbb{A}\right)h_1 - \left(\Psi\mathbb{B} - \mathbb{A}\right)h_2\right] \right\|_2 \\ &\leq \left\| \left(I + \mathbb{B}^{-1}L\mathbb{A}\right)^{-1}\mathbb{B}^{-1}L \right\|_2 \left\| \left(\Psi\mathbb{B} - \mathbb{A}\right)h_1 - \left(\Psi\mathbb{B} - \mathbb{A}\right)h_2 \right\|_2 \\ &\leq \sup_{\omega\in\mathbb{R}} \Lambda\left\{ \left[1_N + b^{-1}K(j\omega)a\right]^{-1} b^{-1}K(j\omega) \right\} M \left\|h_1 - h_2\right\|_2 \\ &= c\left\|h_1 - h_2\right\|_2 \end{aligned}$$

where

$$c = \sup_{\omega\in\mathbb{R}} \Lambda\left\{ \left[1_N + b^{-1}K(j\omega)a\right]^{-1} b^{-1}K(j\omega) \right\} M < 1.$$

It follows from the contraction mapping fixed point theorem [8, page 300] that there is a unique $f \in L_{2,N}(0,\infty)$ that satisfies (6.8) and that

$$f = \lim_{m\to\infty} T^m 0.$$

Since

$$\left(I + \mathbb{B}^{-1} L \mathbb{A}\right)^{-1}$$

is causal by [14, Lemma 4], T is causal and thus the last assertion of (i) follows (from $f = \lim_{m\to\infty} T^m 0$). Also, since $(T^m 0)(t)$ for $t \in (0, \delta)$ depends only on $g(t)$ for $t \in (0, \delta)$ it follows that the map F is causal.

We also find from (6.10) and $(\Psi\mathbb{B} - \mathbb{A})\, 0 \; = 0$ that

$$\begin{aligned}
h &= \left(I + \mathbb{B}^{-1} L \mathbb{A}\right)^{-1} \mathbb{B}^{-1} g - \left(I + \mathbb{B}^{-1} L \mathbb{A}\right)^{-1} \mathbb{B}^{-1} L \left[(\Psi\mathbb{B} - \mathbb{A})\, h - 0\right] \\
\Rightarrow h &= \left(I + \mathbb{B}^{-1} L \mathbb{A}\right)^{-1} \mathbb{B}^{-1} g \\
&\quad - \left(I + \mathbb{B}^{-1} L \mathbb{A}\right)^{-1} \mathbb{B}^{-1} L \left[(\Psi\mathbb{B} - \mathbb{A})\, h - (\Psi\mathbb{B} - \mathbb{A})\, 0\right] \\
\Rightarrow \|h\|_2 &\leq \left\| \left(I + \mathbb{B}^{-1} L \mathbb{A}\right)^{-1} \mathbb{B}^{-1} \right\|_2 \|g\|_2 + c \, \|h - 0\|_2 \\
\Rightarrow \|h\|_2 &\leq \frac{1}{1-c} \left\| \left(I + \mathbb{B}^{-1} L \mathbb{A}\right)^{-1} \mathbb{B}^{-1} \right\|_2 \|g\|_2 .
\end{aligned}$$

Since $f(t) = (\mathbb{B}h)(t) = b \times h(t)$,

$$\begin{aligned}
\|f\|_2^2 &= \int_0^\infty f^*(t) f(t)\, dt \\
&= \int_0^\infty |f(t)|_2^2 \; dt \\
&= \int_0^\infty |b \times h(t)|_2^2 \; dt \\
&\leq \int_0^\infty \Lambda\{b\}^2 \, |h(t)|_2^2 \; dt \\
&= \Lambda\{b\}^2 \, \|h\|_2^2 ,
\end{aligned}$$

so that

$$\begin{aligned}
\|f\|_2 &\leq \Lambda\{b\} \frac{1}{1-c} \left\| \left(I + \mathbb{B}^{-1} L \mathbb{A}\right)^{-1} \mathbb{B}^{-1} \right\|_2 \|g\|_2 \\
&\leq \Lambda\{b\} \frac{1}{1-c} \sup_{\omega\in\mathbb{R}} \Lambda \left\{ \left(1_N + b^{-1} K(j\omega) a\right)^{-1} b^{-1} \right\} \|g\|_2 \\
&= \rho \, \|g\|_2
\end{aligned}$$

where

$$\rho = \Lambda\{b\} \frac{1}{1-c} \sup_{\omega\in\mathbb{R}} \Lambda \left\{ \left(1_N + b^{-1} K(j\omega) a\right)^{-1} b^{-1} \right\}$$

depends only on k and Ψ. (Although a and b appear in the equation, whether an a and b exist that satisfy the conditions for applying the lemma, is dependent only on k and Ψ.)

Similarly, with f_1 and f_2 the unique solutions in $L_{2,N}(0,\infty)$ of

$$\begin{aligned} g_1 &= f_1 + L\Psi f_1 \\ g_2 &= f_1 + L\Psi f_2 \end{aligned}$$

we find with $f_1 = \mathbb{B}h_1,\ f_2 = \mathbb{B}h_2$,

$$\begin{aligned} h_1 - h_2 &= \left(I + \mathbb{B}^{-1}L\mathbb{A}\right)^{-1}\mathbb{B}^{-1}(g_1 - g_2) \\ &\quad - \left(I + \mathbb{B}^{-1}L\mathbb{A}\right)^{-1}\mathbb{B}^{-1}L\left[(\Psi\mathbb{B} - \mathbb{A})\,h_1 - (\Psi\mathbb{B} - \mathbb{A})\,h_2\right] \\ \Rightarrow \|h_1 - h_2\|_2 &\leq \left\|\left(I + \mathbb{B}^{-1}L\mathbb{A}\right)^{-1}\mathbb{B}^{-1}\right\|_2 \|g_1 - g_2\|_2 \\ &\quad + \left\|\left(I + \mathbb{B}^{-1}L\mathbb{A}\right)^{-1}\mathbb{B}^{-1}L\right\|_2 \|[(\Psi\mathbb{B} - \mathbb{A})\,h_1 - (\Psi\mathbb{B} - \mathbb{A})\,h_2]\|_2 \\ &\leq \left\|\left(I + \mathbb{B}^{-1}L\mathbb{A}\right)^{-1}\mathbb{B}^{-1}\right\|_2 \|g_1 - g_2\|_2 + c\,\|h_1 - h_2\|_2 \\ \Rightarrow \|f_1 - f_2\|_2 &\leq \rho\,\|g_1 - g_2\|_2\,. \end{aligned}$$

This proves the theorem.

Making similar changes to the proofs in [14] we also have the following theorem.

Theorem 6 Let

$$g(t) = f(t) + \int_0^t k(t-\tau)\Psi f(\tau)\,d\tau,\ t \geq 0,$$

where $g \in L_{2,N}(0,\infty)$ and $f \in L_{2,N_{loc}}(0,\infty)$, $k \in \mathbb{K}_{1,N}$, $\Psi : \mathbb{H}_N(0,\infty) \to \mathbb{H}_N(0,\infty)$ be causal and satisfy $\Psi 0 = 0$ and let

$$K(s) = \int_0^\infty k(t)e^{-st}\,dt, \sigma \geq 0.$$

Suppose there are a matrix a and an invertible matrix b and an $M > 0$ such that

(i) $\det\left[1_N + b^{-1}K(s)a\right] \neq 0,\ \sigma \geq 0,$

(ii) $\sup_{\omega\in\mathbb{R}} \Lambda\left\{\left[1_N + b^{-1}K(j\omega)a\right]^{-1} b^{-1}K(j\omega)\right\} M < 1$, and

(iii) for any $f \in L_{2,N}(0,\infty)$,

$$\|(\Psi\mathbb{B} - \mathbb{A})f\|_2 \leq M \|f\|_2$$

where $\mathbb{A}$ and $\mathbb{B}$ are defined on $\mathbb{H}_N(0,\infty)$ by $(\mathbb{A}f)(t) = a \times f(t)$ and $(\mathbb{B}f)(t) = b \times f(t)$.

Then $f \in L_{2,N}(0,\infty)$, and there exists a positive constant c that depends only on k and Ψ such that

$$\|f\|_2 \leq c \|g\|_2 .$$

6.3 Extending Results to $L_{\infty,N}(0,\infty)$

For the case where the nonlinearity is diagonal, it is shown in [11] that if in addition to the conditions of Theorem 5, we assume that ξ given by $\xi(t) = t^p k(t),\ t \geq 0$ belongs to $\mathbb{K}_{1,N} \bigcap \mathbb{K}_{2,N}$ for $p \in \{0,1,2\}$ and $g \in L_{\infty,N}(0,\infty)$, then there is a c that depends only on k and Ψ such that

$$\max_j \sup_{t\geq 0} |f_j(t)| \leq c \max_j \sup_{t\geq 0} |g_j(t)|$$

and $\lim_{t\to\infty} f_j(t) = 0$ for $j = 1,2,\ldots,N$ whenever $\lim_{t\to\infty} g_j(t) = 0$ for $j = 1,2,\ldots,N$.

In [15] a simpler proof that $f \in L_{\infty,N}(0,\infty)$ is given under the stronger assumption that there is a $c_1 > 0$ such that $\xi(t) = e^{c_1 t}k(t),\ t \geq 0$ belongs to $\mathbb{K}_{1,N} \bigcap \mathbb{K}_{2,N}$ for $p \in \{0,1,2\}$.

A key idea in the proof given in [11] is to define a function q such that $\psi[f(t),t] = q(t) \times f(t)$. The following lemma is used to generate a q in the case that ψ is not diagonal.

Lemma 6 Let $f,\ g \in \mathbb{H}_N(0,\infty)$. Suppose there is an $M > 0$ such that

$$|f(t)|_2 \leq M\,|g(t)|_2\,,\ t \geq 0.$$

Then there is a matrix valued function q such that

(i) $f(t) = q(t) \times g(t)$, and

(ii) for any $y \in \mathbb{H}_N(0,\infty)$, $q(\cdot) \times y(\cdot) \in \mathbb{H}_N(0,\infty)$ and

$$|q(t) \times y(t)|_2 \leq M\,|y(t)|_2\,,\ t \geq 0.$$

Proof: Let

$$q(t) = \begin{cases} 0,\ g(t) = 0 \\ \dfrac{f(t)}{|g(t)|_2^2} \times g(t)^*,\ g(t) \neq 0. \end{cases}$$

A simple calculation shows that for any $y \in \mathbb{H}_N(0,\infty)$,

$$q(t) \times y(t) = \begin{cases} 0,\ g(t) = 0 \\ \dfrac{1}{|g(t)|_2^2}\,\langle y(t), g(t)\rangle\, f(t),\ g(t) \neq 0. \end{cases}$$

In particular,

$$\begin{aligned} q(t) \times g(t) &= \begin{cases} 0 = f(t),\ g(t) = 0 \\ \dfrac{1}{|g(t)|_2^2}\,\langle g(t), g(t)\rangle\, f(t) = f(t),\ g(t) \neq 0 \end{cases} \\ &= f(t) \end{aligned}$$

and using the Schwarz inequality [8, page 137],

$$\begin{aligned} |q(t) \times y(t)|_2 &= \begin{cases} 0,\ g(t) = 0 \\ \left| \dfrac{1}{|g(t)|_2^2}\,\langle y(t), g(t)\rangle\, f(t) \right|_2,\ g(t) \neq 0 \end{cases} \\ &= \begin{cases} 0,\ g(t) = 0 \\ \dfrac{1}{|g(t)|_2^2}\,|\langle y(t), g(t)\rangle|\,|f(t)|_2\,,\ g(t) \neq 0 \end{cases} \end{aligned}$$

$$
\begin{aligned}
&\leq \begin{cases} 0, \ g(t) = 0 \\ \dfrac{1}{|g(t)|_2^2} \, |y(t)|_2 \, |g(t)|_2 \, |f(t)|_2 \, , \ g(t) \neq 0 \end{cases} \\
&= \begin{cases} 0, \ g(t) = 0 \\ \dfrac{|f(t)|_2}{|g(t)|_2} \, |y(t)|_2 \, , \ g(t) \neq 0 \end{cases} \\
&\leq M \, |y(t)|_2 \, .
\end{aligned}
$$

Since $f, g \in L_{2,N}(0, \infty)$ and the elements of $q(t)$ are

$$
q_{rs} = \begin{cases} 0, \ g(t) = 0, \ r, s \in \{1, 2, \ldots, N\} \\ \dfrac{f_r(t) g_s(t)^*}{|g(t)|_2^2}, \ g(t) \neq 0 \ r, s \in \{1, 2, \ldots, N\}, \end{cases}
$$

it follows that q is measurable and thus for any $y \in \mathbb{H}_N(0, \infty)$, $q(\cdot) y(\cdot)$ is measurable.

This proves the lemma.

To obtain results similar to [11, Theorem 2] and [15, Corollary 3(a)], we need the following two lemmas.

Lemma 7 Let

$$
g(t) = f(t) + \int_0^t k(t - \tau) \psi[f(\tau), \tau] \, d\tau
$$

in which $f, \ g \in L_{2,N_{loc}}(0, \infty)$ and $\psi : \mathbb{R}^N \times [0, \infty) \to \mathbb{R}^N$. If $\psi[h(t), t]$ is a measurable function of t whenever h is measurable and there are a matrix a and an invertible matrix b and an $M > 0$ such that for any $w \in \mathbb{R}^N$,

$$
|\psi[bw, t] - aw|_2 \leq M \, |w|_2 \, , \ t \geq 0
$$

then there is a matrix valued function q such that

$$
g(t) = f(t) + \int_0^t k(t - \tau) q(\tau) f(\tau) \, d\tau
$$

and for any $y \in L_{2,N}(0, \infty)$

$$
[q(\cdot) b - a] \, y(\cdot) \in L_{2,N}(0, \infty)
$$

and

$$\|[q(\cdot)b - a]\, y(\cdot)\|_2 \leq M \|y(\cdot)\|_2 .$$

Proof: With $h(t) = b^{-1}f(t),\ t \geq 0$ we have

$$g(t) = bh(t) + \int_0^t k(t-\tau)\left[\psi[bh(\tau),\tau] - ah(\tau)\right]\, d\tau + \int_0^t k(t-\tau)ah(\tau)\, d\tau.$$

Since there is an $M > 0$ such that

$$|\psi[bh(t),t] - ah(t)|_2 \leq M\, |h(t)|_2 ,\ t \geq 0,$$

by Lemma 6 there is a matrix valued function $\bar{q}$ such that

$$\bar{q}(t)h(t) = \psi[bh(t),t] - ah(t)$$

and for any $y \in L_{2,N}(0,\infty)$,

$$\bar{q}(\cdot)y(\cdot) \in \mathbb{H}_N(0,\infty)$$

and

$$|\bar{q}(t)y(t)|_2 \leq M\, |y(t)|_2 ,\ t \geq 0.$$

From this it follows that $\bar{q}(\cdot)y(\cdot) \in L_{2,N}(0,\infty)$ and

$$\|\bar{q}(\cdot)y(\cdot)\|_2 \leq M \|y\|_2$$

since

$$\begin{aligned} \|\bar{q}(\cdot) \times y(\cdot)\|_2 &= \left(\int_0^\infty |\bar{q}(t) \times y(t)|_2^2\, dt\right)^{0.5} \\ &\leq \left(\int_0^\infty M^2\, |y(t)|_2^2\, dt\right)^{0.5} \\ &= M \|y\|_2 . \end{aligned}$$

We thus have

$$\begin{aligned} g(t) &= bh(t) + \int_0^t k(t-\tau)\left[\psi[bh(\tau),\tau] - ah(\tau)\right]\,d\tau + \int_0^t k(t-\tau)ah(\tau)\,d\tau \\ &= bh(t) + \int_0^t k(t-\tau)\bar{q}(\tau)h(\tau)\,d\tau + \int_0^t k(t-\tau)ah(\tau)\,d\tau \\ &= bh(t) + \int_0^t k(t-\tau)\left[\bar{q}(\tau)h(\tau) + ah(\tau)\right]\,d\tau \\ &= f(t) + \int_0^t k(t-\tau)\left[\bar{q}(\tau)b^{-1} + ab^{-1}\right]f(\tau)\,d\tau \\ &= f(t) + \int_0^t k(t-\tau)q(\tau)f(\tau)\,d\tau \end{aligned}$$

where

$$q(t) = \bar{q}(t)b^{-1} + ab^{-1},\ t \geq 0.$$

Since

$$q(t)b - a = \bar{q}(t)$$

the result follows. This proves the lemma.

Lemma 8 Let

$$\begin{aligned} g_1(t) &= f_1(t) + \int_0^t k(t-\tau)\psi[f_1(\tau),\tau]\,d\tau \\ g_2(t) &= f_2(t) + \int_0^t k(t-\tau)\psi[f_2(\tau),\tau]\,d\tau \end{aligned}$$

in which $f_1,\ g_1,\ f_2,\ g_2 \in L_{2,N_{loc}}(0,\infty)$ and $\psi : \mathbb{R}^N \times [0,\infty) \to \mathbb{R}^N$. If $\psi[h(t),t]$ is a measurable function of t whenever h is measurable and there are a matrix a and an invertible matrix b and an $M > 0$ such that for any $w_1,\ w_2 \in \mathbb{R}^N$,

$$\left|[\psi[bw_1,t] - aw_1] - [\psi[bw_2,t] - aw_2]\right|_2 \leq M\left|w_1 - w_2\right|_2,\ t \geq 0$$

then there is a matrix valued function q such that

$$g_1(t) - g_2(t) = f_1(t) - f_2(t) + \int_0^t k(t-\tau)q(\tau)[f_1(\tau) - f_2(\tau)]\,d\tau$$

and for any $y \in L_{2,N}(0,\infty)$

$$[q(\cdot)b - a]\, y(\cdot) \in L_{2,N}(0,\infty)$$

and

$$\|[q(\cdot)b - a]\, y(\cdot)\|_2 \leq M \|y(\cdot)\|_2 .$$

Proof: With $h_1(t) = b^{-1}f_1(t)$ and $h_2(t) = b^{-1}f_2(t),\ t \geq 0$ we have

$$\begin{aligned} & g_1(t) - g_2(t) \\ = \;& bh_1(t) - bh_2(t) + \int_0^t k(t-\tau)\left[\psi[bh_1(\tau),\tau] - ah_1(\tau) - \psi[bh_2(\tau),\tau] + ah_2(\tau)\right] d\tau \\ & + \int_0^t k(t-\tau)a\left[h_1(\tau) - h_2(\tau)\right] d\tau. \end{aligned}$$

Since there is an $M > 0$ such that

$$|[\psi[bh_1(t),t] - ah_1(t)] - [\psi[bh_2(t),t] - ah_2(t)]|_2 \leq M\,|h_1(t) - h_2(t)|_2\,,\ t \geq 0$$

by Lemma 6 and arguments similar to those in the proof of Lemma 7 there is a matrix valued function $\bar{q}$ such that

$$\bar{q}(t)\left[h_1(t) - h_2(t)\right] = \psi[bh_1(\tau),\tau] - ah_1(\tau) - \psi[bh_2(\tau),\tau] + ah_2(\tau)$$

and for any $y \in L_{2,N}(0,\infty)$,

$$\|\bar{q}(\cdot)y(\cdot)\|_2 \leq M \|y\|_2 .$$

We thus have

$$\begin{aligned} & g_1(t) - g_2(t) \\ = \;& b\left[h_1(\tau) - h_2(\tau)\right] + \int_0^t k(t-\tau)\left[\psi[bh_1(\tau),\tau] - ah_1(\tau) - \psi[bh_2(\tau),\tau] + ah_2(\tau)\right] d\tau \\ & + \int_0^t k(t-\tau)a\left[h_1(\tau) - h_2(\tau)\right] d\tau \end{aligned}$$

$$
\begin{aligned}
&= b\left[h_1(t)-h_2(t)\right]+\int_0^t k(t-\tau)\bar{q}(\tau)\left[h_1(\tau)-h_2(\tau)\right]\,d\tau \\
&\quad +\int_0^t k(t-\tau)a\left[h_1(\tau)-h_2(\tau)\right]\,d\tau \\
&= b\left[h_1(t)-h_2(t)\right]+\int_0^t k(t-\tau)\left[\bar{q}(\tau)+a\right]\left[h_1(t)-h_2(t)\right]\,d\tau \\
&= f_1(t)-f_2(t)+\int_0^t k(t-\tau)\left[\bar{q}(\tau)b^{-1}+ab^{-1}\right]\left[f_1(\tau)-f_2(\tau)\right]\,d\tau \\
&= f_1(t)-f_2(t)+\int_0^t k(t-\tau)q(\tau)\left[f_1(\tau)-f_2(\tau)\right]\,d\tau
\end{aligned}
$$

where

$$q(t)=\bar{q}(t)b^{-1}+ab^{-1},\ t\geq 0.$$

Since

$$q(t)b-a=\bar{q}(t)$$

the result follows. This proves the lemma.

Note that with a q as in Lemma 7 or Lemma 8 and with Ψ defined by $(\Psi f)(t)=q(t)\times f(t)$ we thus have for any $f_1,\ f_2\in L_{2,N}(0,\infty)$ (and $\mathbb{A}$ and $\mathbb{B}$ defined on $\mathbb{H}_N(0,\infty)$ by $(\mathbb{A}f)(t)=a\times f(t)$ and $(\mathbb{B}f)(t)=b\times f(t)$)

$$
\begin{aligned}
&\left\|(\Psi\mathbb{B}-\mathbb{A})f_1-(\Psi\mathbb{B}-\mathbb{A})f_2\right\|_2 \\
&\quad = \left\|(q(\cdot)b-a)\left[f_1(\cdot)-f_2(\cdot)\right]\right\|_2 \\
&\quad \leq M\left\|f_1-f_2\right\|_2.
\end{aligned}
$$

With the aid of Theorem 5 and Lemmas 6–8 and with obvious modifications to the proofs of the lemmas and theorems in [11] we have the following theorems.

Theorem 7 Let ξ given by $\xi(t)=t^pk(t),\ t\geq 0$ belong to $\mathbb{K}_{1,N}\bigcap\mathbb{K}_{2,N}$ for $p\in\{0,1,2\}$. Let

$$g(t)=f(t)+\int_0^t k(t-\tau)\psi[f(\tau),\tau]\,d\tau,\ t\geq 0$$

where $\psi : \mathbb{R}^N \times [0,\infty) \to \mathbb{R}^N$, $g \in L_{\infty,N}(0,\infty)$ and $f \in L_{2,N_{loc}}(0,\infty)$. Let

$$K(s) = \int_0^\infty k(t)e^{-st}\,dt,\ \sigma \geq 0.$$

Suppose that $\psi[h(t),t]$ is a measurable function of t whenever h is measurable and there are a matrix a and an invertible matrix b and an $M > 0$ such that

(i) $\det\left[1_N + b^{-1}K(s)a\right] \neq 0,\ \sigma \geq 0,$

(ii) $\sup\limits_{\omega\in\mathbb{R}} \Lambda\left\{\left[1_N + b^{-1}K(j\omega)a\right]^{-1} b^{-1}K(j\omega)\right\} M < 1$, and

(iii) for any $w \in \mathbb{R}^N$,

$$|\psi[bw,t] - aw|_2 \leq M\,|w|_2\,,\ t \geq 0.$$

Then $f \in L_{\infty,N}(0,\infty)$, there exists a positive constant c which depends only on k and ψ such that

$$\max_{1\leq j\leq N} \sup_{t\geq 0} |f_j(t)| \leq c \max_{1\leq j\leq N} \sup_{t\geq 0} |g_j(t)|\,,$$

and $\lim_{t\to\infty} f_j(t) = 0$ for $j \in \{1,2,\ldots,N\}$ whenever $\lim_{t\to\infty} g_j(t) = 0$ for $j \in \{1,2,\ldots,N\}$.

Theorem 8 Let ξ given by $\xi(t) = t^p k(t),\ t \geq 0$ belong to $\mathbb{K}_{1,N} \bigcap \mathbb{K}_{2,N}$ for $p \in \{0,1,2\}$. Let

$$g_1(t) = f_1(t) + \int_0^t k(t-\tau)\psi[f_1(\tau),\tau]\,d\tau,\ t \geq 0$$
$$g_2(t) = f_2(t) + \int_0^t k(t-\tau)\psi[f_2(\tau),\tau]\,d\tau,\ t \geq 0$$

where $\psi : \mathbb{R}^N \times [0,\infty) \to \mathbb{R}^N$, $g_1,\ g_2,\ f_1,\ f_2 \in L_{2,N_{loc}}(0,\infty)$ and $(g_1 - g_2) \in L_{\infty,N}(0,\infty)$. Let

$$K(s) = \int_0^\infty k(t)e^{-st}\,dt,\ \sigma \geq 0.$$

Suppose that $\psi[0,t]=0,\ t\geq 0$, $\psi[h(t),t]$ is a measurable function of t whenever h is measurable and there are a matrix a and an invertible matrix b and an $M>0$ such that

(i) $\det\left[1_N+b^{-1}K(s)a\right]\neq 0,\ \sigma\geq 0$,

(ii) $\sup\limits_{\omega\in\mathbb{R}}\Lambda\left\{\left[1_N+b^{-1}K(j\omega)a\right]^{-1}b^{-1}K(j\omega)\right\}M<1$, and

(iii) for any $w_1,\ w_2\in\mathbb{R}^N$,

$$|\psi[bw_1,t]-aw_1-\psi[bw_2,t]+aw_2|_2\leq M\,|w_1-w_2|_2\,,\ t\geq 0.$$

Then $(f_1-f_2)\in L_{\infty,N}(0,\infty)$, there exists a positive constant c which depends only on k and ψ such that

$$\max_{1\leq j\leq N}\sup_{t\geq 0}\left|f_{1_j}(t)-f_{2_j}(t)\right|\leq c\max_{1\leq j\leq N}\sup_{t\geq 0}\left|g_{1_j}(t)-g_{2_j}(t)\right|,$$

and $\lim_{t\to\infty}\left[f_{1_j}(t)-f_{2_j}(t)\right]=0$ for $j\in\{1,2,\ldots,N\}$ whenever $\lim_{t\to\infty}\left[g_{1_j}(t)-g_{2_j}(t)\right]=0$ for $j\in\{1,2,\ldots,N\}$.

Under somewhat stronger assumptions it is possible to give a relatively simple proof that $L_{\infty,N}(0,\infty)$ inputs give rise to $L_{\infty,N}(0,\infty)$. The proof is based on [15, p. 880].

Theorem 9 Let

$$g(t)=f(t)+\int_0^t k(t-\tau)\psi[f(\tau),\tau]\,d\tau,\ t\geq 0$$

where $\psi:\mathbb{R}^N\times[0,\infty)\to\mathbb{R}^N$, $g\in L_{\infty,N}(0,\infty)$ and $f\in L_{2,N_{loc}}(0,\infty)$ and let

$$K(s)=\int_0^\infty k(t)e^{-st}\,dt,\sigma\geq 0.$$

Suppose $\psi[h(t),t]$ is a measurable function of t whenever h is measurable and there exist a positive constant c_1 , a matrix a, an invertible matrix b and an $M>0$ such that

(i) $\xi \in \mathbb{K}_{1,N} \bigcap \mathbb{K}_{2,N}$ where ξ is defined by $\xi(t) = e^{c_1 t} k(t),\ t \geq 0$,

(ii) $\det \left[1_N + b^{-1} K(s) a\right] \neq 0,\ \sigma \geq 0$,

(iii) $\sup_{\omega \in \mathbb{R}} \Lambda \left\{ \left[1_N + b^{-1} K(j\omega) a\right]^{-1} b^{-1} K(j\omega) \right\} M < 1$, and

(iv) for any $w \in \mathbb{R}^N$,

$$|\psi[bw, t] - aw|_2 \leq M |w|_2,\ t \geq 0.$$

Then $f \in L_{\infty,N}(0, \infty)$.

Proof: Let $z \in \mathbb{R}^N$. With $w = b^{-1} z$ we have for any $t > 0$

$$\begin{aligned} |\psi[z,t]|_2 &= |\psi[bw,t] - aw + aw|_2 \\ &\leq |\psi[bw,t] - aw|_2 + |aw|_2 \\ &\leq M |w|_2 + |aw|_2 \\ &= M \left|b^{-1} z\right|_2 + \left|a b^{-1} z\right|_2 \\ &\leq M \Lambda \left\{b^{-1}\right\} |z|_2 + \Lambda \{a\} \Lambda \left\{b^{-1}\right\} |z|_2 \\ &= \Lambda \left\{b^{-1}\right\} (M + \Lambda \{a\}) |z|_2 . \end{aligned}$$

Let $y > 0$, $0 < c_2 < c_1$ and

$$d = \int_0^y k(y - \tau) \psi[f(\tau), \tau]\, d\tau.$$

Then for $j \in \{1, 2, \ldots, N\}$,

$$\begin{aligned} |d_j| &= \left| \int_0^y \sum_{l=1}^N k_{j,l}(y - \tau) \psi_l[f(\tau), \tau]\, d\tau \right| \\ &\leq \sum_{l=1}^N \left| \int_0^y k_{j,l}(y - \tau) \psi_l[f(\tau), \tau]\, d\tau \right| \\ &= \sum_{l=1}^N \left| \int_0^y e^{c_2(y-\tau)} k_{j,l}(y - \tau) e^{-c_2(y-\tau)} \psi_l[f(\tau), \tau]\, d\tau \right| \end{aligned}$$

$$
\begin{aligned}
&\leq \sum_{l=1}^{N} \left(\int_0^y \left(e^{c_2(y-\tau)} k_{j,l}(y-\tau) \right)^2 d\tau \right)^{\frac{1}{2}} \left(\int_0^y e^{2c_2\tau} e^{-2c_2 y} \psi_l^2[f(\tau),\tau]\, d\tau \right)^{\frac{1}{2}} \\
&= \sum_{l=1}^{N} \left\| e^{c_2 \cdot} k_{j,l_y} \right\|_{L_2(0,\infty)} e^{-c_2 y} \left\| e^{c_2 \cdot} \psi_{l_y}[f(\cdot),\cdot] \right\|_{L_2(0,\infty)} \\
&\leq \sum_{l=1}^{N} \left\| e^{c_2 \cdot} k_{j,l_y} \right\|_{L_2(0,\infty)} e^{-c_2 y} \left\| e^{c_2 \cdot} \psi_y[f(\cdot),\cdot] \right\|_{L_{2,N}(0,\infty)} \\
&\leq \sum_{l=1}^{N} \left\| e^{c_2 \cdot} k_{j,l_y} \right\|_{L_2(0,\infty)} e^{-c_2 y} \Lambda\left\{b^{-1}\right\} \left(M + \Lambda\{a\}\right) \left\| e^{c_2 \cdot} f_y \right\|_{L_{2,N}(0,\infty)}.
\end{aligned}
$$

Since $c_2 < c_1$ and $e^{c_1 \cdot} k \in \mathbb{K}_{1,N}$,

$$
\begin{aligned}
\left\| e^{c_2 \cdot} k_{j,l_y} \right\|_{L_2(0,\infty)} &\leq \left\| e^{c_2 \cdot} k_{j,l} \right\|_{L_2(0,\infty)} \\
&< \infty
\end{aligned}
$$

and thus

$$
|d_j| \leq c_3 e^{-c_2 y} \left\| e^{c_2 \cdot} f_y \right\|_{L_{2,N}(0,\infty)}
$$

where

$$
c_3 = \sum_{j=1}^{N} \sum_{l=1}^{N} \left\| e^{c_2 \cdot} k_{j,l} \right\|_{L_2(0,\infty)} \Lambda\left\{b^{-1}\right\} \left(M + \Lambda\{a\}\right) < \infty.
$$

Since c_3 does not depend on j,

$$
\max_j |d_j| \leq c_3 e^{-c_2 y} \left\| e^{c_2 \cdot} f_y \right\|_{L_{2,N}(0,\infty)}.
$$

Let $0 < c_4 < c_1$ be such that[2] for any $0 < c_5 < c_4$, with

$$
\tilde{k}(t) = e^{c_5 t} k(t),\ t \geq 0
$$

and

$$
\tilde{K}(s) = \int_0^\infty \tilde{k}(t) e^{-st}\, dt,\ \sigma \geq 0
$$

[2]In the proof of [15, Corollary 2(a)] it is pointed out that the existence of such a c_4 can be proved from the fact that each element of $[K(s) - K(s - c_4)]$ approaches zero uniformly in $\sigma \geq 0$ as $c_4 \to 0+$.

we have

$$\sup_{\omega\in\mathbb{R}} \Lambda\left\{\left[1_N + b^{-1}\tilde{K}(j\omega)a\right]^{-1} b^{-1}\tilde{K}(j\omega)\right\} M < 1.$$

By Lemma 7 there is a matrix-valued function q such that

$$g(t) = f(t) + \int_0^t k(t-\tau)q(\tau)f(\tau)\,d\tau,\ t \geq 0 \tag{6.11}$$

and for any $u \in L_{2,N}(0,\infty)$,

$$[q(\cdot)b - a]\,u(\cdot) \in L_{2,N}(0,\infty)$$

and

$$\|[q(\cdot)b - a]\,u(\cdot)\|_2 \leq M\,\|u\|_2\,.$$

Defining Ψ by $(\Psi u)(t) = q(t)u(t)$, we satisfy the requirements of Theorem 5 and thus we know that the map that associates f with g via (6.11) is causal. Thus, for $y > 0$, if (that there is a unique $\bar{f}$ that satisfies this equation also follows from Theorem 5)

$$g_y(t) = \bar{f}(t) + \int_0^t k(t-\tau)q(\tau)\bar{f}(\tau)\,d\tau,\ t \geq 0,$$

then

$$f(t) = \bar{f}(t),\ t \in [0,y].$$

We have

$$\begin{aligned} g_y(t) &= \bar{f}(t) + \int_0^t k(t-\tau)q(\tau)\bar{f}(\tau)\,d\tau,\ t \geq 0 \\ \Rightarrow e^{c_5 t}g_y(t) &= e^{c_5 t}\bar{f}(t) + \int_0^t e^{c_5(t-\tau)}k(t-\tau)q(\tau)e^{c_5\tau}\bar{f}(\tau)\,d\tau,\ t \geq 0 \\ &= \tilde{f}(t) + \int_0^t \tilde{k}(t-\tau)(\Psi\tilde{f})(\tau)\,d\tau,\ t \geq 0 \end{aligned}$$

where

$$\tilde{f}(t) = e^{c_5 t}\bar{f}(t),\ t \geq 0.$$

By Theorem 5 there is a $\rho > 0$ such that

$$\left\|\tilde{f}\right\|_2 \leq \rho\,\|e^{c_5\cdot}g_y\|_2\,.$$

We can clearly choose $c_2 = c_5 = c_4$ so that we have

$$\begin{aligned}
\max_j |f_j(y)| &\leq \max_j |g_j(y)| + \max_j \left| \int_0^y \sum_{l=1}^N k_{j,l}(y-\tau)\psi_l[f(\tau),\tau]\,d\tau \right| \\
&\leq \max_j |g_j(y)| + c_3 e^{-c_4 y} \|e^{c_4 \cdot} f_y\|_2 \\
&\leq \max_j |g_j(y)| + c_3 e^{-c_4 y} \rho \|e^{c_4 \cdot} g_y\|_2 \\
&\leq \max_j \sup_{t\geq 0} |g_j(t)| + c_3 e^{-c_4 y} \rho \left(\frac{N}{2c_4}\right)^{\frac{1}{2}} e^{c_4 y} \max_j \sup_{t\geq 0} |g_j(t)| \\
&= \left(1 + c_3 \rho \left(\frac{N}{2c_4}\right)^{\frac{1}{2}}\right) \max_j \sup_{t\geq 0} |g_j(t)|
\end{aligned}$$

Since this holds for all $y > 0$, $f \in L_{\infty,N}(0,\infty)$.

6.4 Approximately Finite Memory and Asymptotically Almost Periodic Inputs

In order to obtain results similar to Theorem 2, we can show that under the conditions of Theorem 8, the map G that associates f with g (i.e. $f = Gg$) via

$$g(t) = f(t) + \int_0^t k(t-\tau)\psi[f(\tau)]\,d\tau,\ t \geq 0 \tag{6.12}$$

has approximately finite memory as defined in [16] and show that the map is uniformly continuous on $L_{\infty,N}(0,\infty)$ and is time invariant.

The uniform continuity of the map follows from Theorem 8. We can easily check the time invariance of the map. Let $\lambda > 0$ and

$$g_2(t) = \begin{cases} 0,\ t < \lambda \\ g(t-\lambda),\ t \geq \lambda. \end{cases}$$

Then with

$$g_2(t) = f_2(t) + \int_0^t k(t-\tau)\psi[f_2(\tau)]\,d\tau,\ t \geq 0,$$

we have from Theorem 5 (i) that

$$f_2(t) = 0,\ t < \lambda.$$

Thus

$$\begin{aligned} g_2(t) = g(t-\lambda) &= f_2(t) + \int_0^{\lambda} k(t-\tau)\psi[0]\,d\tau + \int_{\lambda}^{t} k(t-\tau)\psi[f_2(\tau)]\,d\tau,\ t \geq \lambda \\ &= f_2(t) + \int_{\lambda}^{t} k(t-\tau)\psi[f_2(\tau)]\,d\tau,\ t \geq \lambda. \end{aligned}$$

Letting $t - \lambda = y$ and $\tau - \lambda = z$ we have

$$g(y) = f_2(y+\lambda) + \int_0^{y} k(y-z)\psi[f_2(z+\lambda)]\,dz,\ y \geq 0.$$

It follows from Theorem 8 that

$$f_2(y+\lambda) = f(y),\ y \geq 0$$

so that

$$f_2(t) = \begin{cases} 0,\ t < \lambda \\ f(t-\lambda),\ t \geq \lambda. \end{cases}$$

To show that G has approximately finite memory, we can repeat the proof of the theorem in [17] by replacing the matrix $D(\tau)$ there with $q(\tau)$ in accordance with Lemma 8 and using Theorem 5 rather than Lemma 1 of [11] in the proof given there.

Thus, if we satisfy the constraints of Theorem 8, we also satisfy the constraints of [16, Theorem 9] and asymptotically almost periodic inputs (g in (6.12)) produce asymptotically almost periodic outputs (f in (6.12)) with the module of the output a subset of the module of the input.

We also note that apart from the changes to prove that the map G is causal, time invariant, and has approximately finite memory, the proof of Theorem 2 is the same under the conditions of Theorem 8 as under the original conditions of Theorem 2 and we thus also have the conclusions of Theorem 2 if we meet the conditions of Theorem 8.

6.5 Example

Our first example shows that even when the nonlinear function (Ψ in Theorem 5, ψ in Theorems 7– 8) is diagonal the conditions for applying the more general formulation of the lemmas and theorems presented here sometimes may be satisfied while the conditions for the original formulations may not be satisfied.

Consider the integral equation

$$g(t) = f(t) + (L\Psi f)(t), t \geq 0$$

in which $g \in L_2(0, \infty)$, L is a linear operator represented in the Laplace domain by

$$K(s) = \begin{bmatrix} \dfrac{1}{(s+1+2i)(s+1-2i)} & 0 \\ \dfrac{1}{(s+1+2i)(s+1-2i)} & \dfrac{1}{(s+1+2i)(s+1-2i)} \end{bmatrix}$$

and $(\Psi f)(t) = \psi[f(t)]$ where $\psi(z) = (\psi_1(z_1), \psi_2(z_2))^T$ is a differentiable nonlinear function with

$$0 \leq \psi_k'(z) \leq \beta, \ k \in \{1, 2\}, \ z \in \mathbb{R}.$$

We find that for $\beta = 7$

$$3.5 \sup_{\omega \in \mathbb{R}} \Lambda \left\{ (1_2 + 3.5K(j\omega))^{-1} K(j\omega) \right\} > 1.0561.$$

This shows that the standard approach cannot be used to show that e.g. $f \in L_2(0, \infty)$.

However (also for $\beta = 7$), with

$$a = \begin{bmatrix} 2.62480443306255 & 1.93312021534028 \\ 1.70670050011234 & 4.46197306598523 \end{bmatrix}, \text{ and}$$

$$b = \begin{bmatrix} 1.06242868073574 & -0.01596861440091 \\ 0.64819242039704 & 1.15192623108721 \end{bmatrix}$$

we have

$$\sup_{\omega\in\mathbb{R}} \Lambda\left\{(1_2 + b^{-1}K(j\omega)a)^{-1}b^{-1}K(j\omega)\right\} \sup_{z\in\mathbb{R}^2} \Lambda\left\{\psi'(z)\times b - a\right\} < 0.986 < 1.$$

and in the Laplace domain the real parts of all poles of all elements of

$$(1_2 + b^{-1}K(s)a)^{-1}$$

are negative. We thus satisfy all the conditions of Theorem 5. This allows us to conclude that e.g. $f \in L_{2,2}(0,\infty)$, and since every element of k tends to zero exponentially as its argument tends to infinity, the conditions of Theorems 7 and 8 are also satisfied, so we can e.g. also conclude that if $g \in L_{\infty,2}(0,\infty)$, then $f \in L_{\infty,2}(0,\infty)$.

Subtracting $0.5(\alpha+\beta)$ from the nonlinear operator leads to a contraction for $\beta < 6.58$. Using the results presented here, we find that we can obtain a contraction for $\beta < 7.15$[3].

Our second example comes from a practical problem in the area of power electronics.

When multiple MOSFET devices are combined in parallel configurations, such as when multiple MOSFET die are combined in a single package, oscillations can arise due to the effect of parasitic components in the configuration [6]. Oscillations internal to the configuration are especially problematic since very little can be done externally to the configuration to prevent the oscillations. This happens because the common drain, gate and source connections act as virtual grounds (i.e. the common drain, gate and source connections can be connected to ideal voltage sources without altering the current and voltage waveforms) when two MOSFET

[3]To apply the theorems presented here requires a numerical search for matrices a and b as required in the statement of the theorems. From a computational point of view it is thus more economical to first try the original formulation and only use the theorems presented here if the original approach does not work. It also means that we do not know whether there are matrices a and b that give even better results. Since we did extensive numerical searches the latter possibility is unlikely.

devices in the configuration oscillate 180° out of phase. A model of a configuration that arises when two MOSFET die are combined in a single package is shown in Figure 6.1.

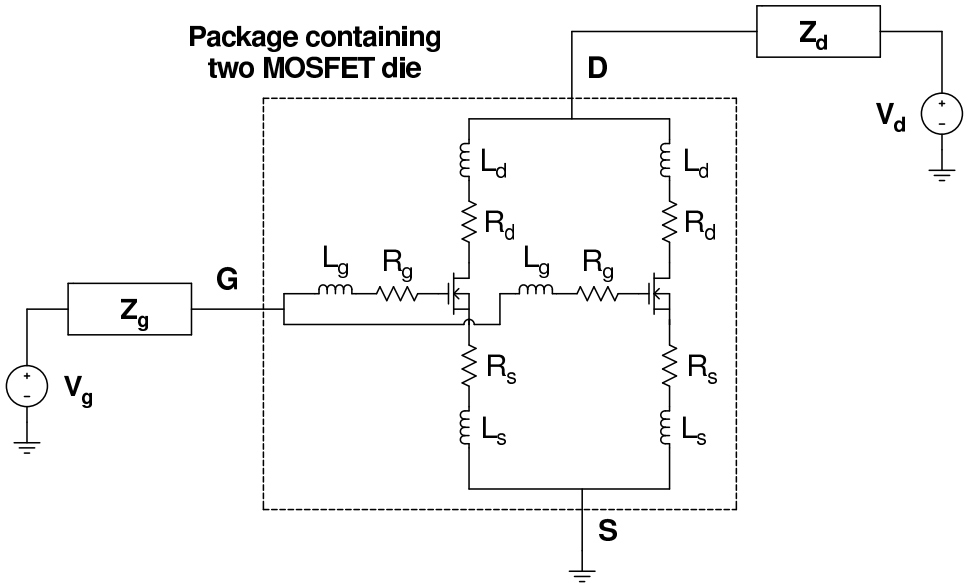

Figure 6.1: Circuit containing a package with two MOSFET die. The nodes labeled D, G and S are the common drain, gate and source terminals of the package. V_d, Z_d, V_g and Z_g represent Thévenin equivalent sources and impedances of the circuits connected respectively to the drain and gate of the package.

The problem can be linearized to predict the onset of instability at various bias points [6]. Here we take the analysis one step further and present a nonlinear analysis of the problem where we take into account the nonlinear dependence of the drain current on the gate-source and drain-source voltages. We simplify the problem by treating the gate-source, drain-source and gate-drain capacitances as linear, and we assume a perfect virtual ground at the common gate, drain and source terminals so that we only need to analyze a single device. We also assume that the gate to source voltage remains in the range 0 to 10 V and the drain to source voltage remains in the range 0 to 150 V. These simplifications are justified by detailed simulations of the nonlinear circuit. The latter simplification allows us

to extend the function that describes the drain current of the intrinsic MOSFET for all values of the gate to source and drain to source voltages in such a way that the partial derivatives of this function remain bounded. (Since one solution with suitable initial conditions is just a constant drain current, we can use Theorem 8 to show that for small perturbations from the initial condition that results in a constant drain current, the solution is close to the constant-drain-current solution. It does thus not matter that we redefined the function describing the drain current in the region far from the constant-drain-current solution.) The simplified circuit is shown in Figure 6.2.

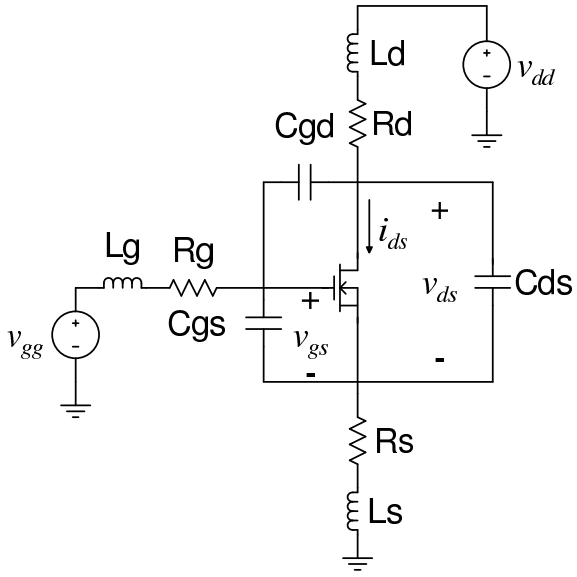

Figure 6.2: Circuit diagram showing the model of a single device (the MOSFET symbol together with C_{gs}, C_{ds} and C_{gd}) and components connecting the single device to the common gate, drain and source terminals.

We assume that the drain to source current, i_{ds}, of the intrinsic MOSFET is given by the solution to

$$\begin{aligned} v_{gs_i} &= v_{gs} - i_{ds} R_{s_i} \\ v_{ds_i} &= v_{ds} - i_{ds} \times (R_{d_i} + R_{s_i}) \end{aligned}$$

$$i_{ds} = \begin{cases} 0, \ (v_{gs_i}, v_{ds_i}) \in A \\ K_M v_{ds_i}(v_{gs_i} - V_{th} - 0.5 v_{ds_i}), \ (v_{gs_i}, v_{ds_i}) \in B \\ 0.5 K_M (v_{gs_i} - V_{th})^2 [1 + \lambda(v_{ds_i} - v_{gs_i} + V_{th})], \ (v_{gs_i}, v_{ds_i}) \in C \end{cases}$$

where

$$\begin{aligned} A &= \{(v_{gs_i}, \ v_{ds_i}) : v_{ds_i} < 0\} \bigcup \{(v_{gs_i}, v_{ds_i}) : v_{gs_i} < V_{th}\}, \\ B &= \{(v_{gs_i}, v_{ds_i}) : v_{ds_i} \geq 0, \ v_{gs_i} \geq V_{th}, \text{ and } v_{ds_i} < (v_{gs_i} - V_{th})\}, \\ C &= \{(v_{gs_i}, v_{ds_i}) : v_{ds_i} \geq 0, \ v_{gs_i} \geq V_{th}, \text{ and } v_{ds_i} \geq (v_{gs_i} - V_{th})\}, \end{aligned}$$

R_{s_i} and R_{d_i} are the intrinsic drain and source resistances (these are different from the external resistances R_d and R_s of Figure 6.2), K_M is a gain factor and V_{th} is the threshold voltage.

The circuit equations can be written in the form

$$\begin{aligned} v_{gs} &= L_1 \tilde{\psi}(v_{gs}, v_{ds}) + L_2 v_{dd} + L_3 v_{gg} + e_1 \\ v_{ds} &= L_4 \tilde{\psi}(v_{gs}, v_{ds}) + L_5 v_{dd} + L_6 v_{dd} + e_2 \end{aligned}$$

in which $L_1, L_2, \ldots, L_6$ are linear operators. Here $\tilde{\psi}(v_{gs}, v_{ds})$ is the drain current as a function of the gate to source and drain to source voltages as described above, except that for $v_{ds} > 150$ and $v_{gs} > 10$ we assign the value of i_{ds} as calculated using the above formulas at $(v_{gs}, 150)$ and $(10, v_{ds})$, respectively. e_1 and e_2 are functions that depend on the initial conditions.

Defining

$$\begin{aligned} f &= \begin{bmatrix} v_{gs} \\ v_{ds} \end{bmatrix}, \\ L &= \begin{bmatrix} -L_1 & 0 \\ -L_4 & 0 \end{bmatrix}, \\ \psi(v_{gs}, v_{ds}) &= \begin{bmatrix} \tilde{\psi}(v_{gs}, v_{ds}) \\ 0 \end{bmatrix}, \text{ and} \end{aligned}$$

Table 6.1: Parameter values for the intrinsic MOSFET of Figure 6.2.

Parameter	Value	Units
K_M	4	A/V^2
V_{th}	3.5	V
λ	0.0015	A/V
R_{d_i}	0.4	Ω
R_{s_i}	0.16	Ω

$$g = \begin{bmatrix} L_2 v_{dd} + L_3 v_{gg} + e_1 \\ L_5 v_{dd} + L_6 v_{dd} + e_2 \end{bmatrix},$$

we can write the circuit equations in the form

$$g = f + L\psi(f).$$

With typical parameters as in Table 6.1, the dependence of the drain to source current of the intrinsic MOSFET on the gate to source and drain to source voltages is shown in Figure 6.3.

To prove that the circuit of Figure 6.2 is stable (i.e. $L_{2,2}(0,\infty)$ inputs produce $L_{2,2}(0,\infty)$ outputs, small differences in the input lead to small differences in the output etc. as in our theorems), we can show that there are a matrix a and an invertible matrix b such that with $K(s)$ the Laplace domain representation of L,

(i) all poles of every element of $K(s)$ have negative real parts

(ii) the zeros of $\det[1_2 + b^{-1}K(s)a]$ all have negative real parts and

(iii) $c \stackrel{\text{def}}{=} \sup_{\omega} \Lambda\left\{[1_2 + b^{-1}K(j\omega)a]^{-1}b^{-1}K(j\omega)\right\} \sup_{(x,y)\in E} \Lambda\left\{\psi'(x,y)b - a\right\} < 1$

where

$$E = \left\{\mathbb{R}^2 \bigcap \left\{(x,y) : \psi'(x,y) \text{ exists}\right\}\right\}.$$

Condition (i) ensures that every element of k, the kernel in the convolution representation of L, tends to zero exponentially as the argument t of $k(t)$ tends to

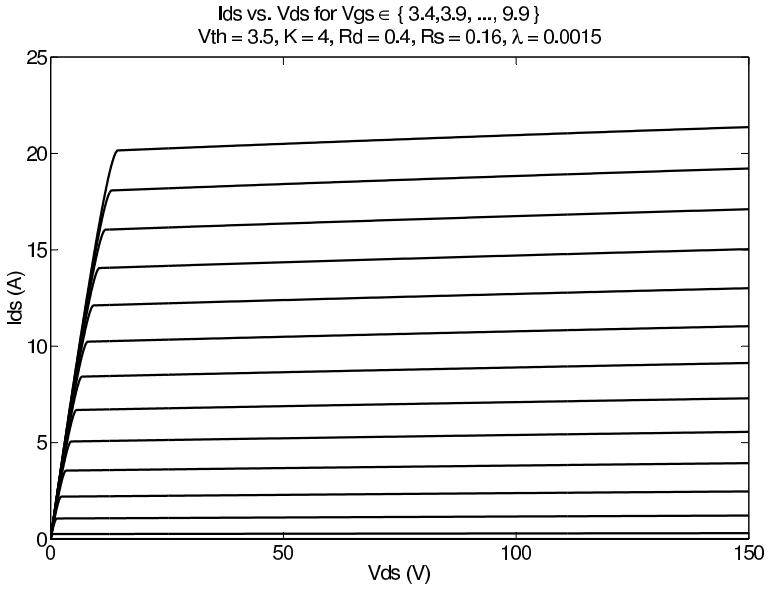

Figure 6.3: Drain to source current of the intrinsic MOSFET with parameters as in Table 6.1 as a function of the gate to source and drain to source voltages.

infinity so that ξ given by $\xi(t) = t^p k(t),\ t \geq 0$ belong to $\mathbb{K}_{1,N} \bigcap \mathbb{K}_{2,N}$ for $p \in \{0, 1, 2\}$. Since ψ is continuous it follows that ψf is measurable whenever f is measurable. Since ψ is continuous and it can be verified that given any two points in the domain of ψ, two points arbitrarily close to the given points can be connected by a line segment along which ψ is differentiable except at a finite number of points, the mean-value theorem can be used to show that for any $w_1,\ w_2 \in \mathbb{R}^N$,

$$|\psi(bw_1) - aw_1 - \psi(bw_2) + aw_2|_2 \leq \sup_{(x,y)\in E} \Lambda\left\{\psi'(x,y)b - a\right\} |w_1 - w_2|_2 .$$

With parameters as in Tables 6.1–6.2 one can verify that e_1 and e_2 are bounded and tend to zero exponentially as their arguments tend to infinity and that the Laplace domain representations of $L_2,\ L_3,\ L_5$ and L_6 are proper rational functions with all poles having negative real parts. From this it follows that if v_{gg} and v_{dd} belong to $L_{2,2}(0,\infty)$ or $L_{\infty,2}(0,\infty)$, then so does g.

It thus follows that if we satisfy the conditions listed above, then we satisfy

the criteria for all our theorems, and we may conclude that e.g. if v_{gg} and v_{dd} belong to $L_{2,2}(0,\infty)$ then so does f, if we make small perturbations to v_{gg} and v_{dd} in either the $L_{2,2}(0,\infty)$ or $L_{\infty,2}(0,\infty)$ sense, then the resulting changes in f are small in the $L_{2,2}(0,\infty)$ or $L_{\infty,2}(0,\infty)$ sense, respectively, etc. In particular, using Theorem 8 we can conclude that if v_{gg} and v_{dd} are constant functions, then f must tend to a constant function as its argument tends to infinity since one solution of the circuit conditions for suitable initial conditions and constant v_{gg} and v_{dd} is clearly a constant function f.[4] In particular, for the simplified circuit we can conclude that the circuit is stable in a very strong sense if we satisfy the above criteria.

For a given problem finding an a and a b that works is non-trivial and we are forced to search for such a and b numerically. With parameters as in Tables 6.1–6.2, we find that

$$a = \begin{bmatrix} 5.1320372 & 5.3409383 \\ 0.052663204 & -0.041466911 \end{bmatrix}, \text{ and} \tag{6.13}$$

$$b = \begin{bmatrix} 1 & -0.4610093 \\ -1.0381752 & 4.8577338 \end{bmatrix} \tag{6.14}$$

can be used to prove that the circuit is stable.

Figure 6.4 plots

$$\Lambda\left\{[1_2 + b^{-1}K(j\omega)a]^{-1}b^{-1}K(j\omega)\right\}$$

as a function of ω, and Figure 6.5 plots

$$\Lambda\left\{\psi'(x,y)b - a\right\}$$

at many points (x_n, y_n) from which we can estimate c.

[4]Set the initial drain and source currents equal to the constant drain to source current that would result for constant gate to source and drain to source voltages, the initial gate current to zero and the initial capacitor voltages equal to the constant intrinsic gate to source, gate to drain and drain to source voltages to obtain a constant drain to source current solution.

Table 6.2: Parameter values for the circuit of Figure 6.2.

Parameter	Value	Units
C_{gs}	2	nF
C_{gd}	200	pF
C_{ds}	200	pF
R_g	1.5	Ω
R_d	0.001	Ω
R_s	0.4	Ω
L_g	6	nH
L_d	1	nH
L_s	2	nH

Figure 6.6 shows the effectiveness of the extended approach suggested here by plotting the bounds we can obtain on c as a function of the gain K_M. In Figure 6.6 the plot labeled (1) corresponds to the original approach in that a is restricted to a constant times the identity matrix and b a diagonal matrix. The plot labeled (2) corresponds to the case where a can be arbitrary, but b is restricted to a diagonal matrix. The plot labeled (3) corresponds to the approach suggested here. We find that with the approach suggested here we can obtain conclusive results for a gain up to $K_M = 13.3$ A/V^2, which is sufficient to handle most practical problems of this type. The original approach provide conclusive results up to a gain of $K_M = 0.00765$ A/V^2 which is insufficient to deal with practical problems of this nature.

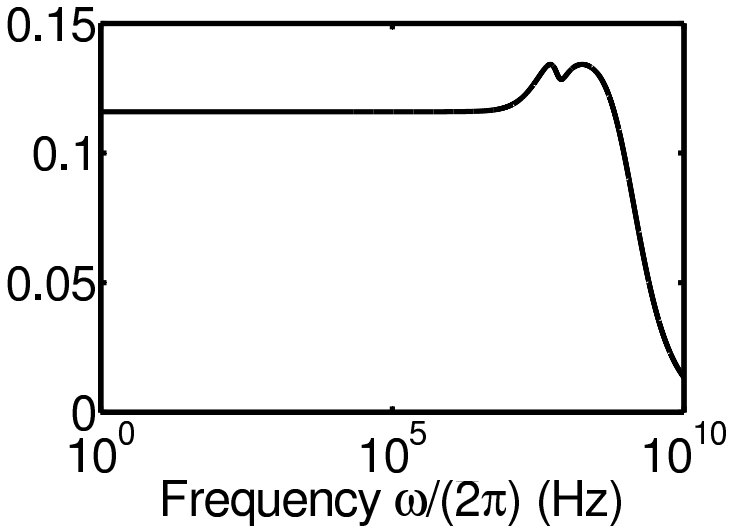

Figure 6.4: A plot of $\Lambda\left\{\left(1_2 + b^{-1}K(j\omega)a\right)^{-1} b^{-1}K(j\omega)\right\}$ as a function of ω for the circuit of Figure 6.2 with a and b as in (6.13) and (6.14) respectively.

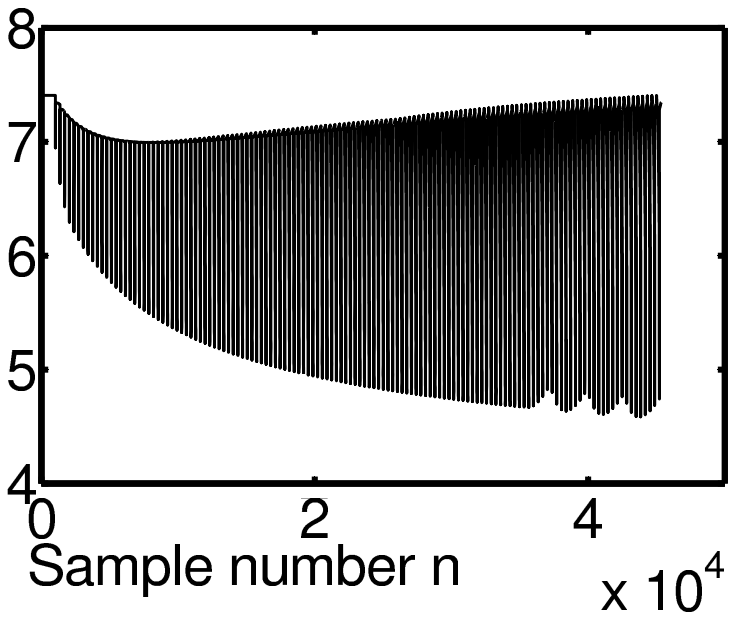

Figure 6.5: A plot of $\Lambda\left\{\psi'(x_n, y_n)b - a\right\}$ for multiple values of (x_n, y_n) for the circuit of Figure 6.2 with a and b as in (6.13) and (6.14) respectively.

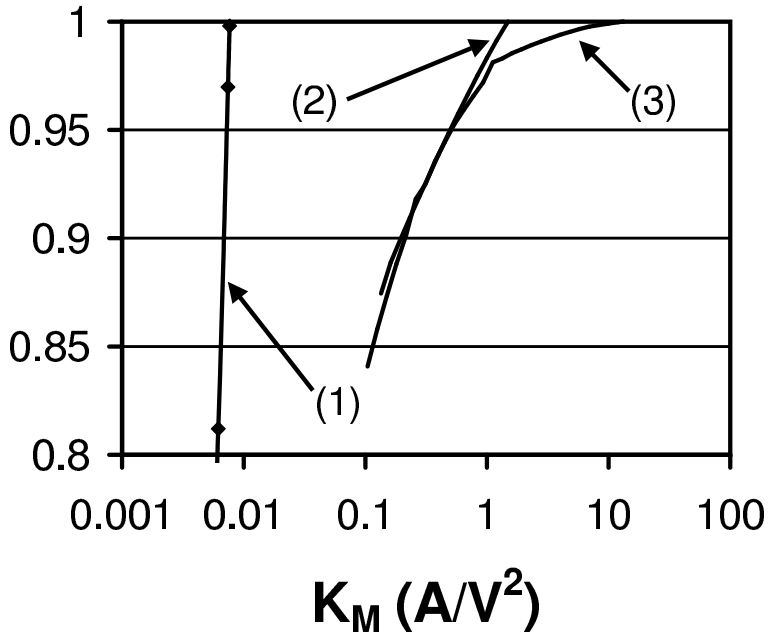

Figure 6.6: Bounds on c as a function of the gain K_M for the circuit of Figure 6.2. The plot labeled (1) corresponds to the original approach in that a is restricted to a constant times the identity matrix and b a diagonal matrix. The plot labeled (2) corresponds to the case where a can be arbitrary, but b is restricted to a diagonal matrix. The plot labeled (3) corresponds to the approach suggested here.

6.6 Conclusion

We have provided a theoretical framework that allows us to obtain conclusive results for a wider class on nonlinear Volterra integral equations of the second kind than was previously possible. These extensions should be useful in practical problems where the nonlinearities are not diagonal and, as we have shown with the aid of a computational example, may even allow us to obtain conclusive results for integral equations containing diagonal nonlinearities for which conclusive results could not previously be obtained.

Chapter 7

The Parallel Nonlinear Resistor and Nonlinear Capacitor Problem

Diodes are often modeled as a parallel combination of a nonlinear capacitor and a nonlinear resistor. In this chapter we derive an integral equation that describes a nonlinear resistor in parallel with a nonlinear capacitor driven by a Thévenin equivalent source. We show how to obtain a contraction mapping operator on $L_2(0,\infty)$.

We provide two bounds for c where T is the chosen contraction mapping operator and $\|Tf - Tg\|_2 < c\,\|f - g\|_2$ for all $f, g \in L_2(0,\infty)$. We show that one of the bounds is always better than the other. We show the optimality of certain constants used in the construction of the contraction mapping operator.

Intuitively the addition of a resistor parallel to a nonlinear capacitor improves the stability of the circuit. However, given the complexity of the contraction operator it is not clear that one can obtain bounds on c such that the addition of a nonlinear parallel resistor stabilizes the circuit subject only to the condition that the minimum incremental conductance is more than some number. With the aid of an example

we show that this is possible (at least for the circuit we used as an example). For this example the minimum incremental conductance required to prove stability is not much more than that of a linear resistor placed in parallel with the varactor for which one can prove that the circuit is stable. We also found that the better of the two bounds on c gives much better results.

7.1 Results in $L_2(0, \infty)$

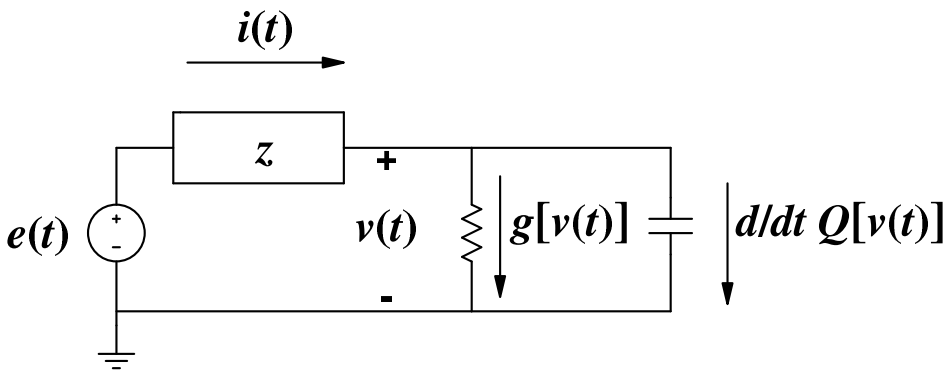

Figure 7.1: Type of circuit considered.

We will be concerned with circuits of the type depicted in Figure. 7.1, in which we consider e as the input and v as the output. In Figure 7.1, e and z represent a Thévenin equivalent source driving a parallel combination of a nonlinear resistor and nonlinear capacitor represented by g and Q, respectively. At time t ($t \geq 0$) the current through the Thévenin equivalent impedance z is $i(t)$, the current through the nonlinear resistor is $g[v(t)]$ and the charge stored in the nonlinear capacitor is $Q[v(t)]$.

The Thévenin equivalent circuit introduces the constraint

$$e(t) + d(t) = v(t) + \int_0^t z(t-\tau) i(\tau)\, d\tau, \ t \geq 0$$

while the nonlinear resistor and capacitor introduce the constraint

$$i(t) = g[v(t)] + \frac{d}{dt}Q[v(t)],\ t \geq 0$$

where d takes into account the initial conditions. Thus

$$e(t) + d(t) = v(t) + \int_0^t z(t-\tau)\left(g[v(\tau)] + \frac{d}{d\tau}Q[v(\tau)]\right) d\tau,\ t \geq 0.$$

Let $Z(s) = \int_0^\infty z(t)e^{-st}\,dt$ be the Laplace domain representation of the Thévenin equivalent driving-point impedance presented to the nonlinear elements. We assume that z is both integrable and square integrable and that Z is a positive real function in the sense of passive network theory (i.e., that $Z(s)$ is real when s is real, and $\mathrm{Re}\,[Z(s)] \geq 0$ for $\mathrm{Re}\,(s) \geq 0$). We also assume that z is differentiable and its derivative z' is Lipschitz continuous on $[0, a]$ for each $a > 0$ and that $z' \in L_1(0, \infty)$.

We assume that $g : \mathbb{R} \to \mathbb{R}$ satisfies $g(0) = 0$ and for any real $r_1 \neq r_2$,

$$0 < \alpha_g \leq \frac{g(r_1) - g(r_2)}{r_1 - r_2} \leq \beta_g$$

and $Q : \mathbb{R} \to \mathbb{R}$ satisfies $Q(0) = 0$ and for any real $r_1 \neq r_2$,

$$0 < \alpha_Q \leq \frac{Q(r_1) - Q(r_2)}{r_1 - r_2} \leq \beta_Q.$$

We seek a solution v such that η defined by $\eta(t) = Q[v(t)]$ is absolutely continuous on every interval $[0, t] \subset \mathbb{R}$. This ensures [31, p. 116] that

$$\frac{d}{dt}Q[v(t)],\ t \geq 0$$

exists a.e. and that charge is conserved in the varactor in the sense that for $0 \leq t_a \leq t_b$,

$$Q[v(t_b)] = \int_{t_a}^{t_b} \frac{d}{d\tau}Q[v(\tau)]\,d\tau + Q[v(t_a)].$$

We furthermore require that both e and d be absolutely continuous. We also assume that e and d are bounded on $[0, \infty)$ and that $\lim_{t\to\infty} d(t) = 0$.

Our assumptions ensure that integration by parts is justified so that

$$\begin{aligned} e(t)+d(t) &= v(t)+\int_0^t z(t-\tau)g[v(\tau)]\,d\tau + z(0)Q[v(t)] - z(t)Q[v(0)] \\ &\quad + \int_0^t u(t-\tau)Q[v(\tau)]\,d\tau,\ t\geq 0 \end{aligned}$$

where

$$u(t)=\frac{d}{dt}z(t),\ t\geq 0.$$

With

$$h(t)=e(t)+d(t)+Q[v(0)]z(t),\ t\geq 0$$

and $I_{\mathbb{R}}$ the identity on $\mathbb{R}$ we thus have

$$h(t)=[I_{\mathbb{R}}+z(0)Q]v(t)+\int_0^t z(t-\tau)g[v(\tau)]\,d\tau+\int_0^t u(t-\tau)Q[v(\tau)]d\tau,\ t\geq 0.$$

It follows from our assumptions that $\lim_{t\to\infty} z(t)=0$ and that $z(0)\geq 0$. (See page 16.)

Since $\alpha_Q>0$ and $z(0)\geq 0$, $(I_{\mathbb{R}}+z(0)Q)^{-1}$ exists. Let y be defined by

$$y(t)=\left(I_{\mathbb{R}}+z(0)Q\right)v(t),\ t\geq 0,$$

$\psi_g:\mathbb{R}\to\mathbb{R}$ by

$$\psi_g=g\left(I_{\mathbb{R}}+z(0)Q\right)^{-1},\text{ and}$$

$\psi_Q:\mathbb{R}\to\mathbb{R}$ by

$$\psi_Q=Q\left(I_{\mathbb{R}}+z(0)Q\right)^{-1}.$$

With these definitions we have

$$\begin{aligned} h(t) &= y(t)+\int_0^t z(t-\tau)g\left[\left(I_{\mathbb{R}}+z(0)Q\right)^{-1}y(\tau)\right]\,d\tau \\ &\quad + \int_0^t u(t-\tau)Q\left[\left(I_{\mathbb{R}}+z(0)Q\right)^{-1}y(\tau)\right]\,d\tau,\ t\geq 0 \\ &= y(t)+\int_0^t z(t-\tau)\psi_g\left[y(\tau)\right]\,d\tau+\int_0^t u(t-\tau)\psi_Q\left[y(\tau)\right]\,d\tau,\ t\geq 0. \end{aligned}$$

Since $(I_{\mathbb{R}} + z(0)Q)\,0 = 0$, $(I_{\mathbb{R}} + z(0)Q)^{-1}\,0 = 0$. Since $g(0) = 0$ and $Q(0) = 0$, we have $\psi_g(0) = \psi_Q(0) = 0$.

Let $r_1 \neq r_2$ be two real numbers. Then

$$\begin{aligned} S_g &\stackrel{\text{def}}{=} \frac{\psi_g(r_1) - \psi_g(r_2)}{r_1 - r_2} \\ &= \frac{g\,(I_{\mathbb{R}} + z(0)Q)^{-1}\,r_1 - g\,(I_{\mathbb{R}} + z(0)Q)^{-1}\,r_2}{r_1 - r_2}. \end{aligned}$$

With

$$y_j \stackrel{\text{def}}{=} (I_{\mathbb{R}} + z(0)Q)^{-1}\,r_j,\ j = 1, 2$$

we have

$$\begin{aligned} S_g &= \frac{gy_1 - gy_2}{(I_{\mathbb{R}} + z(0)Q)\,y_1 - (I_{\mathbb{R}} + z(0)Q)\,y_2} \\ &= \frac{gy_1 - gy_2}{y_1 - y_2 + z(0)\,(Qy_1 - Qy_2)}. \end{aligned}$$

Since $y_1 \neq y_2$ (since $(I_{\mathbb{R}} + z(0)Q)$ is invertible and thus injective) and $\alpha_g > 0$, $gy_1 \neq gy_2$, and we have

$$\begin{aligned} S_g &= \frac{1}{\dfrac{y_1 - y_2}{gy_1 - gy_2} + z(0)\dfrac{Qy_1 - Qy_2}{gy_1 - gy_2}} \\ &= \frac{1}{\dfrac{y_1 - y_2}{gy_1 - gy_2} + z(0)\dfrac{Qy_1 - Qy_2}{y_1 - y_2}\dfrac{y_1 - y_2}{gy_1 - gy_2}} \\ &= \frac{1}{\dfrac{y_1 - y_2}{gy_1 - gy_2}\left(1 + z(0)\dfrac{Qy_1 - Qy_2}{y_1 - y_2}\right)}. \end{aligned}$$

Now

$$\frac{y_1 - y_2}{gy_1 - gy_2}\left(1 + z(0)\frac{Qy_1 - Qy_2}{y_1 - y_2}\right) \begin{cases} \leq \dfrac{1}{\alpha_g}\,(1 + z(0)\beta_Q) \\ \geq \dfrac{1}{\beta_g}\,(1 + z(0)\alpha_Q) \end{cases}$$

so that

$$\frac{\alpha_g}{1 + z(0)\beta_Q} \leq S_g \leq \frac{\beta_g}{1 + z(0)\alpha_Q}.$$

Also, with

$$\begin{aligned} S_Q &\stackrel{\text{def}}{=} \frac{\psi_Q(r_1) - \psi_Q(r_2)}{r_1 - r_2} \\ &= \frac{Q\left(I_{\mathbb{R}} + z(0)Q\right)^{-1} r_1 - Q\left(I_{\mathbb{R}} + z(0)Q\right)^{-1} r_2}{r_1 - r_2} \end{aligned}$$

and

$$y_j \stackrel{\text{def}}{=} \left(I_{\mathbb{R}} + z(0)Q\right)^{-1} r_j,\ j = 1, 2$$

we have

$$\begin{aligned} S_Q &= \frac{Qy_1 - Qy_2}{\left(I_{\mathbb{R}} + z(0)Q\right) y_1 - \left(I_{\mathbb{R}} + z(0)Q\right) y_2} \\ &= \frac{Qy_1 - Qy_2}{y_1 - y_2 + z(0)\left(Qy_1 - Qy_2\right)}. \end{aligned}$$

Since $\alpha_Q > 0$ and thus $Qy_1 \neq Qy_2$ we have

$$\begin{aligned} S_Q &= \frac{1}{\frac{y_1 - y_2}{Qy_1 - Qy_2} + z(0)\frac{Qy_1 - Qy_2}{Qy_1 - Qy_2}} \\ &= \frac{1}{\frac{y_1 - y_2}{Qy_1 - Qy_2} + z(0)}. \end{aligned}$$

Now

$$\frac{y_1 - y_2}{Qy_1 - Qy_2} + z(0) \begin{cases} \leq \dfrac{1}{\alpha_Q} + z(0) = \dfrac{1 + z(0)\alpha_Q}{\alpha_Q} \\ \geq \dfrac{1}{\beta_Q} + z(0) = \dfrac{1 + z(0)\beta_Q}{\beta_Q} \end{cases}$$

so that

$$\frac{\alpha_Q}{1 + z(0)\alpha_Q} \leq S_Q \leq \frac{\beta_Q}{1 + z(0)\beta_Q}.$$

Let x_g and x_Q be two real numbers. Then

$$\begin{aligned} h(t) &= y(t) + \int_0^t z(t-\tau)\psi_g\left[y(\tau)\right]\, d\tau + \int_0^t u(t-\tau)\psi_Q\left[y(\tau)\right]\, d\tau,\ t \geq 0 \\ &= y(t) + \int_0^t z(t-\tau)\left(\psi_g - x_g I_{\mathbb{R}}\right) y(\tau)\, d\tau + \int_0^t u(t-\tau)\left(\psi_Q - x_Q I_{\mathbb{R}}\right) y(\tau)\, d\tau \\ &\quad + x_g \int_0^t z(t-\tau) y(\tau)\, d\tau + x_Q \int_0^t u(t-\tau) y(\tau)\, d\tau,\ t \geq 0. \end{aligned}$$

Define the maps L_g and L_Q from $L_2(0,\infty)$ into itself (since $z,\ u \in L_1(0,\infty)$) by

$$\begin{aligned}(L_g f)(t) &= \int_0^t z(t-\tau) f(\tau)\, d\tau,\ t \geq 0, \text{ and} \\ (L_Q f)(t) &= \int_0^t u(t-\tau) f(\tau)\, d\tau,\ t \geq 0.\end{aligned}$$

Define the maps Ψ_g and Ψ_Q on $L_2(0,\infty)$ by

$$\begin{aligned}(\Psi_g f)(t) &= \psi_g[f(t)],\ t \geq 0, \text{ and} \\ (\Psi_Q f)(t) &= \psi_Q[f(t)],\ t \geq 0.\end{aligned}$$

Since both ψ_g and ψ_Q are Lipschitz continuous maps from $\mathbb{R}$ to $\mathbb{R}$ (with Lipschitz constants of $\frac{\beta_g}{1+z(0)\alpha_Q}$ and $\frac{\beta_Q}{1+z(0)\beta_Q}$, respectively), it follows that Ψ_g and Ψ_Q map $L_2(0,\infty)$ into itself.

Let

$$K(s) = \int_0^\infty [x_g z(t) + x_Q u(t)]\, e^{-st}\, dt.$$

If

$$1 + K(s) \neq 0, \sigma \geq 0,$$

then it follows from arguments similar to those in [14, Lemma 5] that $(I + x_g L_g + x_Q L_Q)$ possesses a bounded inverse on $L_2(0,\infty)$.

Suppose (just for now) that both h and y belong to $L_2(0,\infty)$. Then we have

$$\begin{aligned}h &= (I + x_g L_g + x_Q L_Q)\, y + L_g\, (\Psi_g - x_g I)\, y + L_Q\, (\Psi_Q - x_Q I)\, y \qquad (7.1) \\ \Leftrightarrow y &= (I + x_g L_g + x_Q L_Q)^{-1}\, h - (I + x_g L_g + x_Q L_Q)^{-1}\, L_g\, (\Psi_g - x_g I)\, y \\ &\quad - (I + x_g L_g + x_Q L_Q)^{-1}\, L_Q\, (\Psi_Q - x_Q I)\, y.\end{aligned}$$

From this it follows that T defined by

$$\begin{aligned}T(y) &= (I + x_g L_g + x_Q L_Q)^{-1}\, h - (I + x_g L_g + x_Q L_Q)^{-1}\, L_g\, (\Psi_g - x_g I)\, y \\ &\quad - (I + x_g L_g + x_Q L_Q)^{-1}\, L_Q\, (\Psi_Q - x_Q I)\, y\end{aligned}$$

is a suitable candidate for a contraction mapping operator since $T : L_2(0,\infty) \to L_2(0,\infty)$ and $y \in L_2(0,\infty)$ is a fixed point of T (i.e. $Ty = y$) if and only if y satisfies (7.1).

For $y_1,\ y_2 \in L_2(0,\infty)$,

$$\begin{aligned}
&\|Ty_1 - Ty_2\|_2 \\
&\quad = \left\| (I + x_g L_g + x_Q L_Q)^{-1} L_g \left[(\Psi_g - x_g I)\, y_2 - (\Psi_g - x_g I)\, y_1 \right] \right. \\
&\qquad \left. + (I + x_g L_g + x_Q L_Q)^{-1} L_Q \left[(\Psi_Q - x_Q I)\, y_2 - (\Psi_Q - x_Q I)\, y_1 \right] \right\|_2 . \quad (7.2)
\end{aligned}$$

Define

$$\begin{aligned}
f_1 &= \left[(\Psi_g - x_g I)\, y_2 - (\Psi_g - x_g I)\, y_1 \right], \text{ and} \\
f_2 &= \left[(\Psi_Q - x_Q I)\, y_2 - (\Psi_Q - x_Q I)\, y_1 \right]
\end{aligned}$$

and take as the definition of the Fourier transform of $f \in L_2(0,\infty)$

$$(\mathcal{F} f)(\omega) \stackrel{\text{def}}{=} \hat{f}(\omega) \stackrel{\text{def}}{=} \text{ l.i.m.} \int_{-\infty}^{\infty} f(t) e^{-j\omega t}\, dt.$$

Then, for $\gamma > 0$ and using Plancherel's identity and the Cauchy-Schwarz inequality, we have

$$\begin{aligned}
&\|Ty_1 - Ty_2\|_2^2 \\
&\quad = \left\| (I + x_g L_g + x_Q L_Q)^{-1} L_g f_1 + \gamma\, (I + x_g L_g + x_Q L_Q)^{-1} L_Q \frac{1}{\gamma} f_2 \right\|_2^2 \\
&\quad = \frac{1}{2\pi} \left\| \mathcal{F} \left((I + x_g L_g + x_Q L_Q)^{-1} L_g f_1 \right. \right. \\
&\qquad \left. \left. + \gamma\, (I + x_g L_g + x_Q L_Q)^{-1} L_Q \frac{1}{\gamma} f_2 \right) \right\|_{2(-\infty,\infty)}^2 \\
&\quad = \frac{1}{2\pi} \left\| \frac{\hat{z}}{1 + x_g \hat{z} + x_Q \hat{u}} \hat{f}_1 + \gamma \frac{\hat{u}}{1 + x_g \hat{z} + x_Q \hat{u}} \frac{1}{\gamma} \hat{f}_2 \right\|_{2(-\infty,\infty)}^2 \\
&\quad = \frac{1}{2\pi} \int_{-\infty}^{\infty} \left| \frac{\hat{z}(\omega)}{1 + x_g \hat{z}(\omega) + x_Q \hat{u}(\omega)} \hat{f}_1(\omega) \right. \\
&\qquad \left. + \gamma \frac{\hat{u}(\omega)}{1 + x_g \hat{z}(\omega) + x_Q \hat{u}(\omega)} \frac{1}{\gamma} \hat{f}_2(\omega) \right|_2^2 d\omega
\end{aligned}$$

$$
\begin{aligned}
&\leq \frac{1}{2\pi}\int_{-\infty}^{\infty}\left[\left|\frac{\hat{z}(\omega)}{1+x_g\hat{z}(\omega)+x_Q\hat{u}(\omega)}\right|^2+\left|\gamma\frac{\hat{u}(\omega)}{1+x_g\hat{z}(\omega)+x_Q\hat{u}(\omega)}\right|^2\right]\\
&\quad\left[\left|\hat{f}_1(\omega)\right|^2+\left|\frac{1}{\gamma}\hat{f}_2(\omega)\right|^2\right]\,d\omega\\
&\leq \frac{1}{2\pi}\sup_{\omega\in\mathbb{R}}\left[\left|\frac{\hat{z}(\omega)}{1+x_g\hat{z}(\omega)+x_Q\hat{u}(\omega)}\right|^2+\left|\gamma\frac{\hat{u}(\omega)}{1+x_g\hat{z}(\omega)+x_Q\hat{u}(\omega)}\right|^2\right]\\
&\quad\int_{-\infty}^{\infty}\left[\left|\hat{f}_1(\omega)\right|^2+\left|\frac{1}{\gamma}\hat{f}_2(\omega)\right|^2\right]\,d\omega\\
&= \frac{1}{2\pi}\sup_{\omega\in\mathbb{R}}\left[\left|\frac{\hat{z}(\omega)}{1+x_g\hat{z}(\omega)+x_Q\hat{u}(\omega)}\right|^2+\left|\gamma\frac{\hat{u}(\omega)}{1+x_g\hat{z}(\omega)+x_Q\hat{u}(\omega)}\right|^2\right]\\
&\quad\left\|(\hat{f}_1,\frac{1}{\gamma}\hat{f}_2)\right\|^2_{2(-\infty,\infty)}\\
&= \sup_{\omega\in\mathbb{R}}\left[\left|\frac{\hat{z}(\omega)}{1+x_g\hat{z}(\omega)+x_Q\hat{u}(\omega)}\right|^2+\left|\gamma\frac{\hat{u}(\omega)}{1+x_g\hat{z}(\omega)+x_Q\hat{u}(\omega)}\right|^2\right]\left\|(f_1,\frac{1}{\gamma}f_2)\right\|^2_2.
\end{aligned}
$$

Using our bounds on S_g and S_Q it follows that

$$
\begin{aligned}
|f_1(t)| &\leq \gamma_g\,|y_2(t)-y_1(t)|\,,\ \text{and}\\
|f_2(t)| &\leq \gamma_Q\,|y_2(t)-y_1(t)|
\end{aligned}
$$

where

$$
\begin{aligned}
\gamma_g &= \max\left\{\frac{\beta_g}{1+z(0)\alpha_Q}-x_g,\ x_g-\frac{\alpha_g}{1+z(0)\beta_Q}\right\},\ \text{and}\\
\gamma_Q &= \max\left\{\frac{\beta_Q}{1+z(0)\beta_Q}-x_Q,\ x_Q-\frac{\alpha_Q}{1+z(0)\alpha_Q}\right\}.
\end{aligned}
$$

Thus

$$
\begin{aligned}
\left\|(f_1,\frac{1}{\gamma}f_2)\right\|^2_2 &= \int_0^t f_1(t)^2+\frac{1}{\gamma^2}f_2(t)^2\,dt\\
&\leq \int_0^t \gamma_g^2\,|y_2(t)-y_1(t)|^2+\left(\frac{\gamma_Q}{\gamma}\right)^2|y_2(t)-y_1(t)|^2\,dt\\
&= \left[\gamma_g+\left(\frac{\gamma_Q}{\gamma}\right)^2\right]\int_0^t|y_2(t)-y_1(t)|^2\,dt\\
&= \left[\gamma_g^2+\left(\frac{\gamma_Q}{\gamma}\right)^2\right]\|y_2-y_1\|_2^2\,.
\end{aligned}
$$

We thus obtain the bound

$$\begin{aligned}\|Ty_1 - Ty_2\|_2 &\leq \sup_{\omega\in\mathbb{R}}\left[\left|\frac{\hat{z}(\omega)}{1+x_g\hat{z}(\omega)+x_Q\hat{u}(\omega)}\right|^2+\left|\gamma\frac{\hat{u}(\omega)}{1+x_g\hat{z}(\omega)+x_Q\hat{u}(\omega)}\right|^2\right]^{\frac{1}{2}} \\ &\quad \left[\gamma_g^2+\left(\frac{\gamma_Q}{\gamma}\right)^2\right]^{\frac{1}{2}}\|y_2-y_1\|_2\,.\end{aligned}$$

It follows that we can apply the contraction mapping fixed point theorem on $L_2(0,\infty)$ provided that there are x_g, x_Q and γ such that with $K(s)$ as defined on page 92, $1+K(s)\neq 0$ for $\sigma\geq 0$, and

$$\sup_{\omega\in\mathbb{R}}\left[\left|\frac{\hat{z}(\omega)}{1+x_g\hat{z}(\omega)+x_Q\hat{u}(\omega)}\right|^2+\left|\gamma\frac{\hat{u}(\omega)}{1+x_g\hat{z}(\omega)+x_Q\hat{u}(\omega)}\right|^2\right]^{\frac{1}{2}}\left[\gamma_g^2+\left(\frac{\gamma_Q}{\gamma}\right)^2\right]^{\frac{1}{2}}<1.$$

7.1.1 Comments

It is clear that using similar arguments than the ones presented above, another bound on $\|Ty_1 - Ty_2\|_2$ that can be obtained directly from (7.2) is

$$\begin{aligned}\|Ty_1 - Ty_2\|_2 &\leq \gamma_g\sup_{\omega\in\mathbb{R}}\left|\frac{\hat{z}(\omega)}{1+x_g\hat{z}(\omega)+x_Q\hat{u}(\omega)}\right|+\gamma_Q\sup_{\omega\in\mathbb{R}}\left|\frac{\hat{u}(\omega)}{1+x_g\hat{z}(\omega)+x_Q\hat{u}(\omega)}\right| \\ &\stackrel{\text{def}}{=} M_2.\end{aligned}$$

One can show that the bound in the previous section is always at least as good as this bound as follows. (In practice it is often much better since the maxima of the functions $\left|[1+x_g\hat{z}(\omega)+x_Q\hat{u}(\omega)]^{-1}\,\hat{z}(\omega)\right|$ and $\left|[1+x_g\hat{z}(\omega)+x_Q\hat{u}(\omega)]^{-1}\,\hat{u}(\omega)\right|$ often occur at different values of ω.) Let M be the bound obtained in the previous section, i.e.

$$M=\sup_{\omega\in\mathbb{R}}\left[\left|\frac{\hat{z}(\omega)}{1+x_g\hat{z}(\omega)+x_Q\hat{u}(\omega)}\right|^2+\left|\gamma\frac{\hat{u}(\omega)}{1+x_g\hat{z}(\omega)+x_Q\hat{u}(\omega)}\right|^2\right]^{\frac{1}{2}}\left[\gamma_g^2+\left(\frac{\gamma_Q}{\gamma}\right)^2\right]^{\frac{1}{2}}$$

and define p_1 and p_2 as

$$\begin{aligned}p_1 &= \sup_{\omega\in\mathbb{R}}\left|\frac{\hat{z}(\omega)}{1+x_g\hat{z}(\omega)+x_Q\hat{u}(\omega)}\right|, \text{ and} \\ p_2 &= \sup_{\omega\in\mathbb{R}}\left|\frac{\hat{u}(\omega)}{1+x_g\hat{z}(\omega)+x_Q\hat{u}(\omega)}\right|.\end{aligned}$$

Then

$$\begin{aligned} M &= \sup_{\omega\in\mathbb{R}}\left[\left|\frac{\hat{z}(\omega)}{1+x_g\hat{z}(\omega)+x_Q\hat{u}(\omega)}\right|^2+\left|\gamma\frac{\hat{u}(\omega)}{1+x_g\hat{z}(\omega)+x_Q\hat{u}(\omega)}\right|^2\right]^{\frac{1}{2}} \\ &\quad \left[\gamma_g^2+\left(\frac{\gamma_Q}{\gamma}\right)^2\right]^{\frac{1}{2}} \\ &\leq \left[\sup_{\omega\in\mathbb{R}}\left|\frac{\hat{z}(\omega)}{1+x_g\hat{z}(\omega)+x_Q\hat{u}(\omega)}\right|^2+\sup_{\omega\in\mathbb{R}}\left|\gamma\frac{\hat{u}(\omega)}{1+x_g\hat{z}(\omega)+x_Q\hat{u}(\omega)}\right|^2\right]^{\frac{1}{2}} \\ &\quad \left[\gamma_g^2+\left(\frac{\gamma_Q}{\gamma}\right)^2\right]^{\frac{1}{2}} \\ &= \left[p_1^2+\gamma^2p_2^2\right]^{\frac{1}{2}}\left[\gamma_g^2+\left(\frac{\gamma_Q}{\gamma}\right)^2\right]^{\frac{1}{2}} \end{aligned}$$

and

$$M_2 = p_1\gamma_g + p_2\gamma_Q.$$

By the Cauchy-Schwarz inequality,

$$\begin{aligned} M &\leq \left[p_1^2+\gamma^2p_2^2\right]^{\frac{1}{2}}\left[\gamma_g^2+\left(\frac{\gamma_Q}{\gamma}\right)^2\right]^{\frac{1}{2}} \\ &\geq p_1\gamma_g + p_2\gamma_Q \end{aligned}$$

with equality holding in the last inequality above only if

$$(p_1, \gamma p_2) = \delta\left(\gamma_g, \frac{\gamma_Q}{\gamma}\right) \tag{7.3}$$

for some real number δ. This means we can minimize

$$\left[p_1^2+\gamma^2p_2^2\right]^{\frac{1}{2}}\left[\gamma_g^2+\left(\frac{\gamma_Q}{\gamma}\right)^2\right]^{\frac{1}{2}}$$

if we choose γ such that (7.3) is satisfied. It follows that we need $\delta = p_1/\gamma_g$ and $\gamma = [(p_1\gamma_Q)/(p_2\gamma_g)]^{\frac{1}{2}}$. With this value of γ we have

$$M \leq \left[p_1^2+\gamma^2p_2^2\right]^{\frac{1}{2}}\left[\gamma_g^2+\left(\frac{\gamma_Q}{\gamma}\right)^2\right]^{\frac{1}{2}}$$

$$
\begin{aligned}
&= p_1\gamma_g + p_2\gamma_Q \\
&= M_2.
\end{aligned}
$$

If the functions e_1 and e_2 defined by

$$
\begin{aligned}
e_1(\omega) &= \left| \frac{\hat{z}(\omega)}{1 + x_g\hat{z}(\omega) + x_Q\hat{u}(\omega)} \right| \text{ and} \\
e_2(\omega) &= \left| \frac{\hat{u}(\omega)}{1 + x_g\hat{z}(\omega) + x_Q\hat{u}(\omega)} \right|
\end{aligned}
$$

attain their maxima at the same value of ω, then the above bound on M is equal to M and the optimal value of γ is $[(p_1\gamma_Q)/(p_2\gamma_g)]^{\frac{1}{2}}$. In this case M and M_2 are also equal.

Another extreme case which may approximately hold is if the support e_1 and e_2 are disjoint sets. In this case

$$
M = \max\{p_1, \gamma p_2\} \left[\gamma_g^2 + \left(\frac{\gamma_Q}{\gamma} \right)^2 \right]^{\frac{1}{2}}.
$$

We have two cases to consider. The first case is when $\gamma p_2 \geq p_1$. In this case we have

$$
\begin{aligned}
M^2 &= \gamma^2 p_2^2 \left(\gamma_g^2 + \left(\frac{\gamma_Q}{\gamma} \right)^2 \right) \\
&= \gamma_g^2 p_2^2 \gamma^2 + p_2^2 \gamma_Q^2
\end{aligned}
$$

and M is minimized by choosing γ as small as possible while still satisfying $\gamma \geq p_1/p_2$. With $\gamma = p_1/p_2$ we have

$$
\begin{aligned}
M &= \left(\gamma_g^2 p_2^2 \left(\frac{p_1}{p_2} \right)^2 + p_2^2 \gamma_Q^2 \right)^{\frac{1}{2}} \\
&= \left(p_1^2 \gamma_g^2 + p_2^2 \gamma_Q^2 \right)^{\frac{1}{2}}.
\end{aligned}
$$

The second case is when $p_1 \geq \gamma p_2$. In this case we have

$$
\begin{aligned}
M^2 &= p_1^2 \left(\gamma_g^2 + \left(\frac{\gamma_Q}{\gamma} \right)^2 \right) \\
&= p_1^2 \gamma_g^2 + p_1^2 \left(\frac{\gamma_Q}{\gamma} \right)^2
\end{aligned}
$$

and M is minimized by choosing γ as large as possible while still satisfying $\gamma \leq p_1/p_2$. With $\gamma = p_1/p_2$ we have

$$\begin{aligned} M &= \left(p_1^2\gamma_g^2 + p_1^2\gamma_Q^2 \left(\frac{p_2}{p_1}\right)^2 \right)^{\frac{1}{2}} \\ &= \left(p_1^2\gamma_g^2 + p_2^2\gamma_Q^2\right)^{\frac{1}{2}}. \end{aligned}$$

In practice none of the extreme cases usually hold and we are forced to search for a γ that works using optimization. The two special cases, namely $\gamma = [(p_1\gamma_Q)/(p_2\gamma_g)]^{0.5}$ and $\gamma = p_1/p_2$ can be used as initial estimates in the optimization process.

For M_2, using arguments similar to those in [23], it is possible to show that the choice of

$$\begin{aligned} x_g &= 0.5(\alpha_1 + \beta_1) \stackrel{\text{def}}{=} \delta_g \text{ and} \\ x_Q &= 0.5(\alpha_2 + \beta_2) \stackrel{\text{def}}{=} \delta_Q \end{aligned}$$

where

$$\begin{aligned} \alpha_1 &= \frac{\alpha_g}{1 + z(0)\beta_Q} \\ \beta_1 &= \frac{\beta_g}{1 + z(0)\alpha_Q} \\ \alpha_2 &= \frac{\alpha_Q}{1 + z(0)\alpha_Q} \\ \beta_2 &= \frac{\beta_Q}{1 + z(0)\beta_Q} \end{aligned}$$

is optimal in the following sense. Let

$$\begin{aligned} \mathcal{C} &= \{(x_g, x_Q) : (I + x_gL_g + x_QL_Q) \text{ has a bounded inverse on } L_2(0,\infty)\}, \\ \eta_g(x_g) &= \max\{x_g - \alpha_1, \beta_1 - x_g\}, \\ \eta_Q(x_Q) &= \max\{x_Q - \alpha_2, \beta_2 - x_Q\}, \\ r(x_g, x_Q) &= \left\| [I + x_gL_g + x_QL_Q]^{-1} L_g \right\|_2 \eta_g(x_g) \\ &\quad + \left\| [I + x_gL_g + x_QL_Q]^{-1} L_Q \right\|_2 \eta_Q(x_Q). \end{aligned}$$

We will prove the equivalent of Theorem 3 of [23], namely that if there are $(x_g, x_Q) \in \mathcal{C}$ such that $r(x_g, x_Q) < 1$, then $(\delta_g, \delta_Q) \in \mathcal{C}$ and $r(\delta_g, \delta_Q) \leq r(x_g, x_Q)$.

We note the following facts regarding η_g (and η_Q). Firstly, $\eta_g(\delta_g) = 0.5(\beta_1 - \alpha_1)$. Secondly, if $\beta_1 - x_g \geq x_g - \alpha_1$, then $\eta_g(x_g) = \beta_1 - x_g$ and we have

$$\begin{aligned} & \beta_1 - x_g \geq x_g - \alpha_1 \\ & \Rightarrow x_g \leq 0.5(\alpha_1 + \beta_1) = \delta_g \\ & \Rightarrow \delta_g - x_g \geq 0 \end{aligned}$$

and thus

$$\begin{aligned} \eta_g(x_g) &= \beta_1 - x_g \\ &= \beta_1 - \delta_g + \delta_g - x_g \\ &= 0.5(\beta_1 - \alpha_1) + |\delta_g - x_g| \\ &= \eta_g(\delta_g) + |\delta_g - x_g| \,. \end{aligned}$$

Similarly, if $\beta_1 - x_g \leq x_g - \alpha_1$, then $\eta_g(x_g) = x_g - \alpha_1$ and we have

$$\begin{aligned} & \beta_1 - x_g \leq x_g - \alpha_1 \\ & \Rightarrow x_g \geq 0.5(\alpha_1 + \beta_1) = \delta_g \\ & \Rightarrow x_g - \delta_g \geq 0 \end{aligned}$$

and thus

$$\begin{aligned} \eta_g(x_g) &= x_g - \alpha_1 \\ &= x_g - \delta_g + \delta_g - \alpha_1 \\ &= |x_g - \delta_g| + 0.5(\beta_1 - \alpha_1) \\ &= \eta_g(\delta_g) + |x_g - \delta_g| \,. \end{aligned}$$

So, in summary and using the same arguments for η_Q, we have

$$\begin{aligned} \eta_g(x_g) &= \eta_g(\delta_g) + |x_g - \delta_g| \text{ and} \\ \eta_Q(x_Q) &= \eta_Q(\delta_Q) + |x_Q - \delta_Q| \,. \end{aligned}$$

Now assume that $(x_g, x_Q) \in \mathcal{C}$ and that $r(x_g, x_Q) < 1$ and consider the invertability of $(I + \delta_g L_g + \delta_Q L_Q)$.

Then

$$\begin{aligned} & I + \delta_g L_g + \delta_Q L_Q \\ &= I + x_g L_g + x_Q L_Q + (\delta_g - x_g) L_g + (\delta_Q - x_Q) L_Q \\ &= (I + x_g L_g + x_Q L_Q) \Big(I + (\delta_g - x_g) (I + x_g L_g + x_Q L_Q)^{-1} L_g \\ &\quad + (\delta_Q - x_Q) (I + x_g L_g + x_Q L_Q)^{-1} L_Q \Big) \\ &= (I + x_g L_g + x_Q L_Q) (I + G) \end{aligned}$$

where

$$G = (\delta_g - x_g) (I + x_g L_g + x_Q L_Q)^{-1} L_g + (\delta_Q - x_Q) (I + x_g L_g + x_Q L_Q)^{-1} L_Q.$$

Since

$$\begin{aligned} \|G\|_2 &\leq |\delta_g - x_g| \left\| (I + x_g L_g + x_Q L_Q)^{-1} L_g \right\|_2 \\ &\quad + |\delta_Q - x_Q| \left\| (I + x_g L_g + x_Q L_Q)^{-1} L_Q \right\|_2 \\ &\leq \eta_g(x_g) \left\| (I + x_g L_g + x_Q L_Q)^{-1} L_g \right\|_2 \\ &\quad + \eta_Q(x_Q) \left\| (I + x_g L_g + x_Q L_Q)^{-1} L_Q \right\|_2 \\ &= r(x_g, x_Q) \\ &< 1, \end{aligned}$$

$(I + G)$ is invertible [8, p.375], and thus also $(I + \delta_g L_g + \delta_Q L_Q)$.

We also have

$$\begin{aligned} & r(\delta_g, \delta_Q) \\ &= \eta_g(\delta_g) \left\| (I + \delta_g L_g + \delta_Q L_Q)^{-1} L_g \right\|_2 + \eta_Q(\delta_Q) \left\| (I + \delta_g L_g + \delta_Q L_Q)^{-1} L_Q \right\|_2 \\ &= (\eta_g(x_g) - |x_g - \delta_g|) \left\| (I + \delta_g L_g + \delta_Q L_Q)^{-1} L_g \right\|_2 + \\ &\quad (\eta_Q(x_Q) - |x_Q - \delta_Q|) \left\| (I + \delta_g L_g + \delta_Q L_Q)^{-1} L_Q \right\|_2 \end{aligned}$$

$$
\begin{aligned}
&= \eta_g(x_g) \left\| (I + x_g L_g + x_Q L_Q)^{-1} L_g + (I + \delta_g L_g + \delta_Q L_Q)^{-1} L_g \right. \\
&\quad \left. - (I + x_g L_g + x_Q L_Q)^{-1} L_g \right\|_2 \\
&\quad - |x_g - \delta_g| \left\| (I + \delta_g L_g + \delta_Q L_Q)^{-1} L_g \right\|_2 \\
&\quad + \eta_Q(x_Q) \left\| (I + x_g L_g + x_Q L_Q)^{-1} L_Q + (I + \delta_g L_g + \delta_Q L_Q)^{-1} L_Q \right. \\
&\quad \left. - (I + x_g L_g + x_Q L_Q)^{-1} L_Q \right\|_2 \\
&\quad - |x_Q - \delta_Q| \left\| (I + \delta_g L_g + \delta_Q L_Q)^{-1} L_Q \right\|_2 \\
&\leq \eta_g(x_g) \left\| (I + x_g L_g + x_Q L_Q)^{-1} L_g \right\|_2 \\
&\quad + \eta_g(x_g) \left\| (I + \delta_g L_g + \delta_Q L_Q)^{-1} L_g - (I + x_g L_g + x_Q L_Q)^{-1} L_g \right\|_2 \\
&\quad - |x_g - \delta_g| \left\| (I + \delta_g L_g + \delta_Q L_Q)^{-1} L_g \right\|_2 \\
&\quad + \eta_Q(x_Q) \left\| (I + x_g L_g + x_Q L_Q)^{-1} L_Q \right\|_2 \\
&\quad + \eta_Q(x_Q) \left\| (I + \delta_g L_g + \delta_Q L_Q)^{-1} L_Q - (I + x_g L_g + x_Q L_Q)^{-1} L_Q \right\|_2 \\
&\quad - |x_Q - \delta_Q| \left\| (I + \delta_g L_g + \delta_Q L_Q)^{-1} L_Q \right\|_2 .
\end{aligned}
$$

Since

$$
\begin{aligned}
&(I + \delta_g L_g + \delta_Q L_Q)^{-1} - (I + x_g L_g + x_Q L_Q)^{-1} \\
&\quad = (I + \delta_g L_g + \delta_Q L_Q)^{-1} \left[(I + x_g L_g + x_Q L_Q) \right. \\
&\qquad \left. - (I + \delta_g L_g + \delta_Q L_Q) \right] (I + x_g L_g + x_Q L_Q)^{-1} \\
&\quad = (x_g - \delta_g) (I + \delta_g L_g + \delta_Q L_Q)^{-1} L_g (I + x_g L_g + x_Q L_Q)^{-1} \\
&\qquad + (x_Q - \delta_Q) (I + \delta_g L_g + \delta_Q L_Q)^{-1} L_Q (I + x_g L_g + x_Q L_Q)^{-1} ,
\end{aligned}
$$

we have (for the sum of the second and fifth terms in our bound on $r(\delta_g, \delta_Q)$)

$$
\begin{aligned}
&\eta_g(x_g) \left\| (I + \delta_g L_g + \delta_Q L_Q)^{-1} L_g - (I + x_g L_g + x_Q L_Q)^{-1} L_g \right\|_2 \\
&\qquad + \eta_Q(x_Q) \left\| (I + \delta_g L_g + \delta_Q L_Q)^{-1} L_Q - (I + x_g L_g + x_Q L_Q)^{-1} L_Q \right\|_2 \\
&\quad \leq \eta_g(x_g) |x_g - \delta_g| \left\| (I + \delta_g L_g + \delta_Q L_Q)^{-1} L_g (I + x_g L_g + x_Q L_Q)^{-1} L_g \right\|_2 \\
&\qquad + \eta_g(x_g) |x_Q - \delta_Q| \left\| (I + \delta_g L_g + \delta_Q L_Q)^{-1} L_Q (I + x_g L_g + x_Q L_Q)^{-1} L_g \right\|_2
\end{aligned}
$$

$$
\begin{aligned}
&+ \eta_Q(x_Q)\,|x_g-\delta_g|\left\|(I+\delta_g L_g+\delta_Q L_Q)^{-1}L_g\,(I+x_g L_g+x_Q L_Q)^{-1}L_Q\right\|_2\\
&+ \eta_Q(x_Q)\,|x_Q-\delta_Q|\left\|(I+\delta_g L_g+\delta_Q L_Q)^{-1}L_Q\,(I+x_g L_g+x_Q L_Q)^{-1}L_Q\right\|_2\\
\leq\ & |x_g-\delta_g|\left\|(I+\delta_g L_g+\delta_Q L_Q)^{-1}L_g\right\|_2\left[\left\|(I+x_g L_g+x_Q L_Q)^{-1}L_g\right\|_2\eta_g(x_g)\right.\\
&\left.+\left\|(I+x_g L_g+x_Q L_Q)^{-1}L_Q\right\|_2\eta_Q(x_Q)\right]\\
&+|x_Q-\delta_Q|\left\|(I+\delta_g L_g+\delta_Q L_Q)^{-1}L_Q\right\|_2\\
&\left[\left\|(I+x_g L_g+x_Q L_Q)^{-1}L_g\right\|_2\eta_g(x_g)+\left\|(I+x_g L_g+x_Q L_Q)^{-1}L_Q\right\|_2\eta_Q(x_Q)\right]\\
=\ &\left(|x_g-\delta_g|\left\|(I+\delta_g L_g+\delta_Q L_Q)^{-1}L_g\right\|_2\right.\\
&\left.+|x_Q-\delta_Q|\left\|(I+\delta_g L_g+\delta_Q L_Q)^{-1}L_Q\right\|_2\right)r(x_g,x_Q)
\end{aligned}
$$

Noting that the sum of the first and fourth terms in our bound on $r(\delta_g,\delta_Q)$ is equal to $r(x_g,x_Q)$ and using our bound above for the sum of the second and fifth terms we have

$$
\begin{aligned}
&r(\delta_g,\delta_Q)\\
&\quad\leq\ r(x_g,x_Q)\\
&\qquad+r(x_g,x_Q)\,|x_g-\delta_g|\left\|(I+\delta_g L_g+\delta_Q L_Q)^{-1}L_g\right\|_2\\
&\qquad-|x_g-\delta_g|\left\|(I+\delta_g L_g+\delta_Q L_Q)^{-1}L_g\right\|_2\\
&\qquad+r(x_g,x_Q)\,|x_Q-\delta_Q|\left\|(I+\delta_g L_g+\delta_Q L_Q)^{-1}L_Q\right\|_2\\
&\qquad-|x_Q-\delta_Q|\left\|(I+\delta_g L_g+\delta_Q L_Q)^{-1}L_Q\right\|_2\\
&\quad=\ r(x_g,x_Q)\\
&\qquad+(r(x_g,x_Q)-1)\,|x_g-\delta_g|\left\|(I+\delta_g L_g+\delta_Q L_Q)^{-1}L_g\right\|_2\\
&\qquad+(r(x_g,x_Q)-1)\,|x_Q-\delta_Q|\left\|(I+\delta_g L_g+\delta_Q L_Q)^{-1}L_Q\right\|_2.
\end{aligned}
$$

Since $r(x_g,x_Q)<1$, the last two terms added to $r(x_g,x_Q)$ in the above equation are not positive, thus

$$
r(\delta_g,\delta_Q)\leq r(x_g,x_Q).
$$

In obtaining M_2, we made use of arguments similar to those of Lemma 5 of [14] to show that

$$\left\|\left(I + x_g L_g + x_Q L_Q\right)^{-1} L_g\right\|_2 \leq \sup_{\omega\in\mathbb{R}} \left|\frac{\hat{z}(\omega)}{1 + x_g\hat{z}(\omega) + x_Q\hat{u}(\omega)}\right|.$$

We can replace "less than or equal" in the above relation with equality by noting that

$$\frac{\hat{z}(\omega)}{1 + x_g\hat{z}(\omega) + x_Q\hat{u}(\omega)}$$

is a continuous function of ω since, as pointed out in Lemma 5 of [14],

$$\inf_{\omega\in\mathbb{R}} |1 + x_g\hat{z}(\omega) + x_Q\hat{u}(\omega)| > 0,$$

and $\hat{z}$ and $\hat{u}$ are continuous functions that tend to zero as the magnitude of their arguments tend to infinity by the Riemann-Lebesgue lemma [1, p. 76] and hence, for any $0 < \varepsilon < 1$, there is an interval $[a, b] \subset \mathbb{R}$ with $0 < a < b$ such that

$$\left|\frac{\hat{z}(\omega)}{1 + x_g\hat{z}(\omega) + x_Q\hat{u}(\omega)}\right| > (1-\varepsilon)\sup_{y\in\mathbb{R}}\left|\frac{\hat{z}(y)}{1 + x_g\hat{z}(y) + x_Q\hat{u}(y)}\right|,\ \omega \in [a, b].$$

It is also easy to show that the Fourier transform $\hat{f}$ of the function f defined by

$$f(t) = \begin{cases} \sin\left(0.5[a+b]t\right),\ 0 \leq t \leq T \\ 0,\ \text{otherwise} \end{cases}$$

has the property that for T sufficiently large,

$$\frac{1}{\sqrt{2\pi}}\left(\int_{-b}^{-a}\left|\hat{f}(\omega)\right|^2 d\omega + \int_a^b \left|\hat{f}(\omega)\right|^2 d\omega\right)^{\frac{1}{2}} \geq (1-\varepsilon)\left\|f\right\|_2.$$

If

$$h = \left(I + x_g L_g + x_Q L_Q\right)^{-1} L_g f,$$

then

$$\begin{aligned} L_g f &= \left(I + x_g L_g + x_Q L_Q\right) h = h + x_g L_g h + x_Q L_Q h \\ \Rightarrow \hat{z}\hat{f} &= \hat{h} + x_g\hat{z}\hat{h} + x_Q\hat{u}\hat{h} \\ \Rightarrow \hat{h}(\omega) &= \frac{\hat{z}(\omega)}{1 + x_g\hat{z}(\omega) + x_Q\hat{u}(\omega)}\hat{f}(\omega),\ \omega \in \mathbb{R} \end{aligned}$$

and we have

$$\begin{aligned}
\|h\|_2^2 &= \frac{1}{2\pi}\left\|\hat{h}\right\|_{2(-\infty,\infty)}^2 \\
&= \frac{1}{2\pi}\int_{-\infty}^{\infty}\left|\frac{\hat{z}(\omega)}{1+x_g\hat{z}(\omega)+x_Q\hat{u}(\omega)}\right|^2\left|\hat{f}(\omega)\right|^2 d\omega \\
&\geq \frac{1}{2\pi}\left(\int_{-b}^{-a}\left|\frac{\hat{z}(\omega)}{1+x_g\hat{z}(\omega)+x_Q\hat{u}(\omega)}\right|^2\left|\hat{f}(\omega)\right|^2 d\omega\right. \\
&\quad \left.+\int_a^b\left|\frac{\hat{z}(\omega)}{1+x_g\hat{z}(\omega)+x_Q\hat{u}(\omega)}\right|^2\left|\hat{f}(\omega)\right|^2 d\omega\right) \\
&\geq \frac{1}{2\pi}\left((1-\varepsilon)^2\sup_{\omega\in\mathbb{R}}\left|\frac{\hat{z}(\omega)}{1+x_g\hat{z}(\omega)+x_Q\hat{u}(\omega)}\right|^2\right. \\
&\quad \left.\left[\int_{-b}^{-a}\left|\hat{f}(\omega)\right|^2 d\omega+\int_a^b\left|\hat{f}(\omega)\right|^2 d\omega\right]\right) \\
&\geq \frac{1}{2\pi}\left((1-\varepsilon)^2\sup_{\omega\in\mathbb{R}}\left|\frac{\hat{z}(\omega)}{1+x_g\hat{z}(\omega)+x_Q\hat{u}(\omega)}\right|^2 2\pi\left(1-\varepsilon\right)^2\|f\|_2^2\right) \\
&= (1-\varepsilon)^4\sup_{\omega\in\mathbb{R}}\left|\frac{\hat{z}(\omega)}{1+x_g\hat{z}(\omega)+x_Q\hat{u}(\omega)}\right|^2\|f\|_2^2.
\end{aligned}$$

Thus

$$\left\|\left(I+x_gL_g+x_QL_Q\right)^{-1}L_g\right\|_2 \geq (1-\varepsilon)^2\sup_{\omega\in\mathbb{R}}\left|\frac{\hat{z}(\omega)}{1+x_g\hat{z}(\omega)+x_Q\hat{u}(\omega)}\right|$$

but since ε was an arbitrary number in $(0,1)$, we have

$$\left\|\left(I+x_gL_g+x_QL_Q\right)^{-1}L_g\right\|_2 \geq \sup_{\omega\in\mathbb{R}}\left|\frac{\hat{z}(\omega)}{1+x_g\hat{z}(\omega)+x_Q\hat{u}(\omega)}\right|$$

and an entirely similar argument shows that also

$$\left\|\left(I+x_gL_g+x_QL_Q\right)^{-1}L_Q\right\|_2 \geq \sup_{\omega\in\mathbb{R}}\left|\frac{\hat{u}(\omega)}{1+x_g\hat{z}(\omega)+x_Q\hat{u}(\omega)}\right|.$$

This means that

$$\begin{aligned}
M_2 &= \gamma_g\sup_{\omega\in\mathbb{R}}\left|\frac{\hat{z}(\omega)}{1+x_g\hat{z}(\omega)+x_Q\hat{u}(\omega)}\right|+\gamma_Q\sup_{\omega\in\mathbb{R}}\left|\frac{\hat{u}(\omega)}{1+x_g\hat{z}(\omega)+x_Q\hat{u}(\omega)}\right| \\
&= \eta_g(x_g)\left\|\left(I+x_gL_g+x_QL_Q\right)^{-1}L_g\right\|_2 \\
&\quad +\eta_Q(x_Q)\left\|\left(I+x_gL_g+x_QL_Q\right)^{-1}L_Q\right\|_2 \\
&= r\left(x_g,x_Q\right)
\end{aligned}$$

so that the choice $x_g = \delta_g$ and $x_Q = \delta_Q$ is optimal in obtaining the smallest possible value for M_2.

7.2 An Example

Our example again concerns the circuit shown in Figure 5.1, with parameters as in Table 5.1. This circuit exhibits period doubling as shown in Chapter 5. It is possible to stabilize this circuit (i.e. prevent the period doubling behavior) by placing a linear resistor, R_2, parallel to the varactor. Using the stability criterion for varactor circuits in Theorem 1 one can show that this circuit is stable if this resistor is less than 36.0185 Ω. If we apply the theory presented in this Chapter, we can prove that the circuit is stable[1] if we replace R_2 with a nonlinear resistor, as long as the largest incremental resistance of the nonlinear resistor is less than 25 Ω. Since nonlinear resistors in practical problems often have very small minimum resistances, this is a very satisfying result. Table 7.1 summarizes the experimental results. Figure 7.2 shows the maximum value of β_g corresponding to each value of α_g for which one can prove the existence of a contraction mapping operator on $L_2(0,\infty)$ corresponding to the varactor circuit of Figure 5.1 using both the M and M_2 estimates. The maximum value of R_2 for which the stability of the varactor circuit can be proved is also plotted. The advantage of the tighter bound M over M_2 in this problem is obvious from Figure 7.2. The bound M is tighter because the maxima of the functions e_1 and e_2 do not occur at the same frequency. This is shown in Figures 7.3–7.4.

We showed that the choice $(x_Q, x_g) = (\delta_Q, \delta_g)$ is optimal when using the bound M_2 for c. It is worth noting that experimentally this choice is also optimal for the estimate M.

[1]Admittedly with only the contraction mapping in $L_2(0,\infty)$ proven, we cannot prove the same strong stability results as in Theorem 1. We do however fully expect that it is possible to obtain the same stronger results now that we have the $L_2(0,\infty)$ results in hand.

Table 7.1: Summary of experimental results. The table lists the minimum incremental conductance (α_g) and corresponding maximum incremental conductance (β_g) of a nonlinear resistor that can be placed in parallel with the varactor in Figure 5.1 for which it can be proved that we can obtain a contraction mapping on $L_2(0,\infty)$. The bounds M and M_2 are also given. The values of γ used to obtain the results as well as the estimates $[(p_1\gamma_Q)/(p_2\gamma_g)]^{\frac{1}{2}}$ and p_1/p_2 are listed in Table 7.2.

α_g	β_g	M	M_2
0.03775	0.22265	0.9999967	1.0275
0.038	0.92652	0.99999997	1.1149
0.039	22.885	0.999999998	1.0176
0.04	> 10000	0.99999992	1.00004
0.04	0.1117	0.9876	0.9996
0.05	0.2682	0.9651	0.9999898
0.06	0.3452	0.9503	0.99998
0.1	0.5463	0.9177	0.999987
0.2	1.329	0.9213	0.99996
0.3	3.144	0.9495	0.999995
0.4	10.53	0.98	0.99999985
0.5	> 10000	0.99997	0.99999798

Table 7.2: The values of γ used to obtain the results in Table 7.1 as well as the estimates $[(p_1\gamma_Q)/(p_2\gamma_g)]^{\frac{1}{2}}$ and p_1/p_2.

α_g	β_g	γ	$[(p_1\gamma_Q)/(p_2\gamma_g)]^{\frac{1}{2}}$	p_1/p_2
0.03775	0.22265	3.5412×10^{-5}	3.4518×10^{-5}	4.9376×10^{-5}
0.038	0.92652	1.6979×10^{-5}	1.1577×10^{-5}	2.4766×10^{-5}
0.039	22.885	3.5827×10^{-6}	1.5134×10^{-6}	1.0668×10^{-5}
0.04	> 10000	1.7372×10^{-7}	7.0135×10^{-8}	1.002×10^{-5}
0.04	0.1117	5.2686×10^{-5}	5.2666×10^{-5}	5.1607×10^{-5}
0.05	0.2682	3.1032×10^{-5}	3.1032×10^{-5}	4.7618×10^{-5}
0.06	0.3452	2.6122×10^{-5}	2.6122×10^{-5}	4.3737×10^{-5}
0.1	0.5463	1.7977×10^{-5}	1.7977×10^{-5}	3.2611×10^{-5}
0.2	1.329	8.9368×10^{-6}	8.9368×10^{-6}	1.9965×10^{-5}
0.3	3.144	4.8678×10^{-6}	4.8678×10^{-6}	1.4439×10^{-5}
0.4	10.53	2.3277×10^{-6}	2.3277×10^{-6}	1.1397×10^{-5}
0.5	> 10000	7.0136×10^{-8}	7.0136×10^{-8}	1.002×10^{-5}

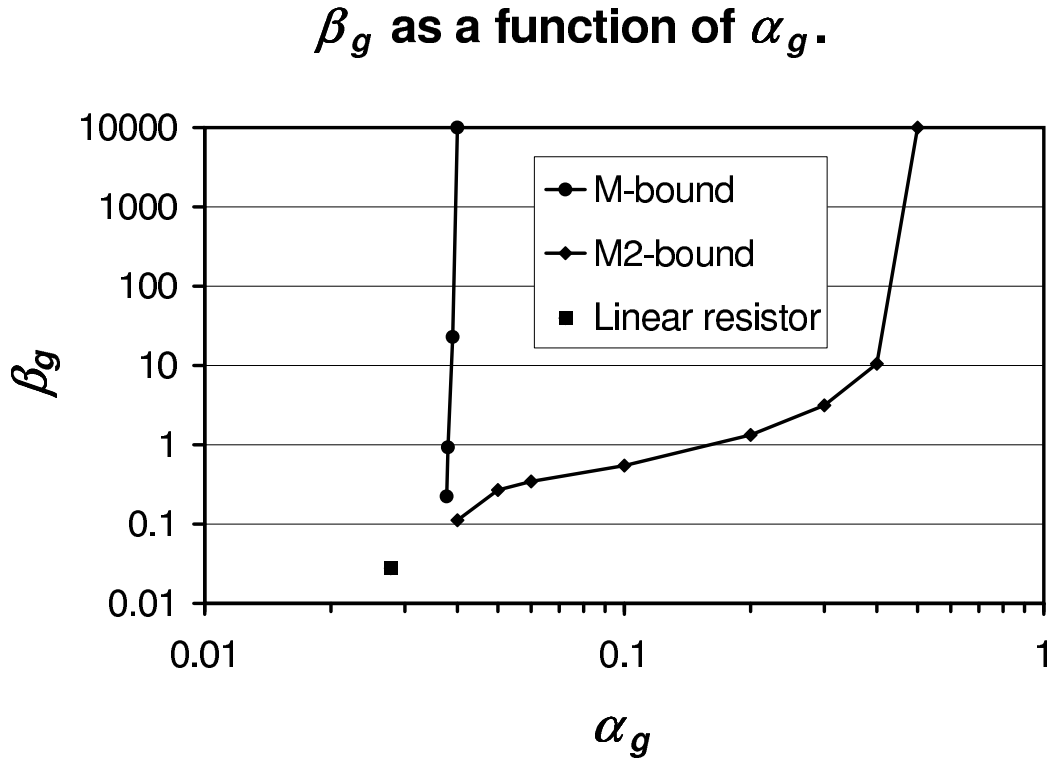

Figure 7.2: The maximum value of β_g corresponding to each value of α_g for which one can prove the existence of a contraction mapping operator on $L_2(0,\infty)$ corresponding to the varactor circuit of Figure 5.1 using both the M and M_2 estimates. The maximum value of a linear resistor, R_2, placed parallel to the varactor for which the stability of the varactor circuit can be proved is also plotted.

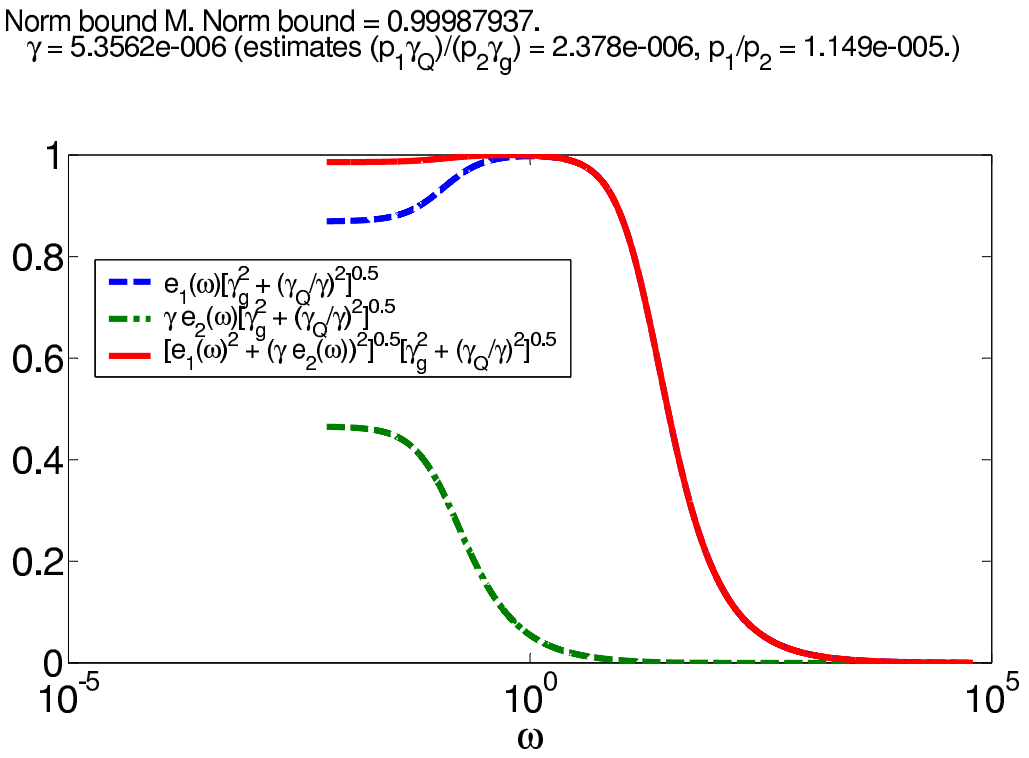

Figure 7.3: Plots of the functions $e_1(\omega)\left[\gamma_g^2+(\gamma_Q/\gamma)^2\right]^{\frac{1}{2}}$, $\gamma e_2(\omega)\left[\gamma_g^2+(\gamma_Q/\gamma)^2\right]^{\frac{1}{2}}$ and $\left(e_1^2(\omega)+[\gamma e_2(\omega)]^2\right)^{\frac{1}{2}}\left[\gamma_g^2+(\gamma_Q/\gamma)^2\right]^{\frac{1}{2}}$ corresponding to the circuit of Figure 5.1 for $\alpha_g = 0.04$ and $\beta_g = 10$. This is one example where the maxima of the functions e_1 and e_2 are at different frequencies allowing a tighter bound using M than M_2.

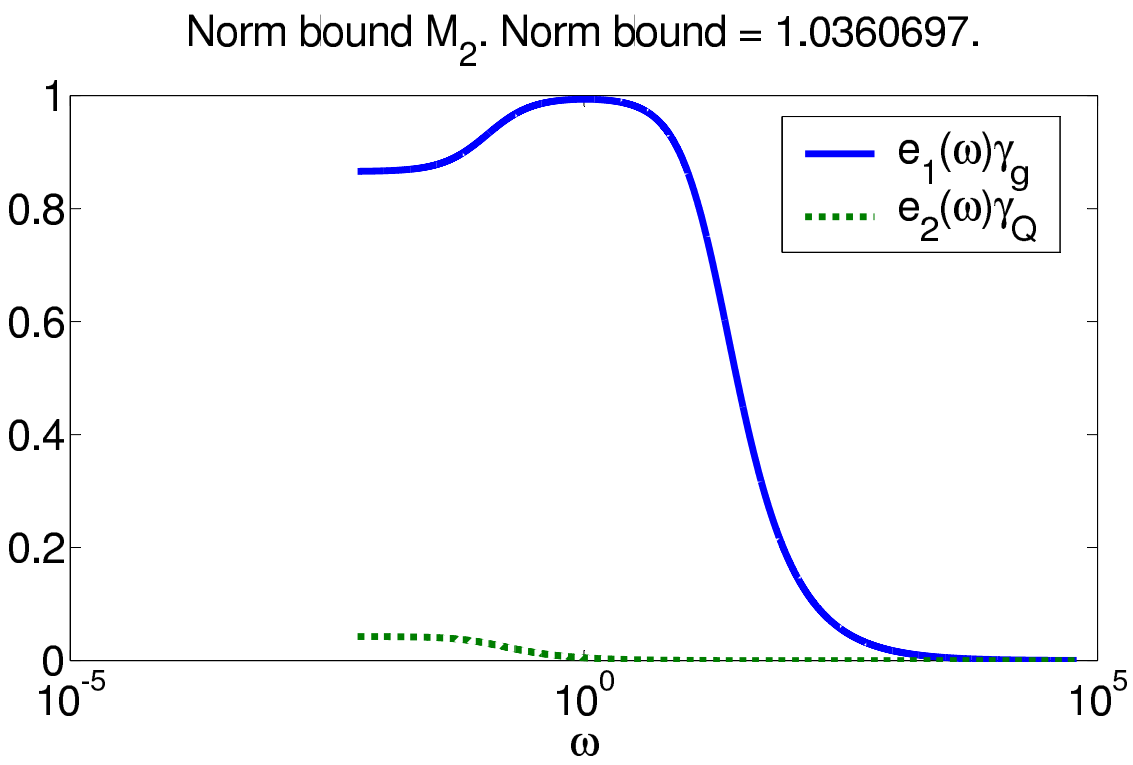

Figure 7.4: Plots of the functions $\gamma_g e_1(\omega)$ and $\gamma_Q e_2(\omega)$ corresponding to the circuit of Figure 5.1 for $\alpha_g = 0.04$ and $\beta_g = 10$. M_2 is the sum of the maxima of these two functions.

Chapter 8

Some Comments on a Perturbational Method of Determining the Stability of Periodic Steady States in Nonlinear Systems

In [10] a perturbation technique for analyzing the stability of periodic steady-state regimes in nonlinear microwave circuits is introduced. The method appears to have reasonable accuracy and has found wide application in both original and modified versions of the theory [26], [25], [30], [29], [27].

This kind of perturbational analysis can be carried out on many circuits and systems that do not satisfy the conditions of the theorems presented in this dissertation. Here we examine one such method, point out a potential problem and suggest a method for working around the problem.

8.1 Introduction

In [10] the analysis starts with the calculated periodic steady state solution, $\tilde{i}$ and $\tilde{v}$, of a nonlinear microwave circuit. The periodic steady state solutions take the form

$$\begin{aligned}\tilde{i}(t) &= \mathrm{Re}\left[\sum_{k=0}^{\infty}\tilde{I}_k\exp(jk\omega_0 t)\right]\\ \tilde{v}(t) &= \mathrm{Re}\left[\sum_{k=0}^{\infty}\tilde{V}_k\exp(jk\omega_0 t)\right].\end{aligned}$$

Conditions are then sought under which $\tilde{i}+\Delta i$ and $\tilde{v}+\Delta v$ can also solve the circuit equations where Δi and Δv are of the form

$$\begin{aligned}\Delta i(t) &= \exp(\sigma t)\cdot\mathrm{Re}\left[\sum_{k=-\infty}^{\infty}\Delta I_k\exp\{j(\omega+k\omega_0)t\}\right]\\ \Delta v(t) &= \exp(\sigma t)\cdot\mathrm{Re}\left[\sum_{k=-\infty}^{\infty}\Delta V_k\exp\{j(\omega+k\omega_0)t\}\right].\end{aligned}$$

It is shown that the conditions are met if the equation

$$\sum_{k=-\infty}^{\infty}A_{k,r-k}\Delta V_k = 0,\ \ -\infty < r < \infty$$

is satisfied in which A is an infinite matrix that depends on the circuit, the steady state solution $\tilde{i}$, $\tilde{v}$ as well as σ and ω. In [10] the system is reduced to a finite system of equations

$$\sum_{k=-N}^{N}A_{k,r-k}\Delta V_k = 0,\ \ -N \le r \le N, \tag{8.1}$$

the determinant of the matrix A (which we will refer to as the system matrix) is denoted by $\Delta(\sigma+j\omega)$, and the problem is reduced to establishing whether $\Delta(\sigma+j\omega)=0$ for some $\sigma>0$. This is done by applying Nyquist's analysis to $\Delta(\sigma+j\omega)$.

A number of steps are problematic.[1] Since this is such a widely accepted method it is worthwhile to examine some of the steps in more detail and try to determine the validity of these steps.

One claim that is made is that $\Delta(\sigma + j\omega)$ is periodic in ω with period $2\omega_0$ if the system is of infinite order. This, together with other claims, allow the Nyquist path to be restricted to an interval of length ω_0 on the imaginary axis.

In Section 8.5 it is shown that this claim does not follow from certain properties of the system matrix A as claimed in [10]. As shown in Section 8.2 it is possible to use a matrix truncation scheme that forces the determinant to be periodic in ω with period $2\omega_0$.

An alternative way of using the results in [10] is to not rely on the periodicity of the system determinant, but to use closed Nyquist paths in the complex plane to search for zeros of the determinant. In Section 8.3.1 we show that this seems to work, at least for a varactor circuit for which we can calculate the waveforms with reasonable confidence.

8.2 A Matrix Truncation Scheme to Restore Periodicity of the Determinant of the System Matrix

Although it has been shown that the periodicity of the determinant of the system matrix does not follow directly from the symmetry of the system matrix as claimed in [10], the problem under investigation is certainly periodic. As a matter of fact, if an infinite number of mixing products are considered and the perturbation frequency is changed by ω_0, the same mixing products as before the change are considered, as

[1] E.g. the large signal solution is found using numerical methods, typically harmonic balance. The harmonic balance solution may converge to a non-physical solution. Truncating the number of harmonics in the large signal solution and truncation of the system matrix A is not justified. The assumption that the determinant of the matrix is periodic in ω_0 may not always hold. The assumed forms of Δi and Δv are not justified.

a simple change in notation reveals.

The challenge is thus to come up with a mathematical formulation of the problem which preserves this periodicity in the determinant of the system matrix so that a finite section of the imaginary axis can be used in a Nyquist analysis.

The following matrix truncation scheme, although lacking physical interpretation, is proposed. Two fixed positive frequencies ω_l and ω_u are chosen such that both are smaller than $N\omega_0$ where the system matrix is truncated to a $2N+1$ by $2N+1$ matrix. All non-diagonal elements of the system matrix (i.e. all elements not lying on the main diagonal) in the columns k (where the columns of the system matrix are numbered from $-N$ to N) such that $\omega_l < |k\omega_0 + \omega| < \omega_u$ (where ω is the perturbation frequency) are reduced in magnitude by the factor

$$\frac{\omega_u - |k\omega_0 + \omega|}{\omega_u - \omega_l}.$$

All non-diagonal elements in columns k such that $|k\omega_0 + \omega| > \omega_u$ are set to zero. The real part of the diagonal elements are tapered to zero using the same scheme. The imaginary part of the diagonal elements are tapered not to zero, but to the imaginary part of the system matrix element on the diagonal in the column $\left\lfloor \frac{\omega_u}{\omega_0} \right\rfloor$ (where $\lfloor x \rfloor = \max\{n \in \mathbb{N} : n \leq x\}$) for zero perturbation frequency.

It is obvious that the determinant of this matrix is truly periodic for a number of changes in perturbation frequency by $2\omega_0$ up to the point where the non-truncated section of the system matrix starts to hit the boundaries of the $2N+1$ by $2N+1$ matrix being used for determinant calculation.

N can be increased at will, so that periodicity for any number of changes in perturbation frequency by ω_0 can be accommodated. The effect on the determinant of increasing N for fixed ω_l and ω_u for perturbation frequencies only a few ω_0 in magnitude is simply to multiply the determinant by the real number $|a_{1,1}|^2$ where $a_{m,n}$ is the element in the m-th row and $n-th$ column of A, the system matrix truncated as per the proposed scheme, so that the increase in size to infinity to

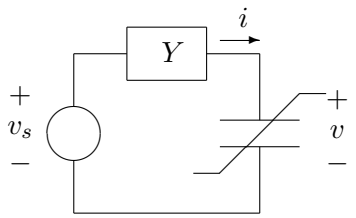

Figure 8.1: Varactor circuit.

obtain true periodicity simply results in a scaling of the determinant. Increasing N will thus not affect the Nyquist plot (except for simple linear scaling) and one can thus safely reduce the Nyquist contour to a finite section of the imaginary axis.

8.3 The Analysis of a Simple Varactor Frequency Divider

Consider the varactor circuit of Figure 8.1 in which the charge stored in the varactor, q, at a voltage, v, is given by the equation

$$q = Q(v).$$

With $\dot{v}$ defined by $\dot{v}(t) = \dfrac{d}{dt}v(t)$, the varactor current and voltage satisfy the equation

$$-i + Q'(v)\dot{v} = 0$$

where $Q'(v) = \dfrac{d}{dv}Q(v)$. In the notation of [10, (1)], this is

$$0 = f[F^0 i, F^0 v, F^1 v] = -F^0 i + Q'(F^0 v)F^1 v.$$

In the notation of [10, (10)] we thus have

$$\begin{aligned} x_0 &= F^0 i \\ y_0 &= F^0 v \\ y_1 &= F^1 v. \end{aligned}$$

With $\sim$ indicating that we evaluate the partial derivatives in the steady state conditions (i.e. $i = \tilde{i}$ and $v = \tilde{v}$), we have

$$\begin{aligned}
\left.\frac{\partial f}{\partial x_0}\right|_{\sim}(t) &= -1 \stackrel{\text{def}}{=} \sum_{p=-\infty}^{\infty} C_{0,p} e^{jp\omega_0 t} \\
\left.\frac{\partial f}{\partial y_0}\right|_{\sim}(t) &= \left[F^1 \tilde{v} Q''(F^0 \tilde{v})\right](t) \stackrel{\text{def}}{=} \sum_{p=-\infty}^{\infty} D_{0,p} e^{jp\omega_0 t} \approx \sum_{p=-P}^{P} D_{0,p} e^{jp\omega_0 t} \quad (8.2) \\
\left.\frac{\partial f}{\partial y_1}\right|_{\sim}(t) &= \left[Q'(F^0 \tilde{v})\right](t) \stackrel{\text{def}}{=} \sum_{p=-\infty}^{\infty} D_{1,p} e^{jp\omega_0 t} \approx \sum_{p=-P}^{P} D_{1,p} e^{jp\omega_0 t} \quad (8.3)
\end{aligned}$$

where $Q''(F^0\tilde{v})$ is the second derivative of $Q(v)$ with respect to v evaluated at $\tilde{v}$.

For the varactor circuit $A_{k,p}(\sigma + j\omega)$[2] as defined in [10, (14)] is thus given by

$$A_{k,p}(\sigma + j\omega) = \begin{cases} D_{0,0} + (\sigma + j\omega + jk\omega_0)D_{1,0} + Y(\sigma + j\omega + jk\omega_0), & p = 0 \\ D_{0,p} + (\sigma + j\omega + jk\omega_0)D_{1,p}, & p \neq 0. \end{cases}$$

As noted in [10, (20)], for fixed p and k large and positive

$$A_{-k,p}(\sigma + j\omega) \approx (-1)^n A_{k,p}(\sigma + j\omega). \quad (8.4)$$

Here n is the highest derivative appearing in f. For the varactor circuit $n = 1$. This follows from

$$A_{k,p}(\sigma + j\omega) \approx \begin{cases} jk\omega_0 D_{1,0} + Y(jk\omega 0), & p = 0 \\ jk\omega_0 D_{1,p}, & p \neq 0 \end{cases}$$

and assuming that

$$Y(\sigma + jk\omega) \approx Y(jk\omega) \approx -Y(-jk\omega) \approx -Y(\sigma - jk\omega)$$

or

$$|jk\omega_0 D_{1,0}| >> |Y(\sigma + jk\omega)|$$

for k large. (These last assumptions are not explicitly made in [10]. The first is true if the admittance Y is shunted by a small capacitor as is commonly assumed

[2] In [10] the dependence of $A_{k,p}$ on σ and ω is suppressed in most equations, i.e. $A_{k,p}(\sigma + j\omega)$ is written simply as $A_{k,p}$

and $\sigma \approx 0$. The second is true if $D_{1,0} > 0$ (which will be the case if the incremental capacitance of the varactor is positive for all voltages) and the Thévenin equivalent impedance contains a series resistor as the first element so that $|Y(\sigma + jk\omega)|$ is bounded.)

In addition it is noted that

$$A_{k,r-k}(\sigma + j[\omega + h\omega_0]) = A_{k+h,r-k}(\sigma + j\omega). \tag{8.5}$$

In [10] it is argued that these two properties ((8.4) and (8.5)) imply that the determinant of the system

$$\sum_{k=-\infty}^{\infty} A_{k,r-k}\Delta V_k = 0, -\infty < r < \infty$$

is periodic in ω.

In Section 8.5 it is shown that the periodicity of the system matrix does not follow from these two properties. This presents a problem as the ability to restrict the Nyquist path to a section on the imaginary axis of the complex plane relies on this periodicity. It should be noted that in many practical problems this periodicity does approximately hold. In fact, even for our counter example in Section 8.5, if we reduce the magnitude of the off-diagonal terms to less than 0.5 this periodicity holds to a high degree of accuracy. On the other hand, we also have examples of circuits in which this periodicity does not hold and we have to use the techniques presented in Section 8.2 to achieve periodicity.

8.3.1 Avoiding issues with periodicity

We again consider the circuit shown in Figure 5.1 with parameters as in Table 5.1. In this circuit the incremental varactor capacitance (i.e. the slope of the plot of charge stored versus voltage) is piecewise linear with one value, C_p, if the voltage is positive and another, C_m, if the voltage is negative.

Using the method of harmonic balance, we obtain an unstable non-period-doubling solution as well as a stable period doubling solution. These solutions are shown in Figures 8.2 and 8.3.

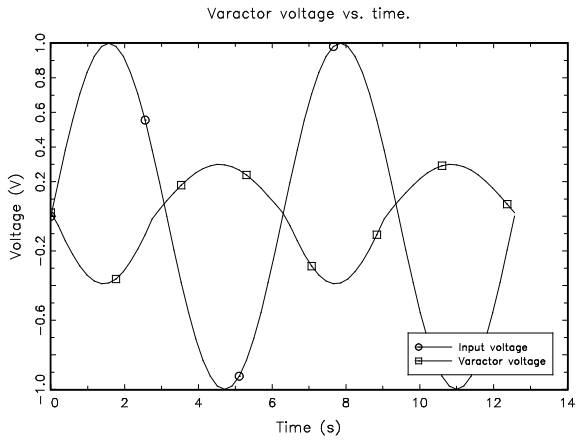

Figure 8.2: Unstable varactor voltage waveform.

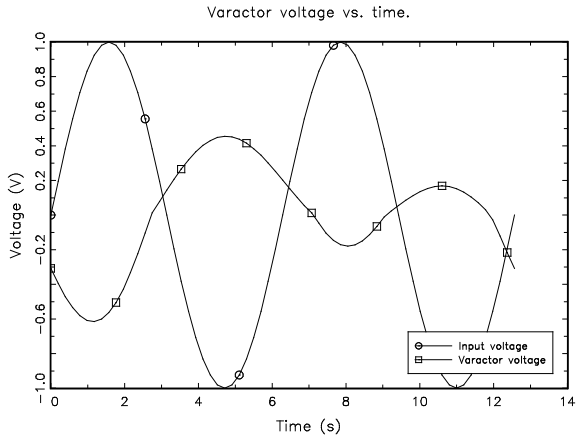

Figure 8.3: Stable varactor voltage waveform.

By numerically finding the unstable fixed point (in the two dimensional state space of zero crossing time and inductor current at the zero crossing) for this circuit, and then perturbing the solution, we can solve for the varactor voltage and current in the time domain. Using the obtained time domain waveform of the perturbed

solution, we find that the difference between the perturbed and unperturbed unstable solutions is a real exponential function (i.e. a function of the form $e^{\sigma t}$) mixed with harmonics of the input signal. The difference between the unperturbed and perturbed unstable solutions for the varactor current is shown in Figure 8.4.

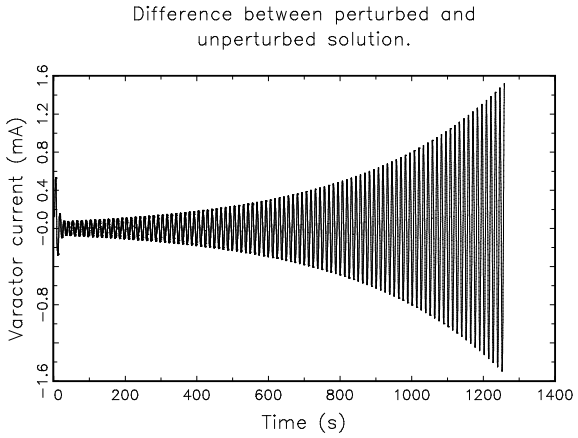

Figure 8.4: The difference between the unperturbed and perturbed unstable solutions for the varactor current.

If this difference is multiplied with the function $e^{-0.00247t}$ (of time t), the waveform shown in Figure 8.5 results. It is seen that this is a function that is periodic with the period of input. In terms of the theory presented in [10], the perturbed signal is thus a real exponential function mixed with the harmonics of the input, corresponding to a zero of the generalized eigenvalue problem located at $0.00247 + 0i$ in the complex plane.

By plotting the determinant of the system matrix along circles in the complex plane and noting whether or not the origin is encircled, we can find the position of zeros. Using this method we find that for the stable period doubling waveform no zero is predicted in the circle centered at $0.00247 + 0j$ with radius 0.001235 . For the unstable waveform we predict a zero at $0.002323 + 0j$, which is fairly close the observed zero. By finding closed paths in which the zero is located and ones in which it is not, we can localize the predicted position as shown in Figure 8.6.

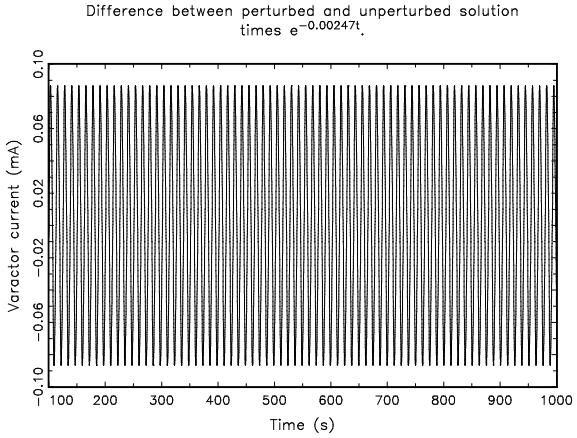

Figure 8.5: The difference between the unperturbed and perturbed unstable solutions for the varactor current multiplied by $e^{-0.00247t}$.

Figures 8.7 and 8.8 show the result of establishing whether or not a zero is located in the vicinity of $0.00247 + 0j$ for the unstable and stable waveforms, respectively. Figure 8.9 shows the predicted and observed locations of the generalized eigenvalue of the system matrix.

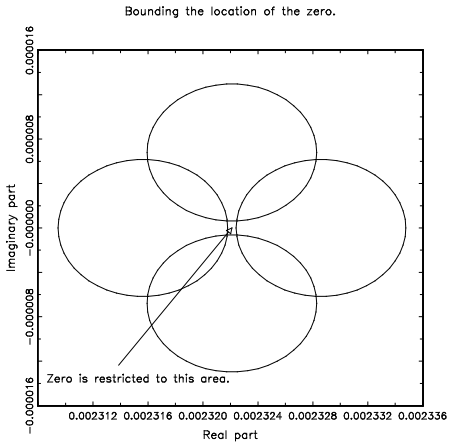

Figure 8.6: Contours used to localize the location of the zero of the generalized eigenvalue problem.

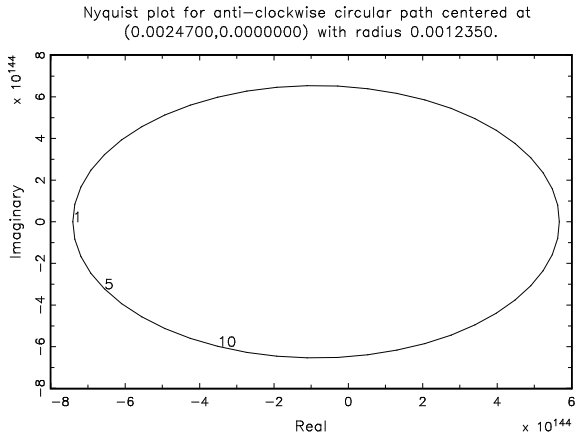

Figure 8.7: The value of the determinant of the system matrix along the circle centered at $0.00247 + 0j$ with radius 0.001235 for the unstable waveform indicating the presence of a zero of the generalized eigenvalue problem within this circle.

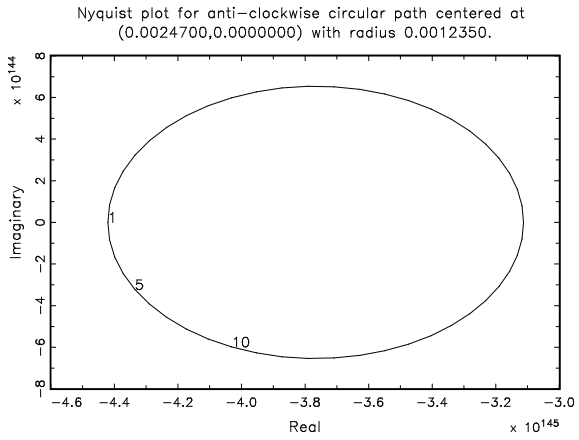

Figure 8.8: The value of the determinant of the system matrix along the circle centered at $0.00247 + 0j$ with radius 0.001235 for the stable waveform indicating the absence of a zero of the generalized eigenvalue problem within this circle.

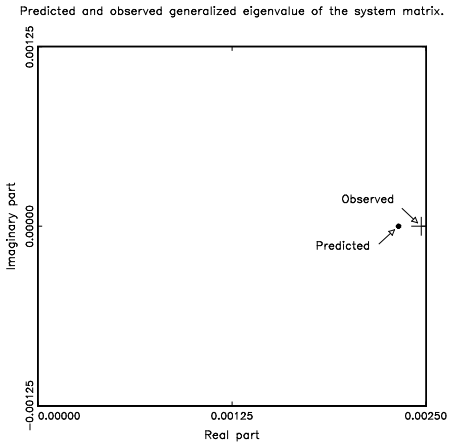

Figure 8.9: The observed and predicted locations of the zero of the generalized eigenvalue problem.

8.3.2 Applying Nyquist analysis to a section of the imaginary axis

The harmonic balance in the previous section was carried out using the modified circuit equations obtained by integrating by parts as is done in Chapter 2. In the transformed set of equations, the role of Y in Figure 8.1 is played by

$$Y(s) = -C^2Ls^2 - C^2Rs - C,$$

the varactor is transformed into a nonlinear resistor with an incremental conductance of $C(C_p - C)(C_p)^{-1}$ for positive voltages, and $C(C_m - C)(C_m)^{-1}$ for negative voltages and v is replaced by w where the correspondence between w and v is given by

$$w(t) = \begin{cases} (C_p/C)v(t), & t \in \{x \in [0,\infty) : v(x) \geq 0\} \\ (C_m/C)v(t), & t \in \{x \in [0,\infty) : v(x) < 0\}. \end{cases}$$

If the value of the determinant in this transformed domain for s going from $-j\omega_0/2$ to $j\omega_0/2$ is plotted as suggested in [10], we find that the plot for the stable period doubling waveform has one counter-clockwise encirclement of the origin and the plot for the unstable waveform does not encircle the origin. These Nyquist plots are shown in Figures 8.10–8.11.

If we carry out the Nyquist analysis in the regular current, voltage domain and plot the value of $e^{-j\pi\omega/\omega_0}\Delta(j\omega)$ for ω going from $-\omega_0/2$ to $\omega_0/2$, we find that the plot of stable waveform does not encircle the origin, whereas the plot of the unstable waveform has one clockwise encirclement of the origin. These Nyquist plots are shown in Figures 8.12–8.13. At least for this example the stability predictions using the Nyquist plots as suggested in [10] give the correct answers.

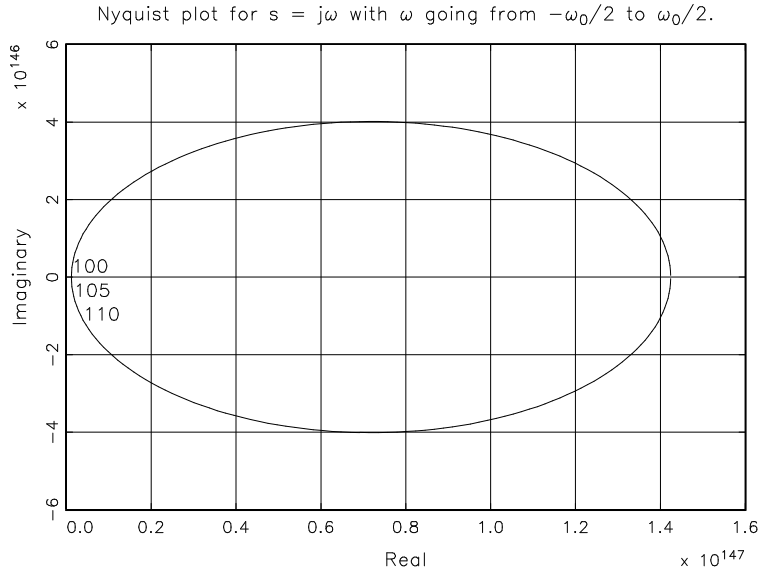

Figure 8.10: The determinant of the system matrix in the transformed domain for s going from $-j\omega_0/2$ to $j\omega_0/2$ on the imaginary axis for the unstable waveform.

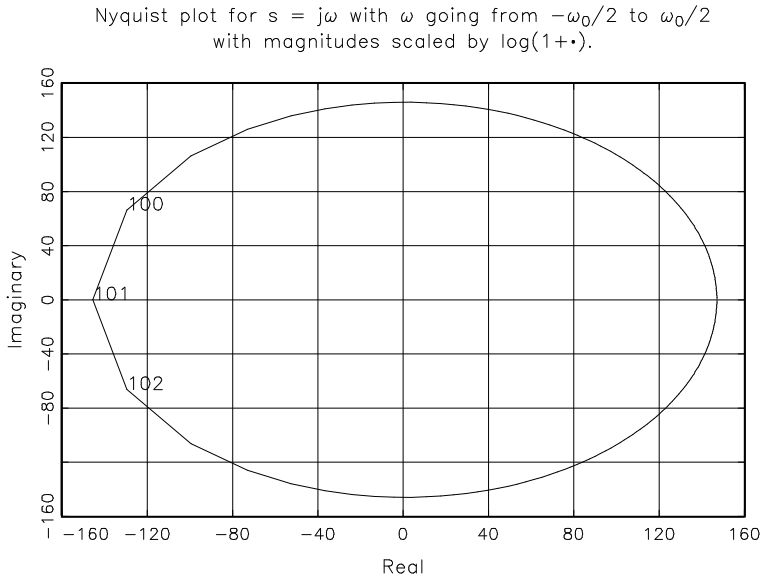

Figure 8.11: The determinant of the system matrix in the transformed domain for s going from $-j\omega_0/2$ to $j\omega_0/2$ on the imaginary axis for the stable waveform. In this plot the magnitude of complex numbers are scaled by $\log_{10}(1+\cdot)$.

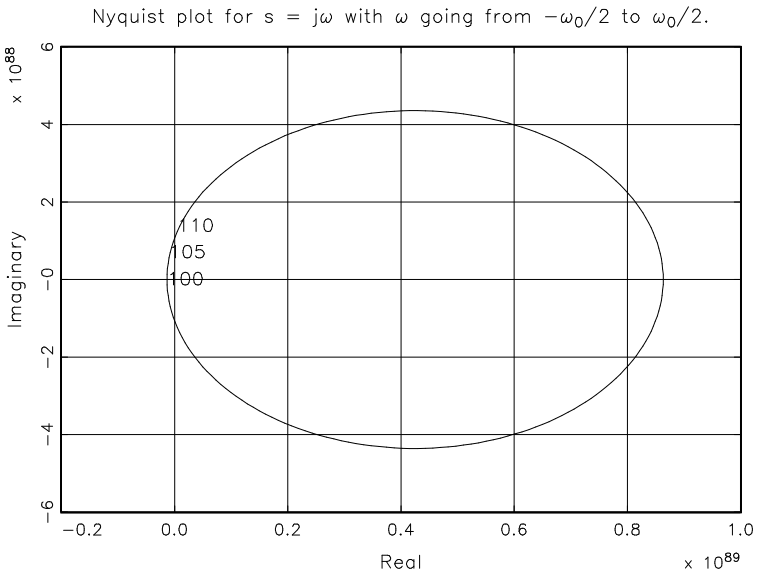

Figure 8.12: A plot of $e^{-j\pi\omega/\omega_0}\Delta(j\omega)$ in the regular current-voltage domain for w going from $-\omega_0/2$ to $\omega_0/2$ for the unstable waveform.

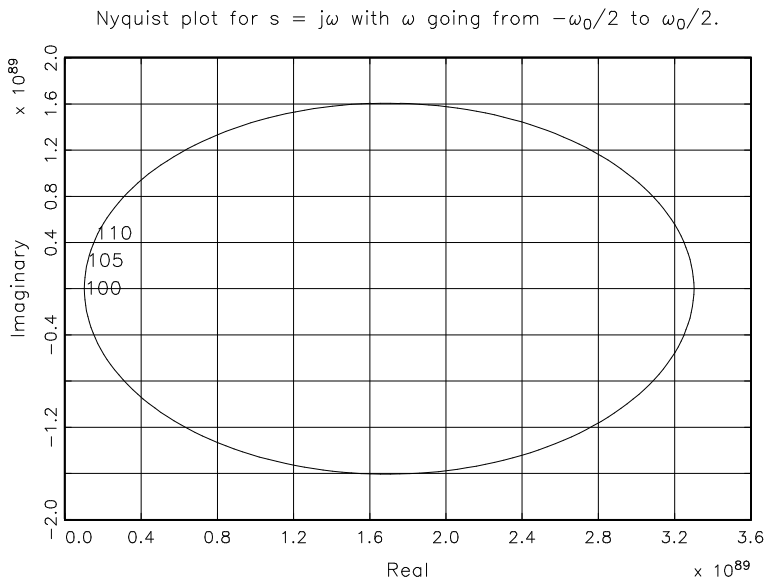

Figure 8.13: A plot of $e^{-j\pi\omega/\omega_0}\Delta(j\omega)$ in the regular current-voltage domain for w going from $-\omega_0/2$ to $\omega_0/2$ for the stable waveform.

8.4 The Analysis of a More Complex Microwave Frequency Divider

In [10] an example of a microwave frequency divider is given. We can use the same circuit to point out a few more things about this type of analysis.

The circuit shown in [10, Figure 2] is reproduced in Fig 8.14. The element values in [10] are unfortunately given in terms of microstrip lengths and widths on a substrate that is described simply as "1.58 mm DUROID". With Rogers DUROID available in different grades and with uncertainty in whether or not the model takes into account open end effects of the microstrip lines as well as uncertainty about some of the diode characteristics, it is not possible to exactly reproduce the results in [10]. The lengths and widths of the lines as well as the estimated impedance, delay and losses are given in Table 8.1. (The impedance, delay and losses were calculated assuming a dielectric thickness of 1.575 mm, dielectric constant of 2.2, dielectric loss tangent of 0.0007, pure copper, and a surface roughness of 1.4 μm.) The model assumed for the diode is shown in Figure 8.15. The intrinsic diode is described by the equation

$$i(t) = I_s \left(e^{\frac{v(t)}{V_b}} - 1 \right) + \left(\frac{C_{T0}}{\sqrt{1 - \frac{v(t)}{\phi}}} + C_{D0} e^{\frac{v(t)}{V_b}} \right) \frac{dv(t)}{dt}$$

with $I_s = 10^{-14}$, $V_b = 0.0442$, $\phi = 0.8$, $C_{T0} = 3.0625 \times 10^{-12}$, and $C_{D0} = \frac{30}{17} \times 10^{-15}$.

Using harmonic balance we obtain the efficiency (defined as the output power at 1.25 GHz divided by the available input power at 2.5 GHz) at a 2.5 GHz input as a function of the available input power as shown in Figure 8.16. Using 64 harmonics in the harmonic balance and keeping 40 harmonics in the system matrix (i.e. $P = 40$ in (8.2) and (8.3)) and using a 101×101 system matrix (i.e. $N = 50$ in 8.1), the stability predictions of Figure 8.17 result. The circuit was also simulated in Saber[3]

[3]Saber is a time domain simulator produced by Synopsys.

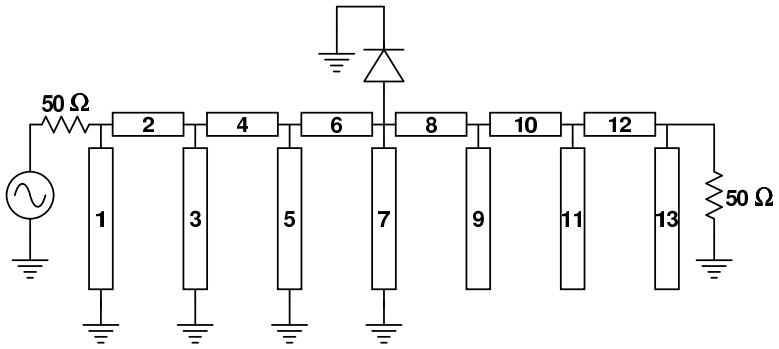

Figure 8.14: Microstip frequency divider.

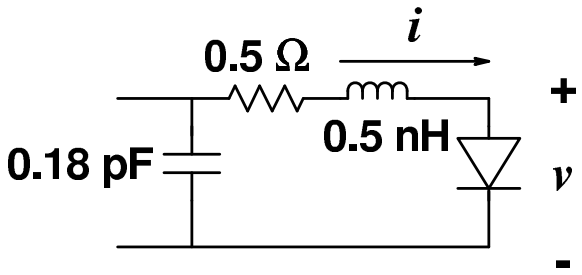

Figure 8.15: Model for the diode in Figure 8.14.

Table 8.1: Parameter values for the circuit of Figure 8.14.

Line	Width mm	Length mm	Impedance Ω	Delay ns	Loss dB/mm
1	8.9	25.4	32.22	0.119	6.5×10^{-4}
2	8.4	18.4	33.66	0.086	6.5×10^{-4}
3	6.6	34.1	40.17	0.158	6.6×10^{-4}
4	6.8	23.6	39.32	0.109	6.5×10^{-4}
5	8.1	19.9	34.59	0.093	6.5×10^{-4}
6	7.7	22.0	35.91	0.102	6.5×10^{-4}
7	8.9	14.0	32.22	0.065	6.5×10^{-4}
8	1.1	13.1	109.03	0.058	8.9×10^{-4}
9	6.1	20.7	42.47	0.096	6.6×10^{-4}
10	5.1	22.5	48.04	0.103	6.7×10^{-4}
11	4.6	14.3	51.44	0.065	6.7×10^{-4}
12	3.2	20.6	64.46	0.093	7×10^{-4}
13	1.3	24.4	101.74	0.108	8.5×10^{-4}

and the stability of the circuit compared with the predictions using the method of [10] as indicated in Figure 8.17. At reasonable input power levels the method of [10] as described here does a good job of predicting the stability of the circuit. At high input power (16, 18 and 19.5 dBm) the stable points of operation predicted are not observed using time domain simulation. The results in Figure 8.17 were produced without using the matrix truncation scheme suggested in Section 8.2. The results were compared with the case where the truncation scheme is used with $\omega_l = 0.9 \times N \times \omega_0$ and $\omega_u = 0.95 \times N \times \omega_0$ and very few differences were observed.

A plot of $e^{-j\pi\omega/\omega_0}\Delta(j\omega)$ as a function of ω as ω is swept from 0 to ω_0 corresponding to an input power level of 7.5 dBm and a period doubling output is shown in Figure 8.18.

For every input power level, harmonic balance can also find a solution without period doubling. (This of course demonstrates how misleading harmonic balance can be.) The number of clockwise encirclements of the origin by the $\Delta(j\omega)e^{-j\pi\omega/\omega_0}$ corresponding to these solutions as ω is swept from 0 to ω_0 as a function of the input power is shown in Figure 8.19. Figure 8.20 shows the number of zeros if we use the matrix truncation scheme suggested in Section 8.2 with $\omega_l = 0.9 \times N \times \omega_0$ and $\omega_u = 0.95 \times N \times \omega_0$. Some small differences are observed. Also shown are the stable non-period-doubling solutions obtained by Saber simulations. As for the period doubling case there is good agreement between the results of the analysis of [10] presented here and the time domain simulations.

The choice of $N = 50$ and $P = 40$ for these plots was not made quite arbitrarily. Three operating conditions were chosen and the accuracy of the method of [10] as described here was analyzed for these three points. The points were a non-period-doubling solution for an input power of -0.46 dBm which is known (from time domain simulations) to be stable, a non-period-doubling solution at 1.5 dBm input which is known to be unstable as well as a stable period doubling solution

corresponding to a 7.5 dBm input. A variety of choices of $N \in \{50, 51, \ldots, 80\}$ and $P \in \{15, 16, \ldots, 50\}$ were used to predict the stability of the periodic steady states. The specific choices that were tested are shown in Tables 8.2–8.4. For this particular circuit and set of conditions the method consistently predicts the stability of the periodic steady states correctly. This is not always the case as we show next.

With circuit parameters as described, the circuit of Fig 8.14 is well suited for the kind of analysis described in [10]. That is because 0.5 Ω series resistance of the diode limits the magnitude of the Thévenin equivalent admittance that is presented to the diode. The periodicity of $\Delta(j\omega)$ thus holds to a high degree of accuracy. If we make a few changes to the circuit including increasing the dielectric constant of the substrate to 2.5, decreasing the diode series resistance to 0.1 Ω, making the diode series inductance very small and changing the input frequency to 2.375 GHz, the analysis does not perform quite as well. From Figure 8.17 one should already suspect that the method is not very accurate at high input power. We thus evaluate the method at an available input power of 16 dBm and look at a non-period-doubling solution. Figure 8.21 shows a plot of $e^{-j\pi\omega/\omega_0}\Delta(j\omega)$ as a function of ω as ω is swept from 0 to ω_0 for $N = 64$ and $P = 35$. The first thing that we notice is that we don't have good periodicity. Figure 8.22 shows the same Nyquist plot with magnitudes scaled by $\log_{10}(1 + 10^4 \cdot)$. If we increase P to 38, the Nyquist plot shown in Figures. 8.23–8.24 results. In this case a change in P from 35 to 38 results in a change in the predicted stability of the periodic steady state. Figures 8.25–8.26 show that the periodicity of $\Delta(j\omega)$ may be recovered using the method of Section 8.2 with $\omega_l = 0.9 \times N \times \omega_0$ and $\omega_u = 0.95 \times N \times \omega_0$ without changing the stability prediction.

With the new parameters, the stability predictions for specific periodic steady states change as more harmonics, P, are taken into account. This is shown in Tables 8.5–8.7 where we consider a non-period-doubling periodic steady state for a

10 dBm input, a non-period-doubling periodic steady state for a 16 dBm input and a period doubling periodic steady state for a 8.5 dBm input.

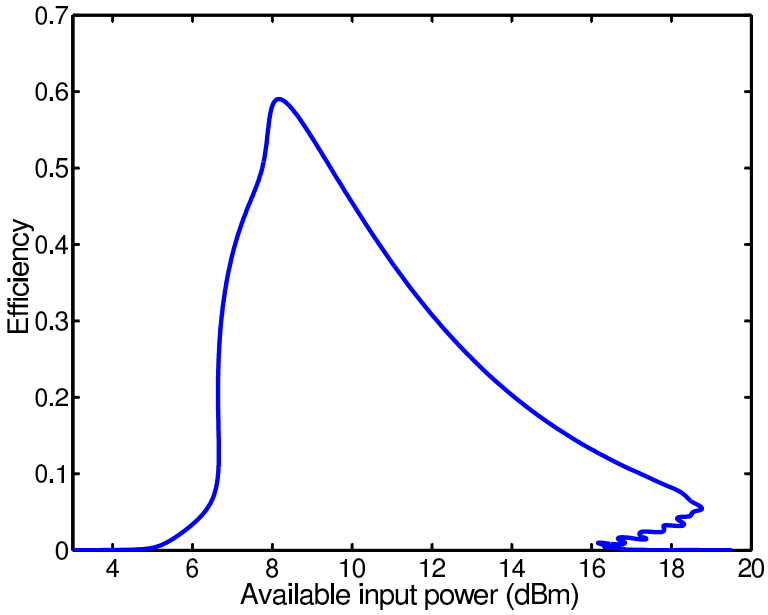

Figure 8.16: Efficiency (defined as the output power at 1.25 GHz divided by the available input power at 2.5 GHz) of the circuit of Figure 8.14 as a function of the available input power at 2.5 GHz obtained by harmonic balance using 64 harmonics.

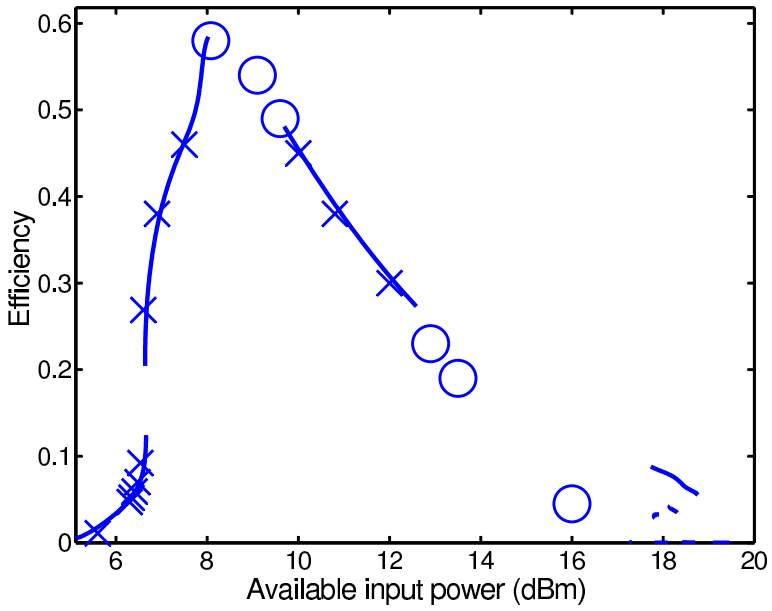

Figure 8.17: Stability of the circuit of Figure 8.14 as a function of the available input power. Stability predicted by the method of [10] as described here is indicated by plotting the efficiency using a solid line only where the circuit is predicted to be stable. Stable points of operation of the circuit verified by time domain simulations are indicated by crosses. Unstable points of operation as verified by time domain simulations are indicated by circles. The unstable operation observed includes generation of subharmonics of 1.25 GHz as well as completely chaotic (unpredictable from cycle to cycle) operation at 16, 18 and 19.5 dBm input levels. The last two points are not indicated on the figure as no efficiency could be assigned to these two points.

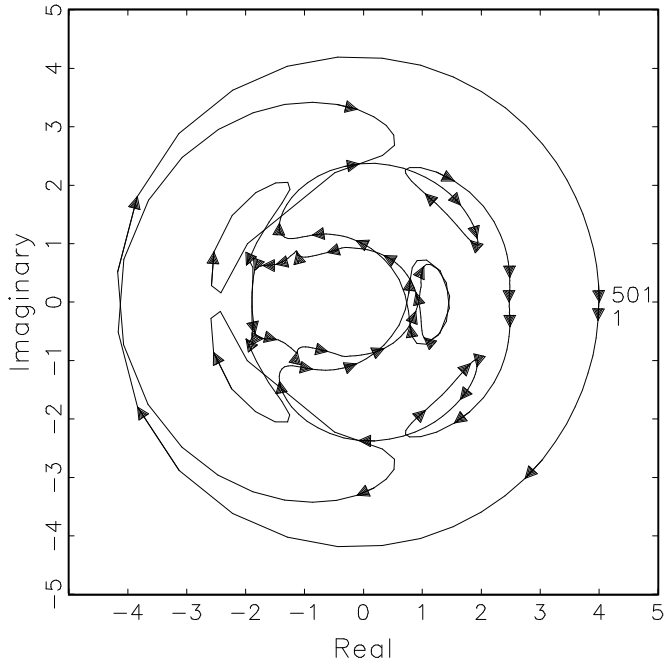

Figure 8.18: A plot of $e^{-j\pi\omega/\omega_0}\Delta(j\omega)$ as a function of ω as ω is swept from 0 to ω_0 corresponding to an input power level of 7.5 dBm and a period doubling output for the circuit of Figure 8.14.

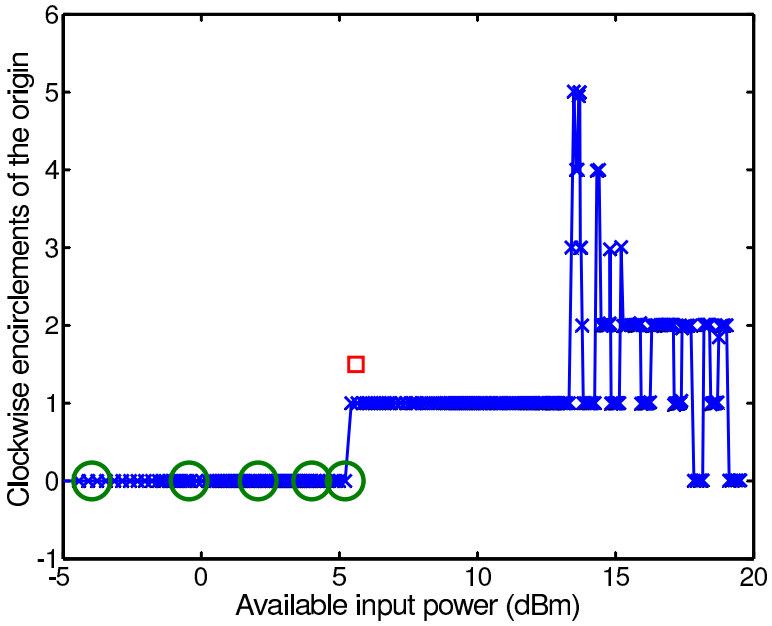

Figure 8.19: Stability of non-period-doubling outputs of the circuit of Figure 8.14 as a function of the available input power. Stability predicted using the method of [10] as described here is indicated by plotting the number of clockwise encirclements of the origin. (The periodic steady state solution is predicted to be unstable if the number of encirclements is positive.) Stable points of non-period-doubling operation of the circuit verified by time domain simulations are indicated by circles. The first input power level at which the time domain simulations indicate only a period doubling solution is indicated with a square.

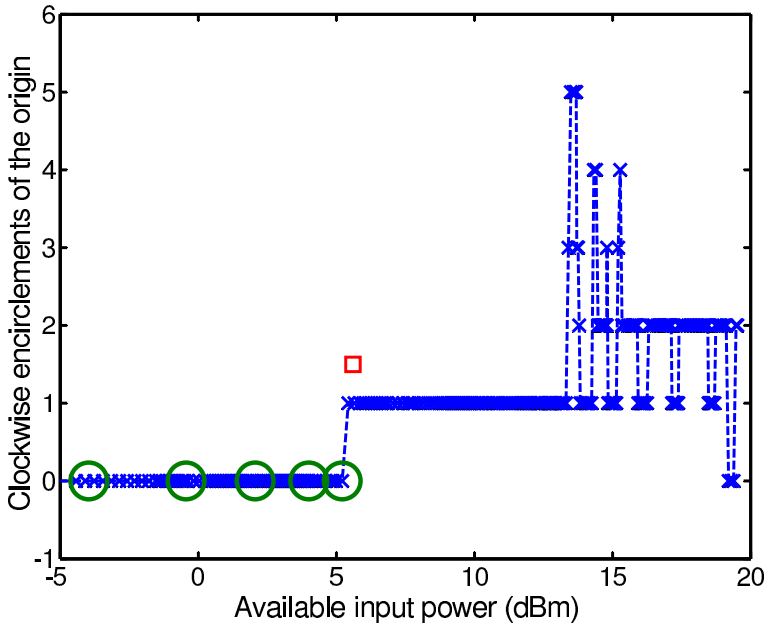

Figure 8.20: Stability of non-period-doubling outputs of the circuit of Figure 8.14 as a function of the available input power. Stability predicted using the method of [10] in combination with the matrix truncation scheme suggested in Section 8.2 with $\omega_l = 0.9 \times N \times \omega_0$ and $\omega_u = 0.95 \times N \times \omega_0$ is indicated by plotting the number of clockwise encirclements of the origin. Stable points of non-period-doubling operation of the circuit verified by time domain simulations are indicated by circles. The first input power level at which the time domain simulations indicate only a period doubling solution is indicated with a square.

Table 8.2: The number of clockwise encirclements of the origin that $e^{-j\pi\omega/\omega_0}\Delta(j\omega)$ makes as ω is swept from 0 to ω_0 as a function of the system matrix size, N in (8.1) in each row, and the number of harmonics, P in (8.2) and (8.3) in each column, for a non-period-doubling output of the circuit of Figure 8.14 with a -0.46 dBm input. From time domain simulations it is known that this is a stable periodic steady state condition.

	15	16	17	18	19	20	21	22	23	24	25	26	27	28	29	30	31	32	33	34	35	36	37	38	39	40	41	42	43	44	45	46	47	48	49	50
50	0	0	0	0	0	0					0					0					0					0										0	0
51	0																																			0
52	0																																			0
53	0																																			0
54	0																																			0
55	0																																			0
56																																				
57																																				
58																																				
59																																				
60	0															0					0					0										0	
61																																				
62																																				
63																																				
64																																				
65	0																																			0
66																																				
67																																				
68																																				
69																																				
70	0															0										0										0
71																																				
72																																				
73																																				
74																																				
75	0																																			0
76																																				
77																																				
78																																				
79																																				
80	0															0										0										0

Table 8.3: The number of clockwise encirclements of the origin that $e^{-j\pi\omega/\omega_0}\Delta(j\omega)$ makes as ω is swept from 0 to ω_0 as a function of the system matrix size, N in (8.1) in each row, and the number of harmonics, P in (8.2) and (8.3) in each column, for a non-period-doubling output of the circuit of Figure 8.14 with a 1.5 dBm input. From time domain simulations it is known that this is an unstable periodic steady state condition.

	15	16	17	18	19	20	21	22	23	24	25	26	27	28	29	30	31	32	33	34	35	36	37	38	39	40	41	42	43	44	45	46	47	48	49	50
50	1	1	1	1	1	1	1	1	1	1	1	1	1	1	1	1	1	1	1	1	1	1	1	1	1	1	1	1	1	1	1	1	1	1	1	
51	1																																			1
52	1																																			1
53	1																																			1
54	1																																			1
55	1																																			1
56																																				
57																																				
58																																				
59																																				
60	1															1										1										1
61																																				
62																																				
63																																				
64																																				
65	1																																			1
66																																				
67																																				
68																																				
69																																				
70	1															1										1										1
71																																				
72																																				
73																																				
74																																				
75	1																																			1
76																																				
77																																				
78																																				
79																																				
80	1															1										1										1

Table 8.4: The number of clockwise encirclements of the origin that $e^{-j\pi\omega/\omega_0}\Delta(j\omega)$ makes as ω is swept from 0 to ω_0 as a function of the system matrix size, N in (8.1) in each row, and the number of harmonics, P in (8.2) and (8.3) in each column, for a period doubling output of the circuit of Figure 8.14 with a 1.5 dBm input. From time domain simulations it is known that this is a stable periodic steady state condition.

	15	16	17	18	19	20	21	22	23	24	25	26	27	28	29	30	31	32	33	34	35	36	37	38	39	40	41	42	43	44	45	46	47	48	49	50
50	0	0	0	0	0	0					0					0					0					0									0	
51	0																																			0
52	0																																			0
53	0																																			0
54	0																																			0
55	0																																			0
56																																				
57																																				
58																																				
59																																				
60	0															0										0										0
61																																				
62																																				
63																																				
64																																				
65	0																																			0
66																																				
67																																				
68																																				
69																																				
70	0															0										0										0
71																																				
72																																				
73																																				
74																																				
75	0																																			0
76																																				
77																																				
78																																				
79																																				
80	0															0										0										0

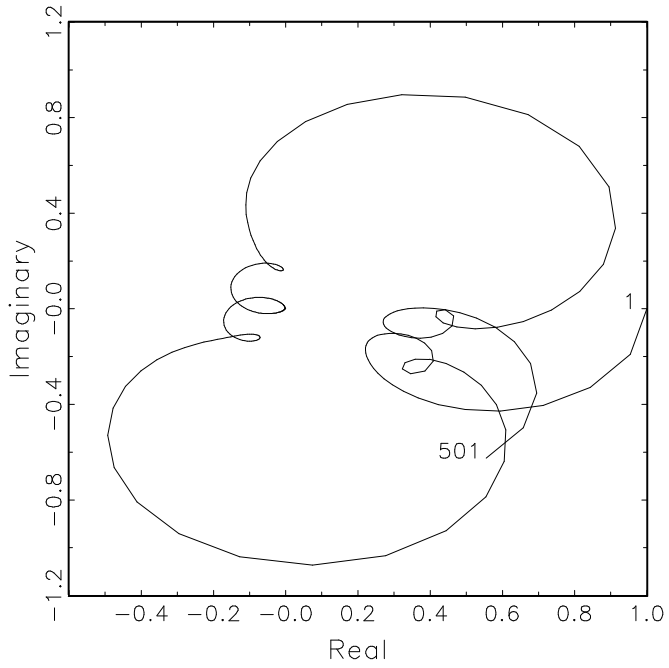

Figure 8.21: A plot of $e^{-j\pi\omega/\omega_0}\Delta(j\omega)$ as a function of ω as ω is swept from 0 to ω_0 corresponding to an input power level of 16 dBm and a non-period-doubling output for the circuit of Figure 8.14 with modified parameters as described in the text, $N = 64$ and $P = 35$.

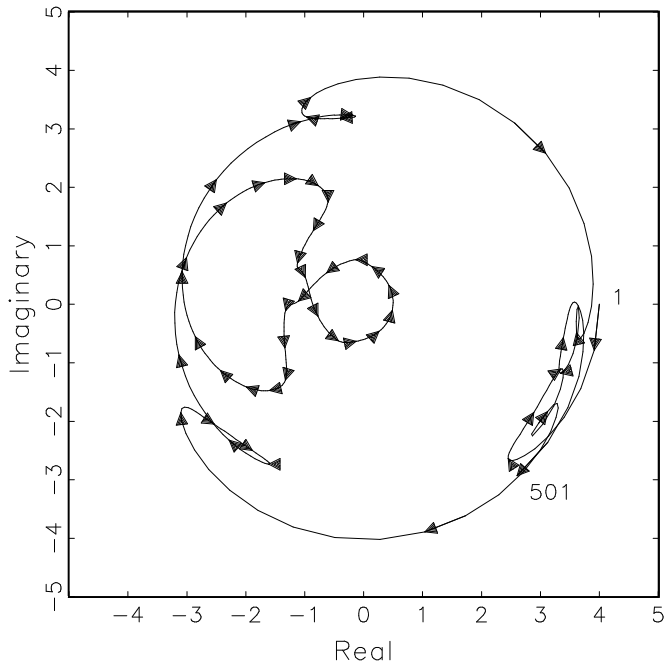

Figure 8.22: A plot of $e^{-j\pi\omega/\omega_0}\Delta(j\omega)$ with magnitudes scaled by $\log_{10}(1+10^4\cdot)$ as a function of ω as ω is swept from 0 to ω_0 corresponding to an input power level of 16 dBm and a non-period-doubling output for the circuit of Figure 8.14 with modified parameters as described in the text, $N = 64$ and $P = 35$.

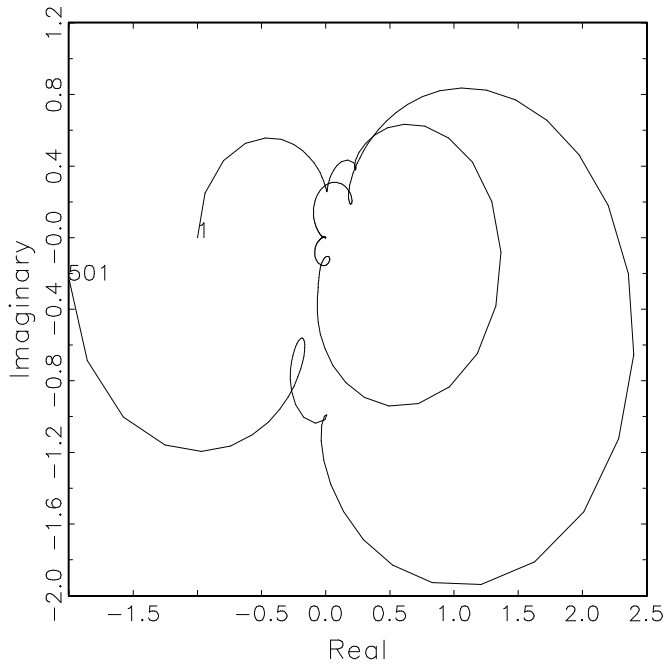

Figure 8.23: A plot of $e^{-j\pi\omega/\omega_0}\Delta(j\omega)$ as a function of ω as ω is swept from 0 to ω_0 corresponding to an input power level of 16 dBm and a non-period-doubling output for the circuit of Figure 8.14 with modified parameters as described in the text, $N = 64$ and $P = 38$.

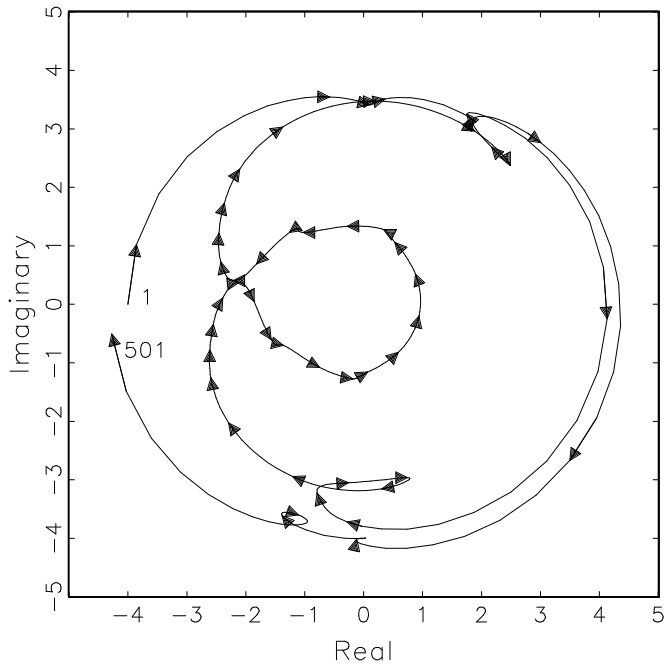

Figure 8.24: A plot of $e^{-j\pi\omega/\omega_0}\Delta(j\omega)$ with magnitudes scaled by $\log_{10}(1+10^4\cdot)$ as a function of ω as ω is swept from 0 to ω_0 corresponding to an input power level of 16 dBm and a non-period-doubling output for the circuit of Figure 8.14 with modified parameters as described in the text, $N = 64$ and $P = 38$.

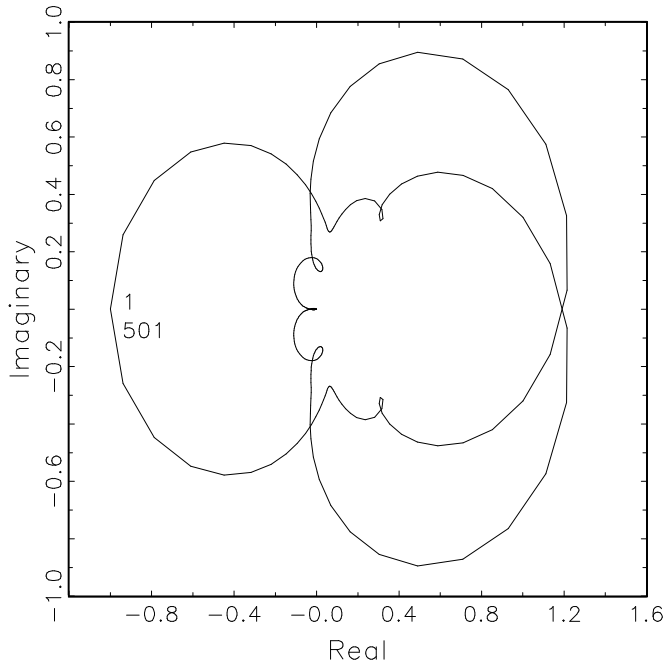

Figure 8.25: A plot of $e^{-j\pi\omega/\omega_0}\Delta(j\omega)$ as a function of ω as ω is swept from 0 to ω_0 corresponding to an input power level of 16 dBm and a non-period-doubling output for the circuit of Figure 8.14 with modified parameters as described in the text, $N = 64$ and $P = 38$. In this plot the matrix truncation scheme suggested in Section 8.2 with $\omega_l = 0.9 \times N \times \omega_0$ and $\omega_u = 0.95 \times N \times \omega_0$ was used.

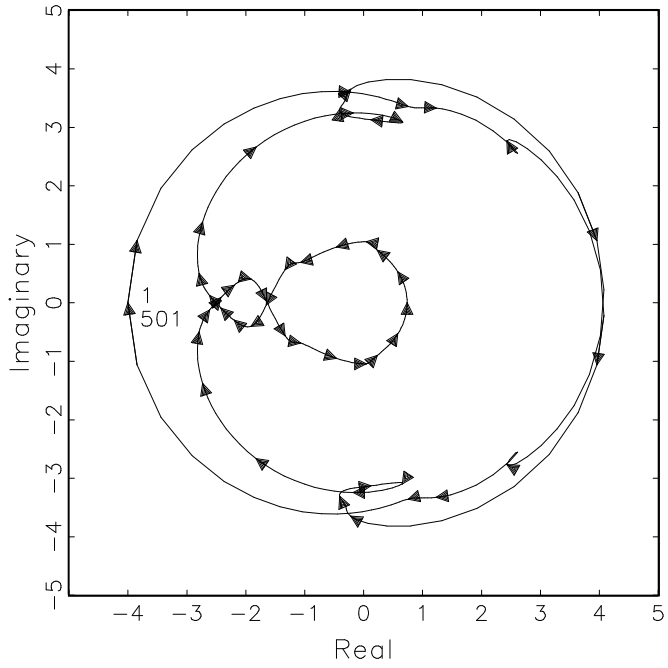

Figure 8.26: A plot of $e^{-j\pi\omega/\omega_0}\Delta(j\omega)$ with magnitudes scaled by $\log_{10}(1+10^4\cdot)$ as a function of ω as ω is swept from 0 to ω_0 corresponding to an input power level of 16 dBm and a non-period-doubling output for the circuit of Figure 8.14 with modified parameters as described in the text, $N = 64$ and $P = 38$. In this plot the matrix truncation scheme suggested in Section 8.2 with $\omega_l = 0.9 \times N \times \omega_0$ and $\omega_u = 0.95 \times N \times \omega_0$ was used.

Table 8.5: The number of clockwise encirclements of the origin that $e^{-j\pi\omega/\omega_0}\Delta(j\omega)$ makes as ω is swept from 0 to ω_0 as a function of the system matrix size, N in (8.1) in each row, and the number of harmonics, P in (8.2) and (8.3) in each column, for a non-period-doubling output of the circuit of Figure 8.14 with modified parameters as described in the text with a 10 dBm input.

	15	16	17	18	19	20	21	22	23	24	25	26	27	28	29	30	31	32	33	34	35	36	37	38	39	40	41	42	43	44	45	46	47	48	49	50
50	2	0	0	0	0	0	0	0	0	1	1	1	1	1	1	1	1	1	1	1	1	1	1	1	1	1	1	1	1	1	1	1	1	1	1	
51									0	1																										
52									0	1																										
53									0	1																										
54									0	1																										
55									0	1																										
56									0	1																										
57									0	1																										
58									0	1																										
59									0	1																										
60	2	0	0	0	0	0	0	0	0	1	1	1	1		1	1					1	1			1			1			1					1
61									0	1																										
62									0	1																										
63									0	1																										
64									0	1																										
65									0	1																										
66									0	1																										
67									0	1																										
68									0	1																										
69									0	1																										
70								0	0	1	1					1										1											1
71									0	1																										
72									0	1																										
73									0	1																										
74									0	1																										
75									0	1																										
76									0	1																										
77									0	1																										
78									0	1																										
79									0	1																										
80								0	0	1	1					1										1											1

Table 8.6: The number of clockwise encirclements of the origin that $e^{-j\pi\omega/\omega_0}\Delta(j\omega)$ makes as ω is swept from 0 to ω_0 as a function of the system matrix size, N in (8.1) in each row, and the number of harmonics, P in (8.2) and (8.3) in each column, for a non-period-doubling output of the circuit of Figure 8.14 with modified parameters as described in the text with a 16 dBm input.

	25	26	27	28	29	30	31	32	33	34	35	36	37	38	39	40	41	42	43	44	45	46	47	48	49	50
50	0	0	0	0	0	0	0	0	0	0	0	1	1	1	1	1	1	2	2	2	2	1	1	1	1	
51											0	1														
52											0	1														
53											0	1														
54											0	1	1	1												
55													0	1												
56													0	1												
57													0	1												
58													0	1												
59													0	1												
60											0		0	1												
61											0		0	1												
62											0		0	1												
63											0	0	0	1												
64											0	0	0	1												
65											0	1														
66											0	1														
67									0	1	1															
68									0	1	1															
69									0	1	1															
70	0					0	0	0	0	1	1	1	1	1	1	2	2	2	2	4	4	1	1	1	1	3
71									0	1	1															
72									0	1	1															
73									0	1	1															
74									0	1	1															
75									0	1	1															
76									0	1	1															
77									0	1	1															
78									0	1	1															
79									0	1	1															
80	0					0		0	0	1	1	1														

Table 8.7: The number of clockwise encirclements of the origin that $e^{-j\pi\omega/\omega_0}\Delta(j\omega)$ makes as ω is swept from 0 to ω_0 as a function of the system matrix size, N in (8.1) in each row, and the number of harmonics, P in (8.2) and (8.3) in each column, for a period doubling output of the circuit of Figure 8.14 with modified parameters as described in the text with a 8.5 dBm input.

	15	16	17	18	19	20	21	22	23	24	25	26	27	28	29	30	31	32	33	34	35	36	37	38	39	40	41	42	43	44	45	46	47	48	49	50
50	1	1	1	1	1	1	1	1	0	0	0	0	0	0	0	0	0	0	0	0	0	0	0	0	0	0	0	0	0	0	0	0	0	0	0	0
51								1	0																											
52								1	0																											
53								1	0																											
54								1	0																											
55								1	0																											
56								1	0																											
57								1	0																											
58								1	0																											
59								1	0																											
60	1	1	1	1	1	1	1	1	0	0	0	0	0		0	0					0	0			0			0			0					0
61								1	0																											
62								1	0																											
63								1	0																											
64								1	0																											
65								1	0																											
66								1	0																											
67								1	0																											
68								1	0																											
69								1	0																											
70							1	1	0	0	0	0													0											0
71								1	0																											
72								1	0																											
73								1	0																											
74								1	0																											
75								1	0																											
76								1	0																											
77								1	0																											
78								1	0																											
79								1	0																											
80								1	0	0	0	0				0						0				0										0

8.5 An example showing that the periodicity of the system matrix does not follow from the properties of the system matrix as claimed in [10]

The system matrix as described in [10] has the property that

$$A[-k,p](\sigma+j\omega) \approx (-1)^m A[k,p](\sigma+j\omega) \tag{8.6}$$

and

$$A[k,p](\sigma+j[\omega+h\omega_0]) = A[k+h,p](\sigma+j\omega) \tag{8.7}$$

where the matrix elements are indexed as shown in Figure 8.27. (Note that the notation has been changed so that elements of matrix A are indicated by $A[i,j]$ rather than $A_{i,j}$ to avoid confusion with notation introduced later. For the same reason n in [10] and the preceding section has been changed to m.)

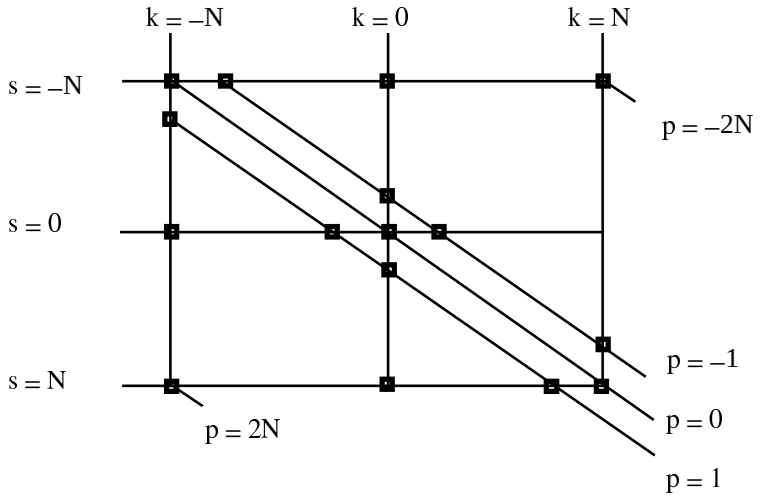

Figure 8.27: Indexing of system matrix elements.

From these two properties it is inferred in [10] that the following holds:

$$\Delta(\sigma+j[\omega+h\omega_0]) = (-1)^{mh}\Delta(\sigma+j\omega)$$

(Where $\Delta(\sigma + j\omega)$ is the determinant of the system matrix evaluated at the perturbation frequency $(\sigma + j\omega)$.)

This inference is based on the matrix symmetry as expressed by equation 8.6 and the fact that a change in perturbation frequency from $(\sigma+j\omega)$ to $(\sigma+j(\omega+h\omega_0))$ results in a shift of the system matrix by h places in the direction of the main diagonal as indicated by equation 8.7.

The following counter example (for the case $m = 1$) shows that the stated matrix symmetry does not translate into the claimed periodicity of the determinant of the matrix when the matrix is shifted in the direction of the main diagonal: Construct a tri-diagonal matrix A_n of order $2n + 1$ with the elements $x, -j, -x^*$ around the diagonal in the upper rows, $0, 1, 0$ in the middle and $-x, j, x^*$ in the lower rows (where $j = \sqrt{-1}$) as shown in equation 8.8 . This matrix possesses the required symmetry property expressed by equation 8.6, yet for any x such that $|x| = 1$ it can be verified that the determinant of this matrix does not have the claimed periodicity if the matrix is shifted in the direction of the main diagonal, regardless of the size of the matrix. In fact, the determinant of this matrix has the property that it takes 6 shifts in the diagonal direction before the determinant repeats with the same pattern. (See Section 8.6.)

In fairness it should be pointed out that numerical analysis shows that if $|x| < 0.5$, then the claimed periodicity of the matrix holds to a high degree of accuracy. It may thus be possible to place additional constraints on the properties of the matrix that will ensure the claimed periodicity for a suitably large matrix.

$$A_n = \begin{bmatrix} -j & x & & & & & & & & & \\ -x^* & -j & x & & & & & & & & \\ & \ddots & \ddots & \ddots & & & & & & & \\ & & -x^* & -j & x & & & & & & \\ & & & -x^* & -j & 0 & & & & & \\ & & & & -x^* & 1 & -x & & & & \\ & & & & & 0 & j & -x & & & \\ & & & & & & x^* & j & -x & & \\ & & & & & & & \ddots & \ddots & \ddots & \\ & & & & & & & & x^* & j & -x \\ & & & & & & & & & x^* & j \end{bmatrix} \tag{8.8}$$

8.6 Derivation of Recursion Formulas for the Determinant of A_n

Start with the matrix

$$A_1 = \begin{bmatrix} -j & 0 & 0 \\ -x^* & 1 & -x \\ 0 & 0 & j \end{bmatrix}$$

.

For any $n \geq 1$ the matrix C_{n+1} is obtained by adding one row and column to A_n such that the first row and column of C_{n+1} are newly added and $C_{n+1}[1,1] = -j$, $C_{n+1}[1,2] = x$ and $C_{n+1}[2,1] = -x^*$. In a similar fashion B_{n+1} is obtained by adding one row and column to A_n such that the last row and column of B_{n+1} are newly added and $B_{n+1}[2n+2, 2n+2] = j$, $B_{n+1}[2n+2, 2n+1] = x^*$ and $B_{n+1}[2n+1, 2n+2] = -x$. The matrix A_{n+1} is obtained by performing the operations to obtain C_{n+1} from A_n as well as the operations to obtain B_{n+1} from A_n on A_n.

Note that for any $n \geq 2$, A_n is of dimension $2n+1$, B_n is the sub-matrix obtained by eliminating the first row and column from A_n and C_n is the matrix obtained by eliminating the last row and column of A_n.

From the construction of the matrices it follows that the following holds for $n \geq 3$.[4]

$$
\begin{aligned}
|C_{n+1}| &= \begin{vmatrix} -j & x & \\ -x^* & \boxed{A_n} & \end{vmatrix} = \begin{vmatrix} -j & x & \\ -x^* & \boxed{\begin{matrix} -j & x \\ -x^* & B_n \end{matrix}} & \end{vmatrix} \\
&= -j|A_n| - x \begin{vmatrix} -x^* & x \\ & \boxed{B_n} \end{vmatrix} = -j|A_n| + |x|^2|B_n|
\end{aligned}
$$

Also

$$
\begin{aligned}
|B_{n+1}| &= \begin{vmatrix} \boxed{A_n} & & -x \\ & x^* & j \end{vmatrix} = \begin{vmatrix} \boxed{C_n} & & \\ & -x & \\ & x^* \quad \text{j} & -x \\ & & x^* \quad j \end{vmatrix} \\
&= j|A_n| - x^* \begin{vmatrix} \boxed{C_n} & \\ & x^* \quad -x \end{vmatrix} = j|A_n| + |x|^2|C_n|
\end{aligned}
$$

and finally

[4] In this section $|M|$ of a matrix M denotes the determinant of M.

$$
|A_{n+1}| = \left|\begin{array}{ccc} -j & x & \\ -x^* & A_n & \\ & & -x \\ & x^* & j \end{array}\right| = \left|\begin{array}{ccc} -j & x & \\ -x^* & \begin{array}{cc} -j & x \\ -x^* & B_n \end{array} & -x \\ & x^* & j \end{array}\right|
$$

$$
= -j\left|\begin{array}{cc} A_n & \\ & -x \\ x^* & j \end{array}\right| - x\left|\begin{array}{ccc} -x^* & x & \\ & B_n & -x \\ & x^* & j \end{array}\right|
$$

$$
= -j(j|A_n| + |x|^2|C_n|) + |x|^2\left|\begin{array}{cc} A_{n-1} & \\ & -x \\ x^* \quad \mathrm{j} & -x \\ x^* & j \end{array}\right|
$$

$$
= -j(j|A_n| + |x|^2|C_n|) + |x|^2(j|B_n| + |x|^2|A_{n-1}|)
$$

$$
= |A_n| - j|x|^2|C_n| + j|x|^2|B_n| + |x|^4|A_{n-1}|
$$

With $|x| = 1$ one obtains the following set of recursion formulas.

$$
\begin{aligned}
|A_{n+1}| &= |A_{n-1}| + |A_n| + j(|B_n| - |C_n|) \\
|B_{n+1}| &= j|A_n| + |C_n| \\
|C_{n+1}| &= -j|A_n| + |B_n|
\end{aligned}
$$

In order to start the recursion one needs (for $|x| = 1$):

$$
\begin{aligned}
|A_1| &= \begin{vmatrix} -j & 0 & 0 \\ -x^* & 1 & -x \\ 0 & 0 & j \end{vmatrix} = 1 \\
|B_2| &= \begin{vmatrix} -j & 0 & 0 & 0 \\ -x^* & 1 & -x & 0 \\ 0 & 0 & j & -x \\ 0 & 0 & x^* & j \end{vmatrix} = 0 \\
|C_2| &= \begin{vmatrix} -j & x & 0 & 0 \\ -x^* & -j & 0 & 0 \\ 0 & -x^* & 1 & -x \\ 0 & 0 & 0 & j \end{vmatrix} = 0 \\
|A_2| &= \begin{vmatrix} -j & x & 0 & 0 & 0 \\ -x^* & -j & 0 & 0 & 0 \\ 0 & -x^* & 1 & -x & 0 \\ 0 & 0 & 0 & j & -x \\ 0 & 0 & 0 & x^* & j \end{vmatrix} = 0
\end{aligned}
$$

Using the formulas one finds that the determinant of $|A_n|$ is a periodic function of n with period 3. This is best shown by referring to table 8.8. From table 8.8 it follows that

$$
|A_n| = \begin{cases} 1 & \text{if} \quad (\text{n mod } 3) = 0 \\ 1 & \text{if} \quad (\text{n mod } 3) = 1 \\ 0 & \text{if} \quad (\text{n mod } 3) = 2 \end{cases}
$$

.

Table 8.8: Calculating $|A_n|$ using recursion

n	$\|A_{n-1}\|$	$\|A_n\|$	$\|B_n\|$	$\|C_n\|$
2	1	0	0	0
3	0	1	0	0
4	1	1	j	-j
5	1	0	0	0

Also from table 8.8 it follows that

$$|C_n| = \begin{cases} 0 & \text{if} \quad (\text{n mod } 3) = 0 \\ \text{-j} & \text{if} \quad (\text{n mod } 3) = 1 \\ 0 & \text{if} \quad (\text{n mod } 3) = 2 \end{cases}$$

.

Next define $X_{n,k}$ as the matrix A_n with k rows and columns added in such a manner that A_n occupies the first n rows and columns of $X_{n,k}$ and for all $m > n$, $X_{n,k}[m,m] = j$, $X_{n,k}[m-1,m] = -x$ and $X_{n,k}[m,m-1] = x^*$. (Note that $X_{n,0} = A_n$.)

In an entirely analogous way to the way $|B_{n+1}|$ is calculated from $|A_n|$ and $|C_n|$ a set of recursion formulas for $|X_{n,k}|$ is obtained as

$$|X_{n,k+1}| = \begin{cases} j|A_n| + |x|^2|C_n| & \text{if } k = 0 \\ j|X_{n,k}| + |x|^2|X_{n,k-1}| & \text{if } k > 0 \end{cases}$$

Next define $A_{n,k}$ (for $k < n$) as the matrix obtained by shifting A_n k places in the direction of the main diagonal towards $A_n[1,1]$, i.e.

$$A_{n,k} = \begin{bmatrix} \boxed{A_{n-k}} & & & & & \\ & -x & & & & \\ x^* & j & -x & & & \\ & \ddots & \ddots & \ddots & & \\ & & x^* & j & -x & \\ & & & x^* & j & \end{bmatrix} = X_{n-k,2k}$$

Thus $|A_{n,k}| = |X_{n-k,2k}|$.

Now consider the case $(n-k) \bmod 3 = 0$:

$$\begin{aligned}
|A_{n,k}| &= |X_{n-k,2k}| \\
|X_{n-k,1}| &= j|A_{n-k}| + |C_{n-k}| = j \times 1 + 0 = j \\
|X_{n-k,2}| &= j|X_{n-k,1}| + |X_{n-k,0}| = j \times j + |A_{n-k}| = -1 + 1 = 0 \\
|X_{n-k,3}| &= j|X_{n-k,2}| + |X_{n-k,1}| = j \times 0 + j = j \\
|X_{n-k,4}| &= j|X_{n-k,3}| + |X_{n-k,2}| = j \times j + 0 = -1 \\
&\vdots
\end{aligned}$$

The rest of the values are readily calculated by referring to table 8.9. From table 8.9 it is clear that for $(n-k) \bmod 3 = 0$, $|X_{n-k,m}|$ is periodic in m with period 12 and as a result

$$\begin{aligned}
|A_{n,k}| &= f_0(k \bmod 6 \text{) with} \\
f_0(1) &= 0 \\
f_0(2) &= -1 \\
f_0(3) &= -1 \\
f_0(4) &= 0 \\
f_0(5) &= 1 \\
f_0(0) &= 1
\end{aligned}$$

Next consider the case $(n-k) \bmod 3 = 1$:

$$\begin{aligned}
|A_{n,k}| &= |X_{n-k,2k}| \\
|X_{n-k,1}| &= j|A_{n-k}| + |C_{n-k}| = j \times 1 + -j = 0
\end{aligned}$$

Table 8.9: Calculating $|X_{n-k,m}|$ for $(n-k)$ mod $3 = 0$

m	$\lvert X_{n-k,m-2}\rvert$	$\lvert X_{n-k,m-1}\rvert$	$\lvert X_{n-k,m}\rvert$
1	-	-	j
2	-	j	0
3	j	0	j
4	0	j	-1
5	j	-1	0
6	-1	0	-1
7	0	-1	-j
8	-1	-j	0
9	-j	0	-j
10	0	-j	1
11	-j	1	0
12	1	0	1
13	0	1	j
14	1	j	0
15	j	0	j

$$
\begin{aligned}
|X_{n-k,2}| &= j|X_{n-k,1}| + |X_{n-k,0}| = j \times 0 + |A_{n-k}| = 0 + 1 = 1 \\
|X_{n-k,3}| &= j|X_{n-k,2}| + |X_{n-k,1}| = j \times 1 + 0 = j \\
|X_{n-k,4}| &= j|X_{n-k,3}| + |X_{n-k,2}| = j \times j + 1 = 0 \\
&\vdots
\end{aligned}
$$

The rest of the values are readily calculated by referring to table 8.9 and noting that the sequence $j, 0$ for $|X_{n-k,m}|$ appear for m equal to 1,2 in table 8.9. The values for $(n-k)$ mod $3 = 1$ thus simply appear at different m. It is thus clear that for $(n-k)$ mod $3 = 1$, $|X_{n-k,m}|$ is periodic in m with period 12 and as a result

$$
\begin{aligned}
|A_{n,k}| &= f_1(k \text{ mod } 6 \text{) with} \\
f_1(1) &= 1 \\
f_1(2) &= 0 \\
f_1(3) &= -1
\end{aligned}
$$

$$
\begin{aligned}
f_1(4) &= -1 \\
f_1(5) &= 0 \\
f_1(0) &= 1
\end{aligned}
$$

Lastly consider the case $(n-k) \bmod 3 = 2$:

$$
\begin{aligned}
|A_{n,k}| &= |X_{n-k,2k}| \\
|X_{n-k,1}| &= j|A_{n-k}| + |C_{n-k}| = j \times 0 + 0 = 0 \\
|X_{n-k,2}| &= j|X_{n-k,1}| + |X_{n-k,0}| = j \times 0 + |A_{n-k}| = 0 + 0 = 0
\end{aligned}
$$

It follows that $|X_{n-k,m}| = 0$ and thus $|A_{n,k}| = 0$ for $(n-k) \bmod 3 = 2$.

Thus for $k < n$

$$
|A_{n,k}| = \begin{cases}
f_0(k \bmod 6) & \text{if} \quad ((n-k) \bmod 3) = 0 \\
f_1(k \bmod 6) & \text{if} \quad ((n-k) \bmod 3) = 1 \\
f_2(k \bmod 6) = 0 & \text{if} \quad ((n-k) \bmod 3) = 2
\end{cases}
$$

The results above can now be put together for the three cases $n \bmod 3 = 0$, $n \bmod 3 = 1$ and $n \bmod 3 = 2$.

First consider the case $n \bmod 3 = 0$. $|A_{n,k}|$ is readily calculated by referring to table 8.10.

$|A_{n,k}|$ for the case $n \bmod 3 = 1$ is calculated by referring to table 8.11.

Lastly $|A_{n,k}|$ for the case $n \bmod 3 = 2$ is calculated by referring to table 8.12.

The final result is summarized in table 8.13.

A matrix satisfying the symmetry requirements of equation 8.6 with $m = 1$ has thus been obtained for which, regardless of the size of the matrix, the determinant never satisfies $|A_{n,k}| = -1^k|A_n|$ for all k (small enough relative to n).

Table 8.10: Calculation of $|A_{n,k}|$ for $n \bmod 3 = 0$

k	$(n-k) \bmod 3$	$k \bmod 6$	function	$\lvert A_{n,k}\rvert$
0	0	0	$f_0(0)$	1
1	2	1	$f_2(1)$	0
2	1	2	$f_1(2)$	0
3	0	3	$f_0(3)$	-1
4	2	4	$f_2(4)$	0
5	1	5	$f_1(5)$	0
6	0	0	$f_0(0)$	1

Table 8.11: Calculation of $|A_{n,k}|$ for $n \bmod 3 = 1$

k	$(n-k) \bmod 3$	$k \bmod 6$	function	$\lvert A_{n,k}\rvert$
0	1	0	$f_1(0)$	1
1	0	1	$f_0(1)$	0
2	2	2	$f_2(2)$	0
3	1	3	$f_1(3)$	-1
4	0	4	$f_0(4)$	0
5	2	5	$f_2(5)$	0
6	1	0	$f_1(0)$	1

Table 8.12: Calculation of $|A_{n,k}|$ for $n \bmod 3 = 2$

k	$(n-k) \bmod 3$	$k \bmod 6$	function	$\lvert A_{n,k}\rvert$
0	2	0	$f_2(0)$	0
1	1	1	$f_1(1)$	1
2	0	2	$f_0(2)$	-1
3	2	3	$f_2(3)$	0
4	1	4	$f_1(4)$	-1
5	0	5	$f_0(5)$	1
6	2	0	$f_2(0)$	0

Table 8.13: $|A_{n,k}|$ as a function of n and k for $k < n$ and $n > 2$.

k mod 6	$\lvert A_{n,k}\rvert$, n mod 3 $\in \{0,1\}$	$\lvert A_{n,k}\rvert$, n mod 3 $= 2$
0	1	0
1	0	1
2	0	-1
3	-1	0
4	0	-1
5	0	1

8.7 Conclusion

Under favorable conditions, the method proposed in [10] is quite useful to predict the stability of periodic steady states in nonlinear circuits. If the conditions are not favorable the stability predictions tend to change as the size of the system matrix is increased and more harmonics are taken into account in the system matrix. Under reasonable conditions it is thus possible to obtain reasonable predictions of the stability, but the results may also be misleading.

We noted that a required periodicity of the determinant of the system matrix does not necessarily follow from the properties of the matrix. We proposed an alternative matrix truncation scheme that solves the periodicity problem, but we do not claim that it improves the ability to predict the stability with any more accuracy than the original method.

If anything, the investigation suggests that the stability analysis described in [10] cannot be relied upon completely. This highlights the importance of the theorems presented in this dissertation as a design guideline wherever possible.

Appendix A

Collected results

This section contains a number of results that are needed in the proofs but would hamper the flow if included in the proofs themselves.

Lemma 9 Let $Q : \mathbb{R} \to \mathbb{R}$ satisfy $Q(0) = 0$ and let there be real constants α and β such that for all $a \neq b$,

$$0 < \alpha \leq \frac{Q(b) - Q(a)}{b - a} \leq \beta.$$

Then with I the identity map from $\mathbb{R}$ onto $\mathbb{R}$ we have that for any $k \geq 0$, $I + kQ$ is invertible and $\psi : \mathbb{R} \to \mathbb{R}$ defined by $\psi = Q[I + kQ]^{-1}$ satisfies $\psi(0) = 0$ and

$$0 < \frac{\alpha}{1 + k\alpha} \leq \frac{\psi(b) - \psi(a)}{b - a} \leq \frac{\beta}{1 + k\beta}.$$

Proof: The invertability of $I+kQ$ follows from the fact that it is a strictly increasing continuous function defined on all of $\mathbb{R}$. $\psi(0) = 0$ follows from

$$[I + kQ](0) = 0 \Rightarrow 0 = [I + kQ]^{-1}(0) \Rightarrow \psi(0) = Q[I + kQ]^{-1}(0) = Q(0) = 0.$$

For the rest of the assertion, let $a, b \in \mathbb{R}$ with $b \neq a$. Since $[I + kQ]$ is injective, $c \stackrel{\text{def}}{=} [I + kQ]^{-1}a \neq d \stackrel{\text{def}}{=} [I + kQ]^{-1}b$.

$$\begin{aligned}\frac{\psi(b)-\psi(a)}{b-a} &= \frac{Qd-Qc}{b-a}\\ &= \frac{Qd-Qc}{d+kQd-c-kQc}\\ &= \frac{\frac{Qd-Qc}{d-c}}{1+k\frac{Qd-Qc}{d-c}}\end{aligned}$$

Now the derivative of the function

$$\frac{x}{1+kx},\ x>0$$

with respect to x is

$$\frac{1}{(1+kx)^2}>0.$$

Thus

$$\frac{\frac{Qd-Qc}{d-c}}{1+k\frac{Qd-Qc}{d-c}}$$

reaches its minimum, when $\dfrac{Qd-Qc}{d-c}$ is minimum, and likewise its maximum when $\dfrac{Qd-Qc}{d-c}$ is maximum.

Thus

$$0\le\frac{\alpha}{1+k\alpha}\le\frac{\psi(b)-\psi(a)}{b-a}\le\frac{\beta}{1+k\beta}$$

as claimed.

Lemma 10 Let h, z and Q be real valued functions with h and z defined on $\mathbb{R}^+$ and Q on $\mathbb{R}$. Consider

$$h(t)=v(t)+\int_0^t z(t-\tau)\frac{d}{d\tau}Q[v(\tau)]d\tau,\quad t\ge 0. \tag{A.1}$$

Assume that h is absolutely continuous on any interval $[0,t]$, $z(0)\ge 0$, z is differentiable, and its derivative z' is Lipschitz continuous on $[0,a]$ for each $a>0$, $Q(0)=0$ and there exist two real constants α and β such that

$$0<\alpha\le\frac{Q(v_2)-Q(v_1)}{v_2-v_1}\le\beta$$

for all real $v_1 \neq v_2$.

Then (A.1) has a unique absolutely continuous solution v defined on $\mathbb{R}^+$, and integration by parts leading to

$$\begin{aligned} h(t) &= v(t) + z(0)Q[v(t)] - z(t)Q[v(0)] + \\ &\quad \int_0^t u(t-\tau)Q[v(\tau)]d\tau, \quad t \geq 0 \end{aligned} \tag{A.2}$$

is justified, where $u(t) = \dfrac{d}{dt}z(t)$.

Proof: Let

$$\begin{aligned} \tilde{h}(t) &= h(t) + Q[v(0)]z(t) \\ \psi &= Q[I + z(0)Q]^{-1} \text{ (which exists by Lemma 9)} \end{aligned}$$

and consider the integral equation

$$\tilde{h}(t) = y(t) + \int_0^t z'(t-\tau)\psi[y(\tau)]\, d\tau \tag{A.3}$$

that results from formally integrating (A.1) by parts and defining y by $y(t) = v(t) + z(0)Q[v(t)]$.

Fix p in $\mathbb{N}$. It follows from our assumptions that $\tilde{h}$ and z' are continuous and thus in $L_{p\,\mathrm{loc}}$. Together with the Lipschitz continuity of ψ (see Lemma 9) it follows from [9, page 167, theorem 5.3] that (A.3) has a unique solution y in $L_{p\,\mathrm{loc}}$.

Since

$$y(t) = \tilde{h}(t) - \int_0^t z'(t-\tau)\psi[y(\tau)]\, d\tau \tag{A.4}$$

and $\tilde{h}$ is continuous, y is continuous since the function

$$J(t) = \int_0^t z'(t-\tau)\psi[y(\tau)]\, d\tau$$

is continuous. This follows by noting that z' is continuous, and $\eta(t) \stackrel{\text{def}}{=} \psi[y(t)]$ is in $L_{p\,\mathrm{loc}}$ since y is and ψ is Lipschitz continuous. We can extend z' and η by zero to all

of $\mathbb{R}$ and apply [31, Theorem 9.3 page 147] on any interval $[0, a]$. (When calculating J on $[0, a]$, one can set the extensions of z' and η to zero outside $[0, a+1]$ so that the extension of z' is compactly supported and the extension of η is in $L_p(-\infty, \infty)$ and all conditions for applying [31, Theorem 9.3 page 147] are met.)

Fix any interval $[0, t]$, $t > 0$. Since $\tilde{h}$ is absolutely continuous, y will be absolutely continuous if J is. We prove the stronger assertion that J is Lipschitz continuous on $[0, t]$ by a simple bounding argument. Let $a, b \in [0, t]$ with $b > a$.

$$
\begin{aligned}
|J(b) - J(a)| &= \left| \int_0^b z'(b-\tau)\psi[y(\tau)]\, d\tau - \int_0^a z'(a-\tau)\psi[y(\tau)]\, d\tau \right| \\
&= \left| \int_0^a \left[z'(b-\tau) - z'(a-\tau) \right] \psi[y(\tau)]\, d\tau + \int_a^b z'(b-\tau)\psi[y(\tau)]\, d\tau \right| \\
&\leq \int_0^a \gamma(b-a)|\psi[y(\tau)]|\, d\tau \\
&\quad + \sup_{\tau\in[0,t]} |z'(\tau)| \frac{\beta}{1+z(0)\beta} \sup_{\tau\in[0,t]} |y(\tau)|(b-a) \\
&\leq \gamma(b-a) \int_0^t |\psi[y(\tau)]|\, d\tau \\
&\quad + \frac{\beta}{1+z(0)\beta} \sup_{\tau\in[0,t]} |z'(\tau)| \sup_{\tau\in[0,t]} |y(\tau)|(b-a) \\
&\leq \left[\gamma t \frac{\beta}{1+z(0)\beta} \sup_{\tau\in[0,t]} |y(\tau)| \right. \\
&\quad \left. + \frac{\beta}{1+z(0)\beta} \sup_{\tau\in[0,t]} |z'(\tau)| \sup_{\tau\in[0,t]} |y(\tau)| \right] (b-a)
\end{aligned}
$$

where γ is the Lipschitz constant of z' on $[0, t]$ and the various supremums are finite because the functions are continuous on the compact set $[0, t]$. This shows that J is Lipschitz continuous on any interval $[0, t]$.

Thus y is an absolutely continuous solution of (A.3). Since ψ is Lipschitz continuous, η is also absolutely continuous and (A.3) can be integrated by parts to give (A.1). Note that $v = [I + z(0)\mathcal{Q}]^{-1} y$ is an absolutely continuous solution of (A.1) since y is absolutely continuous and $[I + z(0)\mathcal{Q}]^{-1}$ is Lipschitz continuous

(with Lipschitz constant $\frac{1}{1+z(0)\alpha}$). This solution has to be the only absolutely continuous solution of (A.1), for if there is another absolutely continuous solution v_2 of (A.1), $y_2 = [I + z(0)\mathcal{Q}]v_2$ is another absolutely continuous solution of (A.3) (as integrating (A.1) by parts shows) contradicting the uniqueness of the solution y in $L_{p\,\mathrm{loc}}$. This completes the proof.

Lemma 11 Let f and g be $\mathbb{R}^{N_1}$ and $\mathbb{R}^{N_2}$-valued AP functions, respectively. Then the $\mathbb{R}^{N_1+N_2}$-valued function (f, g) is an AP function.

Proof: This is an easy consequence of a theorem in [2]. In order to state and use this theorem we have to introduce notation used in [2]. A set E of real numbers is said to be *relatively dense* if there exists a number $l > 0$ such that any interval of length l contains at least one number of E. With f a real or complex valued function defined on $\mathbb{R}$, a number τ is called a *translation number of f belonging to* $\varepsilon > 0$ if

$$\sup_{t\in\mathbb{R}} |f(t+\tau) - f(t)| < \varepsilon.$$

We denote the set of all translation numbers of a function f belonging to ε by $E\{\varepsilon, f\}$. The following theorem is proved in [2, p. 5].

Theorem 10 For any $\varepsilon > 0$ and any $f_1, f_2 \in$AP, the set $E\{\varepsilon, f_1\} \bigcap E\{\varepsilon, f_2\}$ is r.d.

Let $\varepsilon > 0$. By Theorem 10,

$$A = E(\varepsilon, f_1) \bigcap E(\varepsilon, f_2) \bigcap \ldots \bigcap E(\varepsilon, f_{N_1}) \bigcap E(\varepsilon, g_1) \bigcap E(\varepsilon, g_2) \bigcap \ldots \bigcap E(\varepsilon, g_{N_2})$$

is r.d.

Let $\tau \in A$. Then

$$|(f, g)(t+\tau) - (f, g)(t)|_\infty = \max_k |(f, g)_k(t+\tau) - (f, g)_k(t)| < \varepsilon.$$

Since A is r.d. this means that there is a length l such that every interval of length l in $\mathbb{R}$ contains at least one number τ such that

$$|(f,g)(t+\tau)-(f,g)(t)|_{\infty}<\varepsilon.$$

Thus (f,g) is an $\mathbb{R}^{N_1+N_2}$-valued AP function.

Appendix B

Glossary

almost everywhere A statement holds almost everywhere (a.e.) in a set S if it holds on all of S except maybe in a set of measure zero. If the set is obvious we will simply say a statement holds a.e. See [31, page 52].

absolutely continuous A finite function f on a finite interval $[a, b]$ is said to be *absolutely continuous* on $[a, b]$ if given $\varepsilon > 0$, there exists $\delta > 0$ such that for any collection $\{[a_i, b_i]\}$ (finite or not) of nonoverlapping subintervals of $[a, b]$,

$$\sum_i |f(b_i) - f(a_i)| < \varepsilon \text{ if } \sum_i (b_i - a_i) < \delta.$$

See [31, page 115].

Appendix C

Facts that are used

This section collects well known facts and theorems for convenience.

C.1 Existence of Solutions

The first result is a simple (and known, see [17, page 475]) extension from real valued functions to N-vector-valued functions of an existence and uniqueness theorem appearing in [28, page 42–47].

Theorem 11 Let $h > 0$, $f \in L_{2,N}(0,h)$ and define $\mathcal{D} = \{(x,y) \subset \mathbb{R}^2 : 0 \leq y \leq x \leq h\}$ and let

$$F : \mathcal{D} \times \mathbb{R}^N \to \mathbb{R}^N$$

be such that for a.e. x, $F[x,y,\phi(y)]$ is a (Lebesgue) measurable function of y whenever $\phi(y)$ is a measurable function of y. Suppose that there are real valued functions a and b and positive constants A and M such that for a.e. x

1. for any $z_1, z_2 \in \mathbb{R}^N$, $|F(x,y,z_1) - F(x,y,z_2)| \leq a(x,y)\,|z_1 - z_2|$,
2. $\left| \int_0^x F[x,y,f(y)]dy \right| \leq b(x)$,

3. $\int_0^h \left[\int_0^x a^2(x,y)dy\right] dx \leq A^2$, and

4. $\int_0^h b^2(y)dy \leq M^2$.

Then the equation

$$\phi(x) = f(x) + \int_0^x F[x, y, \phi(y)]dy \tag{C.1}$$

has a unique solution ϕ in $L_{2,N}(0,h)$. The solution is the limit of the sequence $\{\phi_m\}_{m=1}^{\infty}$ where

$$\begin{aligned} \phi_0 &= f \\ \phi_n(x) &= f(x) + \int_0^x F[x, y, \phi_{n-1}(y)]dy,\ n = 1, 2, \ldots. \end{aligned}$$

Moreover, this sequence converges uniformly a.e. to the solution ϕ.

Proof: See [28, page 43–47].

Corollary 1 Let $k \in \mathbb{K}_{2,N}$ and let $\eta : \mathbb{R}^N \to \mathbb{R}^N$ be Lipschitz continuous and $\eta(0) = 0$. Then for each $u \in L_{\infty,N_{loc}}(0,\infty)$ there exists a unique $v \in L_{\infty,N_{loc}}(0,\infty)$ such that

$$u(t) = v(t) + \int_0^t k(t-\tau)\eta[v(\tau)]d\tau,\ t \geq 0.$$

Proof: Fix $h > 0$ and let C be the Lipschitz constant of η. (I.e. for arbitrary $z_1, z_2 \in \mathbb{R}^N$, $|\eta(z_1) - \eta(z_2)|_2 \leq C\,|z_1 - z_2|_2$.) Check all conditions for applying Theorem 11. The measurability of $k(t-\tau)\eta[v(\tau)]$ as a function of τ for almost every t if v is measurable follows immediately from the continuity of η and the measurability of k.

Condition 1 is satisfied with

$$a(t,\tau) = C\left(\sum_{l=1}^{N}\sum_{m=1}^{N} k_{lm}^2(t-\tau)\right)^{\frac{1}{2}}$$

since (with $F(x,y,z) = -k(x-y)\eta(z)$)

$$\begin{aligned}
&|F(t,\tau,z_1) - F(t,\tau,z_2)|_2^2 \\
&= |-k(t-\tau)\eta(z_1) + k(t-\tau)\eta(z_2)|_2^2 \\
&= |k(t-\tau)[\eta(z_1) - \eta(z_2)]|_2^2 \\
&= \sum_{l=1}^{N}\left(\sum_{m=1}^{N} k_{lm}(t-\tau)[\eta_m(z_1) - \eta_m(z_2)]\right)^2 \\
&\leq \sum_{l=1}^{N}\sum_{m=1}^{N} k_{lm}^2(t-\tau)\sum_{m=1}^{N}[\eta_m(z_1) - \eta_m(z_2)]^2 \\
&= |\eta(z_1) - \eta(z_2)|_2^2 \sum_{l=1}^{N}\sum_{m=1}^{N} k_{lm}^2(t-\tau) \\
&\leq C^2\,|z_1 - z_2|_2^2 \sum_{l=1}^{N}\sum_{m=1}^{N} k_{lm}^2(t-\tau).
\end{aligned}$$

Condition 2 is satisfied with

$$b(\tau) = Ch^{\frac{1}{2}}\left(\sum_{l=1}^{N}\sum_{m=1}^{N}\|k_{lm}\|_2^2\right)^{\frac{1}{2}} \sup_{y\in(0,h)}|u(y)|_2$$

since

$$\begin{aligned}
&\left|\int_0^t F[t,\tau,u(\tau)]\,d\tau\right|_2^2 \\
&= \left|\int_0^t -k(t-\tau)\eta[u(\tau)]\,d\tau\right|_2^2 \\
&= \sum_{l=1}^{N}\left(\int_0^t \sum_{m=1}^{N} -k_{lm}(t-\tau)\eta_m[u(\tau)]\,d\tau\right)^2 \\
&= \sum_{l=1}^{N}\left(\sum_{m=1}^{N}\int_0^t -k_{lm}(t-\tau)\eta_m[u(\tau)]\,d\tau\right)^2 \\
&\leq \sum_{l=1}^{N}\left(\sum_{m=1}^{N}\left(\int_0^t k_{lm}^2(t-\tau)\,d\tau\right)^{\frac{1}{2}}\left(\int_0^t \eta_m^2[u(\tau)]\,d\tau\right)^{\frac{1}{2}}\right)^2 \text{ (Schwarz's inequality.[1])} \\
&\leq \sum_{l=1}^{N}\left(\left(\sum_{m=1}^{N}\int_0^t k_{lm}^2(t-\tau)\,d\tau\right)^{\frac{1}{2}}\left(\sum_{m=1}^{N}\int_0^t \eta_m^2[u(\tau)]\,d\tau\right)^{\frac{1}{2}}\right)^2 \text{ (C.S. inequality.[2])}
\end{aligned}$$

$$
\begin{aligned}
&= \sum_{l=1}^{N}\sum_{m=1}^{N}\int_0^t k_{lm}^2(t-\tau)\,d\tau \int_0^t \sum_{m=1}^{N}\eta_m^2[u(\tau)]\,d\tau \\
&= \int_0^t |\eta[u(\tau)]|_2^2\,d\tau \sum_{l=1}^{N}\sum_{m=1}^{N}\int_0^t k_{lm}^2(t-\tau)\,d\tau \\
&\leq h\left(C\sup_{y\in[0,h]}|u(\tau)|_2\right)^2 \sum_{l=1}^{N}\sum_{m=1}^{N}\int_0^\infty k_{lm}^2(\tau)\,d\tau \\
&= h\left(C\sup_{y\in[0,h]}|u(\tau)|_2\right)^2 \sum_{l=1}^{N}\sum_{m=1}^{N}\|k_{lm}\|_2^2
\end{aligned}
$$

Condition 3 is satisfied with

$$A = C^2 h\sum_{l=1}^{N}\sum_{m=1}^{N}\|k_{lm}\|_2^2$$

since

$$
\begin{aligned}
&\int_0^h\left(\int_0^t a^2(t,\tau)\,d\tau\right)dt \\
&\quad= \int_0^h\left(\int_0^t C^2\sum_{l=1}^{N}\sum_{m=1}^{N}k_{lm}^2(t-\tau)\,d\tau\right)dt \\
&\quad\leq \int_0^h\left(C^2\sum_{l=1}^{N}\sum_{m=1}^{N}\int_0^\infty k_{lm}^2(\tau)\,d\tau\right)dt \\
&\quad= C^2h\sum_{l=1}^{N}\sum_{m=1}^{N}\|k_{lm}\|_2^2 \\
&\quad< \infty.
\end{aligned}
$$

Condition 4 is satisfied with

$$M = C^2h^2\sup_{y\in[0,h]}|u(y)|_2^2\sum_{l=1}^{N}\sum_{m=1}^{N}\|k_{lm}\|_2^2$$

since

$$\int_0^h b^2(\tau)\,d\tau$$

[1]Schwarz's inequality for $L_{2n}(0,\infty)$. See e.g. [31, page 128].
[2]Cauchy-Schwarz inequality for $\mathbb{R}^N$. See e.g. [31, page 3].

$$
\begin{aligned}
&= \int_0^h C^2 h \sum_{l=1}^{N} \sum_{m=1}^{N} \|k_{lm}\|_2^2 \sup_{y\in[0,h]} |u(y)|_2^2 \, d\tau \\
&= C^2 h^2 \sup_{y\in[0,h]} |u(y)|_2^2 \sum_{m=1}^{N} \|k_{lm}\|_2^2 \\
&< \infty.
\end{aligned}
$$

Thus, by Theorem 11,

$$u(t) = v(t) + \int_0^t k(t-\tau)\eta[v(\tau)]d\tau,\ t \in [0,h]$$

has a unique solution in $L_{2,N}(0,h)$.

Since u is bounded on $[0,h]$ and

$$
\begin{aligned}
&\left| \int_0^t k(t-\tau)\eta[v(\tau)]\, d\tau \right|_2^2 \\
&= \sum_{l=1}^{N} \left(\int_0^t \sum_{m=1}^{N} -k_{lm}(t-\tau)\eta_m[v(\tau)]\, d\tau \right)^2 \\
&= \sum_{l=1}^{N} \left(\sum_{m=1}^{N} \int_0^t -k_{lm}(t-\tau)\eta_m[v(\tau)]\, d\tau \right)^2 \\
&\leq \sum_{l=1}^{N} \left(\sum_{m=1}^{N} \left(\int_0^t k_{lm}^2(t-\tau)\, d\tau \right)^{\frac{1}{2}} \left(\int_0^t \eta_m^2[v(\tau)]\, d\tau \right)^{\frac{1}{2}} \right)^2 \text{ (Schwarz's inequality.[3])} \\
&\leq \sum_{l=1}^{N} \left(\left(\sum_{m=1}^{N} \int_0^t k_{lm}^2(t-\tau)\, d\tau \right)^{\frac{1}{2}} \left(\sum_{m=1}^{N} \int_0^t \eta_m^2[v(\tau)]\, d\tau \right)^{\frac{1}{2}} \right)^2 \text{ (C.S. inequality.[4])} \\
&= \sum_{l=1}^{N} \sum_{m=1}^{N} \int_0^t k_{lm}^2(t-\tau)\, d\tau \int_0^t \sum_{m=1}^{N} \eta_m^2[v(\tau)]\, d\tau \\
&\leq \int_0^h |\eta[v(\tau)]|_2^2 \, d\tau \sum_{l=1}^{N} \sum_{m=1}^{N} \int_0^t k_{lm}^2(t-\tau)\, d\tau \\
&\leq \int_0^h C^2 \, |v(\tau)|_2^2 \, d\tau \sum_{l=1}^{N} \sum_{m=1}^{N} \int_0^\infty k_{lm}^2(\tau)\, d\tau \\
&= C^2 \, \|v\|_2^2 \sum_{l=1}^{N} \sum_{m=1}^{N} \|k_{lm}\|_2^2 \\
&< \infty,
\end{aligned}
$$

so is v.

The solution v is unique in $L_{\infty,N}(0,h)$, for if v_2 were a different solution in $L_{\infty,N}(0,h)$, we have

$$\begin{aligned} u(t) &= v(t) + \int_0^t k(t-\tau)\eta[v(\tau)]d\tau,\ t \in [0,h],\ \text{and} \\ u(t) &= v_2(t) + \int_0^t k(t-\tau)\eta[v_2(\tau)]d\tau,\ t \in [0,h]. \end{aligned}$$

Since the solution v is unique in $L_{2,N}(0,h)$, we have $v = v_2$ a.e. in $[0,h]$ [31, Theorem 5.11]. Since $\eta(0) = 0$, $\eta[v(t)] - \eta[v_2(t)] = 0$ a.e. in $[0,h]$ and thus

$$\begin{aligned} v_2(t) - v(t) &= \int_0^t k(t-\tau)\left(\eta[v(\tau)] - \eta[v_2(\tau)]\right)\,d\tau,\ t \in [0,h] \\ &= 0. \end{aligned}$$

Since this holds for every choice of h, the result follows.

Fact 1 Lipschitz continuity ⇒ Absolute Continuity ⇒ Bounded variation. See [31, page 115].

Lemma 12 Let $u \in L_1(0,\infty)$. Then with U the Laplace transform of u, we have (for $\sigma \in \mathbb{R}$),

$$\lim_{\sigma\to\infty} U(\sigma) = 0.$$

Proof: Let $\varepsilon > 0$. Let

$$F(x) = \int_0^x |u(t)|\ dt.$$

Since F is continuous and $F(0) = 0$, there exists a $k > 0$ such that $F(k) < \varepsilon/2$. Thus, for $\sigma > 0$,

$$|U(\sigma)| = \left|\int_0^\infty e^{-\sigma t}u(t)\,dt\right|$$

[3]Schwarz's inequality for $L_{2n}(0,\infty)$.
[4]Cauchy-Schwarz inequality for $\mathbb{R}^N$.

$$
\begin{aligned}
&= \left| \int_0^k e^{-\sigma t} u(t)\, dt + \int_k^\infty e^{-\sigma t} u(t)\, dt \right| \\
&\leq \int_0^k |u(t)|\ dt + e^{-\sigma k} \int_k^\infty |u(t)|\ dt \\
&< \varepsilon/2 + e^{-\sigma k} \left\| u \right\|_{L_1(0,\infty)} \\
&\leq \varepsilon
\end{aligned}
$$

provided

$$
\sigma \geq \frac{1}{k} \left[-\ln\left(\frac{\varepsilon}{2}\right) + \ln\left(\left\| u \right\|_{L_1(0,\infty)} \right) \right].
$$

C.2 Description of the Theorems used in Chapter 2

The theorems stated here are much simplified versions of two of the theorems given in [15]. They are used to prove the claims concerning the stability of the varactor circuit. The original theorems deal with the more general case of vector-valued Lebesgue measurable functions and time-varying nonlinearities. The interested reader is referred to the original publication. Here we restrict ourselves to measurable real-valued functions of a real variable (unless otherwise noted) and the case in which $\alpha > 0$.

The statement below that $\psi \in \Psi(\alpha, \beta)$ means that $\psi(0) = 0$ and

$$
\alpha \leq \frac{\psi(x_2) - \psi(x_1)}{x_2 - x_1} \leq \beta
$$

for $x_1 \neq x_2$. The statement that $u \in \Phi(\alpha, \beta)$ means that $u \in L_1(0, \infty)$ and, with U the Laplace transform of u, the locus of $U(j\omega)$ for $-\infty < \omega < \infty$ lies outside the circle of radius $\frac{1}{2}(\alpha^{-1} - \beta^{-1})$ centered on the real axis of the complex plane at $[-\frac{1}{2}(\alpha^{-1} + \beta^{-1}), 0]$ and does not encircle it.

Theorem 12 below corresponds to Theorem 4 of [15] and establishes the claim that if the input approaches a periodic function of time with period T as time increases then the output approaches a unique periodic function of time with the

same period T and this function depends only on the periodic function that the input approaches. To state the theorem, define $\mathcal{D}$ by

$$\mathcal{D} \;=\; \{f : f \in L^{\infty}(-\infty,\infty), f(t) = f(t+T) \text{ for } -\infty < t < \infty\}.$$

Theorem 12 Let $u \in \Phi(\alpha,\beta)$ with $t^p u(t) \in L_1 \bigcap L_2$ for $p \in \{0,1,2\}$. Let $g_1 \in \mathcal{D}$, $g_2 \in L_\infty(0,\infty)$, $\lim_{t\to\infty} g_2(t) = 0$, and $\psi \in \Psi(\alpha,\beta)$. Let $y \in L_{2\,\mathrm{loc}}$ satisfy

$$g_1(t) + g_2(t) = y(t) + \int_0^t u(t-\tau)\psi[y(\tau)]d\tau,\ t \geq 0. \tag{C.2}$$

Then $\mathcal{D}$ contains a (unique) element $\hat{y}$ which does not depend on g_2 such that

$$\lim_{t\to\infty} [y(t) - \hat{y}(t)] = 0.$$

Comment concerning describing-functions: The periodic function $\hat{y}$ in Theorem 12 satisfies the equation

$$g_1(t) = \hat{y}(t) + \int_{-\infty}^t u(t-\tau)\psi[\hat{y}(\tau)]d\tau,\ \ -\infty < t < \infty. \tag{C.3}$$

Under the conditions of the theorem, the describing-function technique for determining $\hat{y}$ is valid [16].

Theorem 13 below corresponds to Corollary 3(a) of [15] and makes precise the claim that small changes in the input result in small changes in the output.

Theorem 13 Let $u \in \Phi(\alpha,\beta)$ with $t^p u \in L_1 \bigcap L_2$ for $p \in \{0,1,2\}$ let $\psi \in \Psi(\alpha,\beta)$, and let

$$\begin{aligned} g_1(t) &= y_1(t) + \int_0^t u(t-\tau)\psi[y_1(\tau)]d\tau,\ t \geq 0 \\ g_2(t) &= y_2(t) + \int_0^t u(t-\tau)\psi[y_2(\tau)]d\tau,\ t \geq 0 \end{aligned} \tag{C.4}$$

where $g_1, g_2, y_1, y_2 \in L_{2\,\mathrm{loc}}$ and $(g_1 - g_2) \in L_\infty(0,\infty)$. Then $(y_1 - y_2) \in L_\infty(0,\infty)$, there exists a positive constant ρ which depends only on u, α, and β such that

$$\sup_{t\geq 0} |y_1(t) - y_2(t)| \leq \rho \sup_{t\geq 0} |g_1(t) - g_2(t)|$$

and $[y_1(t) - y_2(t)] \to 0$ as $t \to 0$ whenever $[g_1(t) - g_2(t)] \to 0$ as $t \to 0$.

Index

Bibliography

[1] T. Arbogast and J. Bona. Applied mathematics I. Class notes, Department of Mathematics, The University of Texas at Austin, Fall Semester 1999.

[2] A. S. Besicovitch. *Almost Periodic Functions*. Dover Publications, Inc., 1954.

[3] C. B. Burckhardt. Analysis of varactor frequency multipliers for arbitrary capacitance variation and drive level. *The Bell System Technical Journal*, vol. 44, no. 4, pages 675–692, April 1965.

[4] C. Corduneanu. *Almost Periodic Functions*. Interscience Publishers, 1968.

[5] A. M. Fink. *Almost Periodic Differential Equations*. Number 377 in Lecture Notes in Mathematics. Springer, 1970.

[6] D. A. Grant and J. Gowar. *POWER MOSFETS Theory and applications*, chapter 7, pages 179–182. John Wiley & Sons, 1989.

[7] D. Hente and R. H. Jansen. Frequency domain continuation method for the analysis and stability investigation of nonlinear microwave circuits. *IEE Proceedings*, vol. 133, Pt. H, no. 5, pages 351–362, October 1986.

[8] E. Kreyszig. *Introductory Functional Analysis with Applications*. John Wiley & Sons, 1989.

[9] R. K. Miller. *Nonlinear Volterra Integral Equations*. Menlo Park: Benjamin, 1971.

[10] V. Rizzoli and A. Lipparini. General stability analysis of periodic steady-state regimes in nonlinear microwave circuits. *IEEE Transactions on Microwave Theory and Techniques*, vol. 33, no. 1, pages 30–37, January 1985.

[11] I. W. Sandberg. On the boundedness of solutions of nonlinear integral equations. *The Bell System Technical Journal*, pages 439–453, March 1965.

[12] I. W. Sandberg and G. J. J. van Zyl. The spectral coefficients of the response of nonlinear systems to asymptotically almost periodic inputs. *IEEE Transactions on Circuits and Systems I: Fundamental Theory and Applications*, vol. 48, no. 2, pages 170–176, February 2001.

[13] I. W. Sandberg. Signal distortion in nonlinear feedback systems. *The Bell System Technical Journal*, pages 2533–2550, November 1963.

[14] I. W. Sandberg. On the $\mathcal{L}_2$–boundedness of solutions of nonlinear functional equations. *The Bell System Technical Journal*, pages 1581–1599, July 1964.

[15] I. W. Sandberg. Some results on the theory of physical systems governed by nonlinear functional equations. *The Bell System Technical Journal*, vol. 44, no. 5, pages 871–898, May 1965.

[16] I. W. Sandberg. Approximately finite memory and input-output maps. *IEEE Transactions on Circuits and Systems–I:Fundamental Theory and Applications*, vol. 39, no. 7, pages 549–556, July 1992.

[17] I. W. Sandberg. Approximately finite memory and the circle criterion. *IEEE Transactions on Circuits and Systems–I:Fundamental Theory and Applications*, vol. 41, no. 7, pages 473–476, July 1994.

[18] I. W. Sandberg and G. J. J. van Zyl. An algorithm with error bounds for calculating intermodulation products. *IEEE Microwave and Guided Wave Letters*, vol. 10, no. 11, pages 463–465, November 2000.

[19] I. W. Sandberg and G. J. J. van Zyl. Evaluation of the response of nonlinear systems to asymptotically almost periodic inputs. In *The 2001 IEEE International Symposium on Circuits and Systems*, vol. 2, pages 77–80, 2001.

[20] I. W. Sandberg and G. J. J. van Zyl. Harmonic balance and almost periodic inputs. In *IEEE International Symposium on Circuits and Systems*, vol. 1, pages 637–640, 2002.

[21] I. W. Sandberg and G. J. J. van Zyl. Designing periodically driven varactor circuits with guaranteed stability. *IEEE Microwave and Guided Wave Letters*, vol. 9, no. 6, pages 230–232, June 1999.

[22] I. W. Sandberg and G. J. J. van Zyl. A frequency-domain stability criterion for periodically driven varactor circuits. In *42nd Midwest Symposium on Circuits and Systems*, vol. 2, pages 943–946. IEEE, 2000.

[23] I. W. Sandberg. A note on the application of the contraction-mapping fixed-point theorem to a class of nonlinear functional equations. *SIAM Review*, vol. 7, no. 2, pages 199–204, April 1965.

[24] I. W. Sandberg and G. J. J. van Zyl. Harmonic balance and almost periodic inputs. *IEEE Transactions on Circuits and Systems I: Fundamental Theory and Applications*, vol. 49, no. 4, pages 459–464, April 2002.

[25] S. Basu, S. A. Maas and T. Itoh. Piecewise stability analysis in microwave circuits. *IEEE Microwave and Guided Wave Letters*, vol. 5, no. 5, pages 159–160, May 1995.

[26] S. Basu, S. A. Maas and T. Itoh. Predicting the onset of instabilities in frequency multipliers. In *IEEE MTT-S International Symposium Digest*, vol. III, pages 1511–1514, 1995.

[27] S. Mons, J. Nallatamby, R. Quéré, P. Savary and J. Obregon. A unified approach for the linear and nonlinear stability analysis of microwave circuits using commercially available tools. *IEEE Transactions on Microwave Theory and Techniques*, vol. 47, no. 12, pages 2403–2409, December 1999.

[28] F. C. Tricomi. *Integral Equations*. New York: Interscience, 1963.

[29] V. Iglesias, A. Suárez and J. L. García. New technique for the determination through commercial software of the stable-operation parameter ranges in nonlinear microwave circuits. *IEEE Microwave and Guided Wave Letters*, vol. 8, no. 12, pages 424–426, December 1998.

[30] V. Rizzoli, A. Neri and D. Masotti. Local stability analysis of microwave oscillators based on Nyquist's theorem. *IEEE Microwave and Guided Wave Letters*, vol. 7, no. 10, pages 341–343, October 1997.

[31] R. L. Wheeden and A. Zygmund. *Measure and Integral: An Introduction to Real Analysis*. Monographs and textbooks in pure and applied mathematics; 43. Marcel Dekker, Inc., 1977.

Vita

Gideon Johannes Jacobus van Zyl was born in Stellenbosch, South Africa on February 26, 1963, the son of Gideon Johannes Jacobus van Zyl and Wilhelmina Dorethea van Zyl. After completing his work at Pearson High School, Port Elizabeth, South Africa in 1981, he entered the University of Stellenbosch in South Africa. He received the B.Eng. and M.Eng. degrees in electronic engineering and the Hons.-B.Sc. degree in mathematics from the University of Stellenbosch in 1985, 1991, and 1996 respectively. He worked at Reutech Radar Systems, Stellenbosch, South Africa from 1987 to 1998. In 2001 he joined Advanced Energy Industries, Inc. in Fort Collins, Colorado.

Permanent Address: 3018 Rockborough Court, Fort Collins, Colorado, 80525

This dissertation was typeset with LaTeX 2_ε[5] by the author.

[5] LaTeX 2_ε is an extension of LaTeX. LaTeX is a collection of macros for TeX. TeX is a trademark of the American Mathematical Society. The macros used in formatting this dissertation were written by Dinesh Das, Department of Computer Sciences, The University of Texas at Austin, and extended by Bert Kay and James A. Bednar.